



Published in final edited form as:

*Chem Soc Rev.* 2017 October 30; 46(21): 6492–6531. doi:10.1039/c7cs00372b.

## Implications of Peptide Assemblies in Amyloid Diseases

**Pu Chun Ke<sup>a</sup>, Marc-Antonie Sani<sup>b</sup>, Feng Ding<sup>c</sup>, Aleksandr Kakinen<sup>a</sup>, Ibrahim Javed<sup>a</sup>, Frances Separovic<sup>b</sup>, Thomas P. Davis<sup>a,d</sup>, and Raffaele Mezzenga<sup>\*,e</sup>**

<sup>a</sup>ARC Center of Excellence in Convergent Bio-Nano Science and Technology, Monash Institute of Pharmaceutical Sciences, Monash University, 381 Royal Parade, Parkville, VIC 3052, Australia

<sup>b</sup>School of Chemistry, Bio21 Institute, The University of Melbourne, 30 Flemington Rd, Parkville, VIC 3010, Australia

<sup>c</sup>Department of Physics and Astronomy, Clemson University, Clemson, SC 29634, United States

<sup>d</sup>Department of Chemistry, University of Warwick, Gibbet Hill, Coventry, CV4 7AL, United Kingdom

<sup>e</sup>ETH Zurich, Department of Health Science & Technology, Schmelzbergstrasse 9, LFO, E23, 8092 Zurich, Switzerland

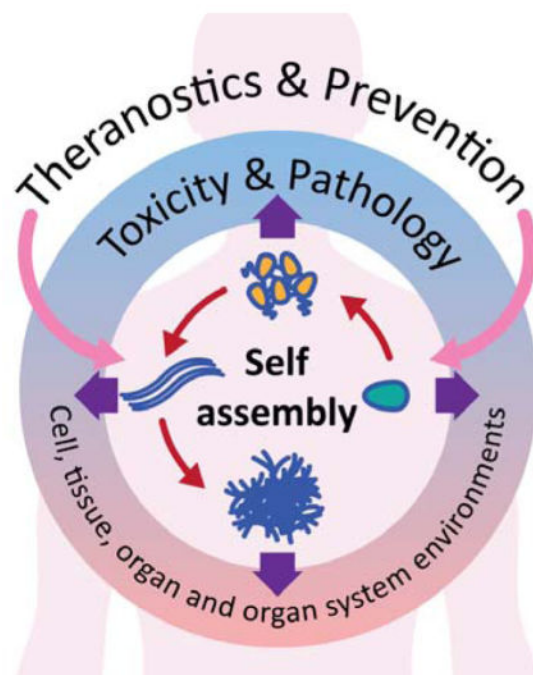
### Abstract

Neurodegenerative disorders and type 2 diabetes are global epidemics compromising the quality of life of millions worldwide, with profound social and economic implications. Despite the significant differences in pathology – much of which are poorly understood – these diseases are commonly characterized by the presence of cross- $\beta$  amyloid fibrils as well as the loss of neuronal or pancreatic  $\beta$ -cells. In this review, we document research progress on the molecular and mesoscopic self-assembly of amyloid-beta, alpha synuclein, human islet amyloid polypeptide and prions, the peptides and proteins associated with Alzheimer's, Parkinson's, type 2 diabetes and prions diseases. In addition, we discuss the toxicities of these amyloid proteins based on their self-assembly as well as their interactions with membranes, metal ions, small molecules and engineered nanoparticles. Through this presentation we show the remarkable similarities and differences in the structural transitions of the amyloid proteins through primary and secondary nucleation, the common evolution from disordered monomers to alpha-helices and then to  $\beta$ -sheets when the proteins encounter the cell membrane, and, the consensus (with a few exceptions) that off-pathway oligomers, rather than amyloid fibrils, are the toxic species regardless of the pathogenic protein sequence or physicochemical properties. In addition, we highlight the crucial role of molecular self-assembly in eliciting the biological and pathological consequences of the amyloid proteins within the context of their cellular environments and their spreading between cells and organs. Exploiting such structure-function-toxicity relationship may prove pivotal for the detection and mitigation of amyloid diseases.

### Graphical Abstract

---

\*Address correspondence to: Raffaele Mezzenga: raffaele.mezzenga@hest.ethz.ch.



## Keywords

amyloid; oligomer; self-assembly; neurodegenerative disorders; A $\beta$ ; IAPP;  $\alpha$ -synuclein; prion; theranostics

## 1. Introduction

Molecular self-assembly is an ubiquitous phenomenon across all living systems: from the polymerization of tubulins and actins into microtubules and actin filaments, to the organization of lipids, transmembrane/peripheral proteins and ion channels into cell membranes, to the assembly of DNA and histones into chromatin fibers and solenoids, and to the aggregation of peptides and proteins intra- or extracellularly evolving from functional monomers to toxic oligomers, amyloid fibrils and plaques. Fundamental to these processes are interactions between the molecular constituents of the assemblies, as well as interactions between the molecular constituents and their associated chaperones, ligands, ions, molecular complexes and organizations, driven by kinetic and thermodynamic processes to elicit desirable biological functions or malfunctions and diseases.

In this review, we attempt to draw parallels from the atomic and mesoscopic structures of five major classes of amyloid proteins in self-assembly, namely, amyloid-beta (A $\beta$ ), tau, alpha-synuclein ( $\alpha$ S), prions, and human islet amyloid polypeptide (IAPP), as well as the biological and pathological endpoints these assemblies elicit in host systems (Fig. 1). The amyloid aggregation of these peptides has been implicated in Alzheimer's, Parkinson's, prion diseases and type 2 diabetes mellitus, or generically referred to as neurodegenerative disorders and T2D that debilitate hundreds of millions of people worldwide. *In vitro*, such peptides/proteins fibrillate on the timescales of tens of minutes for IAPP to days for A $\beta$  and

$\alpha$ S, characterized by a sigmoidal kinetic curve consisting of a lag phase, an elongation phase, and a saturation phase.<sup>1</sup> The lag phase is where nucleation is initiated through protein misfolding and where intrinsic seeds and/or oligomers are formed, the elongation phase corresponds to the addition of monomers to growing protofilaments, while the saturation phase is where protofilaments associate through self-assembly to render amyloid fibrils. In addition to primary nucleation, secondary nucleation through the combination of both monomeric and aggregated species is also feasible.<sup>2, 3</sup> It has been suggested that the amyloid state is perhaps available to any polypeptide chain<sup>4-9</sup> and represents the energetically most favorable state even compared to native proteins.<sup>1</sup> *In vivo*, however, the development of amyloids and plaques in the brain or pancreatic islets often takes decades, or ~10,000 times longer. Such drastic differences in fibrillization may originate from the crowded hierarchical cellular environments, where amyloid proteins are synthesized and then translocate and spread through inter- and intra-molecular assembly, chaperoned by proteins (e.g. insulin for IAPP) or modulated by pH and ionic strength. Accordingly, while the main purpose of this review is to highlight the structure-function-toxicity triangle of a selected few amyloid proteins, another goal of this presentation is to draw the readers' attention from focusing exclusively on amyloid proteins to the environments of the culprits at large, which undoubtedly also contribute to the pathologies of the amyloid diseases. Such perspective may prove beneficial to the development of mitigation strategies and therapeutics against amyloidogenesis that has become increasingly perilous to modern society.

In terms of content, this review consists of 6 sections: section 1 offers an introduction to protein self-assembly and amyloid diseases; sections 2-5 review the structure, function and toxicity characteristics of A $\beta$ , tau, IAPP,  $\alpha$ S and prions, loosely following their increasing numbers of amino acids (residues); section 6 provides a summary. A $\beta$  and tau, despite their great contrast in chain length, both contribute to the AD pathology and hence are presented together. Although A $\beta$  is slightly longer than IAPP in chain length, A $\beta$  is the most studied of all amyloid proteins<sup>10</sup> and is therefore discussed in the early section of this review.

## 2. A $\beta$ , tau and Alzheimer's disease

The hallmark of Alzheimer's disease (AD) is the accumulation of toxic aggregates that impair synaptic function and induce cognitive decline. The first reported occurrence of cognitive disorder linked to AD was in 1907 by Alzheimer, who observed two types of abnormality in a brain autopsy that he attributed to be the cause of an unusual type of dementia.<sup>11</sup> The discovery of neuritic plaques (or miliary foci) and neurofibrillary tangles (NFTs) was immediately linked to the dystrophic neuronal process, and later A $\beta$  fibrils<sup>12, 13</sup> and hyperphosphorylated tau tangles<sup>14</sup> were isolated and characterized (and proposed to cause dementia). Characterizations of the monomeric forms of the molecules found in these neurotoxic deposits have led to greater understanding of the pathways leading to AD, with a particular focus on the structure-function relationship between aggregates and neurotoxicity. However, almost all drugs tested thus far in clinical trials have failed or shown limited impact on AD.

Tau is a neuronal protein associated with microtubules and may regulate neuron morphology. There are six main tau isoforms in the brain and central nervous system (CNS).

The longest human isoform has 441 residues with a high proportion of phosphorylatable residues (serine and threonine) and a low proportion of hydrophobic amino acids. Tau protein in solution is considered an intrinsically disorder protein (IDP) and behaves as a random coil,<sup>15</sup> although modifications by phosphorylation may lead to an increase in  $\alpha$ -helix or  $\beta$ -sheet regions. Aggregation of totally or partially disordered proteins is associated with many neurodegenerative diseases, including AD.<sup>16</sup> However, the molecular mechanism of aggregation and the structure of the aggregated form remain controversial. Tau is mainly an axonal protein but in AD and other tauopathies it is also present at dendritic spines and may play a toxic role. The tau hypothesis of AD considers that excessive phosphorylation of tau protein can result in the self-assembly of tangles of paired helical filaments (PHFs) and straight filaments which are involved in the pathogenesis of AD and other tauopathies. These neurofibrillary tangles are insoluble structures that impair axonal transport and lead to cell death. The molecular structures of PHFs and tau protein are not well defined.

NMR data<sup>17</sup> have revealed that 343 of the 441 amino acids in tau are disordered with six segments of the sequence displaying propensity to form  $\beta$ -strands, three segments showing poly-Pro helices and two segments with a transient  $\alpha$ -helix structure. In particular, aggregation of tau is believed to be strongly associated with two short residue sequences:<sup>18–21</sup> the first in the third repeat fragment (R3, i.e.

VQIVYKPVDLSKVTSKCGSLGNIHKK) of the microtubule binding domain of tau, VQIVYK, or the mutant VQIINK, in the second repeat fragment. The aggregation of the R3 fragment has been extensively studied in the presence of polyanions, such as heparin, pointing at the formation of fibrillar structures with similar features as those assembled from the pristine tau protein.<sup>22</sup> In the absence of heparin, however, the same R3 fragment has been shown to self-assemble into giant amyloid ribbons of remarkable aspect ratios.<sup>23</sup>

The tau protein is a highly dynamic structure. An NMR study of a peptide derived from tau showed that phosphorylation stabilized the  $\alpha$ -helix structure,<sup>24</sup> suggesting a possible higher content of  $\alpha$ -helices in hyperphosphorylated tau in PHFs. Tau protein can form dimers, oligomers and larger aggregates and fibrils. However, in this review we focus on the A $\beta$  peptide rather than tau aggregates, as greater structural details are available for the former.

## 2.1 Role of APP and production of A $\beta$

A $\beta$  peptides are produced by an intrinsic cleavage of the amyloid precursor protein (APP) that is an integral membrane protein encoded on chromosome 21 by the APP gene.<sup>25</sup> It is accepted that patients with trisomy 21 (Down syndrome) overexpress APP and develop AD-like senile plaques in their brain.<sup>26, 27</sup> Yet, the physiological function of APP remains uncertain, mostly because APP is part of a gene family with overlapping function (e.g. producing the amyloid precursor-like proteins APLP1 and APLP2) and is subject to various post-expression modifications.<sup>28</sup> Still, only APP generates the A $\beta$  fragment. APP modulates critical features in brain development since APP knock-out mice are viable but exhibit reduced body weight and brain mass<sup>29</sup> with increased brain levels of copper,<sup>30</sup> cholesterol and sphingolipid.<sup>31</sup> Interestingly, reintroducing the APP ectodomain, which is produced by cleavage of the membrane-anchored APP, improved cognitive function and synaptic density<sup>32, 33</sup> and acted as an apoptosis modulator through caspases activations.<sup>34</sup> The

intracellular C-terminal domain also has a functional role in sorting APP and, in particular, the highly conserved YENPTY cytoplasmic sequence is prone to interaction with other proteins, such as X11 and Fe65, which are postulated to regulate APP internalization.<sup>35</sup>

The location and sequence of the proteolytic cleavage of APP are critical to AD. APP is primarily translocated to the cell surface (short residence time) where  $\alpha$ -secretase and then  $\gamma$ -secretase produce APP $\alpha$ , p3 and AICD fragments, which are not amyloidogenic. However, when APP is relocated through endocytosis (rapid turnover due to the YENPTY sequence) into endosomes containing the  $\beta$ -secretase (also called BACE1) and the  $\gamma$ -secretase, then APP $\beta$ , the toxic A $\beta$  peptides and AICD fragments are produced (Fig. 2). BACE1 is an aspartyl protease that has optimum efficiency at pH 4.5.<sup>36</sup> Interestingly, acid pH can promote greater aggregation rate of A $\beta$  peptides<sup>37</sup> due to the protonation state of the three histidines (His6, His13 and His14), and also attenuate lysosomal degradation of A $\beta$  peptides.<sup>38</sup> Furthermore, if APP is relocated to the trans Golgi network instead of the ER, BACE1 can produce N-truncated A $\beta$  peptides which are prone to rapid pyroglutamylation.<sup>39</sup> These species have been characterized as highly toxic<sup>40</sup> and found in intracellular, extracellular and vascular A $\beta$  deposits in AD brain tissue,<sup>41</sup> while unmodified peptides are primarily located in endosomal compartments and are eventually exocytosed into the extracellular space.

It is noteworthy that intracellular pools of A $\beta$  peptides are pointed as the most toxic species causing the death of neurons.<sup>42, 43</sup> The physiological function of these A $\beta$  peptides, usually 39–43 residues in length, is unconfirmed. However, during excitatory neuronal activity, an increase in excretion of A $\beta$  peptides is observed<sup>44</sup> with the effect of downregulating excitatory synaptic transmission.<sup>45</sup> Thus, A $\beta$  peptides are an important modulator of memory, since inhibition of peptide production impairs learning.<sup>46</sup> A $\beta$ (1–40) is the most abundant A $\beta$  isoform found in its soluble form in plasma, cerebrospinal fluid and brain interstitial fluid<sup>47</sup> but is also a major component in amyloid plaques. Interestingly, the level of the fast-aggregating isoform A $\beta$ (1–42) is a biomarker for detecting amyloid pathologic changes in the brain and cerebral vessels<sup>48</sup> and, moreover, the relative A $\beta$ (1–42)/A $\beta$ (1–40) ratio is markedly increased in AD.<sup>49</sup> Overall, both the concentration and location of A $\beta$  peptides are critical for brain function, thereby complicating therapeutic strategies against AD.

## 2.2 Atomic structures of A $\beta$ 40 & A $\beta$ 42, post-modifications and amyloid fibrils

A $\beta$  peptides vary in length due to the multiple cleavage sites recognized by the secretases, but the most abundant species are A $\beta$ (1–40) and A $\beta$ (1–42), whose sequences are shown in Fig. 3. Furthermore, A $\beta$  peptides can be degraded by proteases such as insulin degrading enzymes,<sup>50</sup> neprilysin<sup>51</sup> and cathepsin B,<sup>52</sup> which render the fragments non-amyloidogenic. A $\beta$  peptides can be subject to post-translational modifications including pyroglutamate formation (Glu3, 11 and 22),<sup>53</sup> phosphorylation (Ser8 and 26),<sup>54</sup> dityrosine formation (Tyr10)<sup>55</sup> and oxidation (Met35)<sup>56</sup> (see Fig. 3).

The A $\beta$  peptide primary sequence exhibits two stretches of hydrophobic residues (17–21 and 32 until C-terminus), which are predicted to adopt a  $\beta$ -sheet conformation.<sup>57</sup> Two turn regions are also predicted between residues His6 and Ser8, and between Asp23 and Asn27.

Finally, the hydrophilic patches between Asp1 and Lys16 and between Glu22 and Lys28 have either  $\beta$ -sheet or  $\alpha$ -helical propensity.<sup>58, 59</sup>

A missing piece in the AD puzzle is the secondary structures of A $\beta$  peptides immediately after cleavage by the  $\gamma$ -secretase. Firstly,  $\beta$ -CTF is likely to remain structured after cleavage by BACE1, at least up to the transmembrane  $\alpha$ -helical segment that contains part of A $\beta$  sequence (Ala28 until C-terminus). Secondly, cleavage by the  $\gamma$ -secretase occurs at intra-membrane and A $\beta$  peptides have a demonstrated affinity for lipid membranes. Thus immediate trafficking is unclear: do A $\beta$  peptides remain in, on or away from the membrane interface? Since lipid membranes modulate the aggregation kinetics,<sup>60</sup> this step could play a critical role in subsequent trafficking and AD pathology.

Several A $\beta$  peptide structures have been compiled in the past two decades,<sup>61</sup> with a consensus that an unstructured to  $\beta$ -sheet transition first occurs followed by a seeded aggregation process to form oligomeric structures that eventually proceeds to mature amyloid fibrils of 70–120 Å in diameter and an indeterminate length according to electron microscopy.<sup>62</sup> Determination of the initial structure of A $\beta$  peptides in native conditions is challenging since the rapid self-aggregation rate accompanied by poor solubility prevents the application of high-resolution techniques such as solution NMR. Nevertheless, several structures of the monomeric peptides have been determined in either organic solvents (dimethylsulfoxide, hexafluoroisopropanol, trifluoroethanol), aqueous solution or detergent micelles (sodium dodecyl sulfate or SDS). In general, A $\beta$  peptides adopted helical conformations with unstructured termini and various turn regions in organic solvents,<sup>63–65</sup> aqueous buffer<sup>66</sup> and in membrane mimetic detergent micelles.<sup>67, 68</sup> Interestingly, most structural studies show that physiological pH,<sup>69</sup> low salt concentration<sup>70</sup> and higher temperature<sup>71</sup> could heavily modulate the peptide conformational transition to  $\beta$ -sheet structure and thereby promoting rapid self-aggregation. The  $\alpha$ -helical conformation is proposed as a transient on-pathway intermediate during the complex amyloid fibril formation.<sup>72</sup> Indeed, the multistep kinetics of amyloid assembly comprise a lag phase, during which little or no fibril material is formed, followed by an exponential growth of  $\beta$ -sheet-rich aggregates that propagate into amyloid fibrils.<sup>1</sup> Increasing evidence suggests that the native partly helical intermediates form the early nucleation seeds during the lag phase.<sup>73</sup> The intramolecular interactions stabilizing the  $\beta$ -sheet structure are shown in Fig. 3. In both A $\beta$  isoforms, the turn conformation is stabilized by hydrophobic interactions and by a salt bridge between Asp23 and Lys28. Many side chain contacts are observed, in particular between Phe19 and Ile32, Leu34 and Val36, and between pairs Gln15 - Val36 and His13 - Val40.<sup>57,74</sup>

Phosphorylation of A $\beta$  peptides, however, does not modify their primary unstructured conformation but leads to a 5-fold reduction in the lag phase due to a faster transition to  $\beta$ -sheet structures, more efficient nucleation and a greater number of oligomeric seeds.<sup>75</sup> N-truncated and/or pyroglutamate-modified A $\beta$  peptides form  $\beta$ -sheet structures<sup>76</sup> with faster aggregation kinetics than the corresponding full-length peptides, which suggests they could be potential seeding species for aggregate formation. More dramatically, the pyroglutamate-modified A $\beta$  peptides also inhibit the full-length peptide fibrillogenesis and lead to a greater content of small oligomeric species<sup>77</sup> that have been demonstrated as the most toxic species.

### 2.3 A $\beta$ aggregation kinetics and amyloid fibril formation

Knowledge of A $\beta$  aggregation kinetics and mechanisms has been acquired mainly through *in vitro* studies using synthetic peptides. The kinetics of fibril formation depends on several intrinsic and extrinsic factors. The primary sequence of the peptide modulates the propensity to aggregate into mature fibrils. Post-modifications promote faster aggregation kinetics, as does the A $\beta$ (1–42) sequence compared to the shorter A $\beta$ (1–40) peptide. Extrinsic factors, such as interaction with lipid membranes, can have either a slowing or accelerating effect, rendering determination of a generic model nontrivial.

The lag phase is a period of slow self-aggregation and structural change, likely from helical to  $\beta$ -sheet structures, and characterized by a combination of multiple nucleation and elongation phases<sup>2,78, 79</sup> leading to a large number of oligomeric species. Primary nucleation is a fast process (milliseconds) producing the first seeds that are elongated further into fibrils by the addition of monomers. The formation of new aggregates is thought to be dominated by a second nucleation phase where existing fibrils are fragmented to expose new seeds either co-aggregating or recruiting monomers. Interestingly, changes in the primary nucleation rate do not affect the elongation phase while secondary nucleation and fragmentation modify the lag and elongation phases.<sup>80</sup> The difference in aggregation rate between the amyloid peptide species, however, may be related to their primary nucleation rate. In fact, A $\beta$ (1–40) monomers, in comparison to A $\beta$ (1–42), exhibit a slower nucleation rate inducing (or caused by) a shift towards nucleation on the fibril surface rather than accumulation of small oligomeric species.<sup>79</sup> These fibril-catalyzed secondary nucleation and elongation processes could be a critical difference in relation to the trafficking and toxicity of the A $\beta$  peptide variants.<sup>81</sup> Notably, measuring the kinetics of aggregation is challenged by the difficulty in sample preparation,<sup>81</sup> especially with regard to starting an experiment without any preformed seeds or a controlled amount of seeds.

The elongation phase is due to the addition of oligomers/monomers onto protofibrils (Fig. 4) or association of protofibrils, in competition with fragmentation of the protofibrils. It is often typified by the half time of the aggregation reaction where the monomers and protofibrils are near equimolar. However, intrinsic and extrinsic factors modulate the stability of the oligomeric species and can template seeds thereby shifting the kinetic rate towards primary nucleation with a faster aggregation rate. The stationary phase represents a steady state where the monomer concentration has reached an equilibrium value and the fibrils are the prevalent species. Notably, AFM studies show that fibrils of different amyloid-forming peptides with diverse macroscopic structures/polymorphism (i.e., ribbon-like versus nanotube-like packing) have a similar Young's modulus; and thus all A $\beta$  peptides are anticipated to exhibit similar mechanical strength.<sup>82</sup>

Intrinsic and extrinsic factors also play a critical role in the modulation of the lag and elongation phases by changing the concentration of free monomer in solution and/or acting as seeding interfaces. The molecular factors influencing the aggregation kinetic of A $\beta$  peptides are various and difficult to assign to a particular microscopic event (primary versus secondary nucleation, fragmentation, etc.), although some properties are more straightforward to correlate, for instance, the effect of pH as electrostatic interactions mediate either attraction or repulsion of the monomers.<sup>78</sup>

## 2.4 Mesoscopic structures of A $\beta$ amyloid fibrils

An original molecular model of A $\beta$ (1–40) fibrils<sup>83</sup> based on solid-state NMR data shows the first ~10 residues as structurally disordered while residues 12–24 and 30–40 adopt  $\beta$ -strand conformations and form parallel  $\beta$ -sheets through intermolecular hydrogen bonding. A bend at residues 25–29 brings the two  $\beta$ -sheets in contact through sidechain-sidechain interactions. The cross- $\beta$  motif common to all amyloid fibrils is a double-layered structure, with in-register parallel  $\beta$ -sheets.<sup>83</sup> However, several studies have shown that A $\beta$  peptides form polymorphic fibrils that depend on growth conditions and various oligomeric aggregates. Thus it is unlikely that amyloid fibrils formed *in vitro* resemble those in the brain. Tycko and co-workers<sup>84</sup> seeded fibril growth from brain extract and used solid-state NMR and electron microscopy to gain structural details of the A $\beta$  fibrils. Using tissue from two AD patients they found a single A $\beta$ 40 fibril structure for each patient emphasizing the critical role of the seeding process. The molecular structure for A $\beta$ 40 fibrils from one patient (Fig. 5) revealed differences from *in vitro* fibrils. The authors proposed that fibrils may spread from a single nucleation site and that structural variations may correlate with variations in AD.

In comparison with A $\beta$ 40, A $\beta$ 42 is more neurotoxic and their differences in behaviour may be due to intrinsic differences in structure. An atomic resolution structure of a single form of A $\beta$ 42 amyloid fibrils has been derived from high field magic angle spinning NMR spectra.<sup>85</sup> The structure shows a dimer of A $\beta$ 42 molecules, each containing four  $\beta$ -strands in an S-shaped amyloid fold (Fig. 6). The dimer is arranged to form two hydrophobic cores, capped by a salt bridge at the end with a hydrophilic outer surface. The monomer interface within the dimer shows contacts between M35 of one molecule and L17 and Q15 of the second. Intermolecular constraints show that the amyloid fibrils are parallel in-register. Interestingly, Ishii and co-workers obtained a similar S-shape arrangement (Fig. 6) using ultra-fast spinning solid-state NMR techniques.<sup>86</sup> Although knowing atomic details of the fibril may be useful for drug design, nevertheless, the oligomer species are generally accepted as the toxic species.<sup>87</sup>

## 2.5 Extrinsic factors modulating A $\beta$ structure, aggregation kinetic and toxicity

**2.5.1 A $\beta$ -metal interactions**—The role of transition metals in AD is highly debated and a recent literature search using meta-analysis and systemic review methodologies identified a widespread misconception that iron and, to a lesser degree, zinc and copper levels are increased in AD brain.<sup>88</sup> Metals were primarily thought to be accumulated in AD brain tissue due to positive staining but quantitative analysis failed to confirm a significant increase,<sup>89</sup> and more recent studies have confirmed the artefacts in quantitation due to tissue fixation prior to analysis.<sup>90</sup> Qualitative *ex vivo* and *in vitro* studies have demonstrated that A $\beta$  peptides recruit iron, zinc and copper with high affinity<sup>91</sup> and, more dramatically, induce a redox complex with oxidative stress properties<sup>92</sup> that may be related to the toxicity of A $\beta$  peptides and which has been widely accepted as a potential toxic mechanism in AD.<sup>93</sup> Two binding sites were identified: the Met35 mediating the Fenton reaction through the electron donor sulfide group,<sup>94</sup> and the N-terminal region forming a chelating domain<sup>95</sup> of Asp1, His6, His13 and His14, which undergoes a major structural rearrangement during the redox cycle of ROS production.<sup>96</sup> Interestingly, *in vitro* experiments have also shown that metal



binding noticeably extends the lag time by stabilizing oligomeric and amorphous aggregates,<sup>97</sup> which may explain the poor *in vivo* detection of the peptide amyloids. A $\beta$ -copper complexes have also been shown to promote lipid peroxidation, in particular within the polyunsaturated chains of membrane lipids, which is another potential toxic mechanism due to neuronal membrane disruption.<sup>98</sup>

**2.5.2 A $\beta$ -membrane interactions**—The role of lipids in AD was first suggested by Alzheimer when he discovered adipose inclusions and alterations of lipid composition in brain tissue.<sup>11</sup> Several classes of lipids have been investigated for their specific interactions with A $\beta$  peptides, such as cholesterol, gangliosides or anionic phospholipids.<sup>99</sup> The lipid membrane interface itself is proposed to be a heterogeneous nucleation site, which modulates A $\beta$  peptide folding kinetics and pathways by reducing the seeding mechanism to a two-dimensional system.<sup>100, 101</sup> To date, there is a consensus that lipid bilayer plays a role in A $\beta$  aggregation and may be involved in neurotoxicity. Different model membranes influence the structure and size of A $\beta$  fibrils based on the charge and hydrophobicity of the membrane.<sup>60, 102</sup> Membrane-attached oligomers of A $\beta$ 40 displayed a  $\beta$ -turn, flanked by two  $\beta$ -sheet regions or an anti-parallel beta-hairpin conformation by Raman spectroscopy and solid-state NMR.<sup>103</sup> In contrast to the mature, less-toxic A $\beta$  fibrils, the membrane-attached oligomer appeared to form a  $\beta$ -barrel or ‘porin’-like structure (also refer to Fig. 15b in section 4 for  $\alpha$ S), which may account for a mechanism for A $\beta$  toxicity.

Cholesterol is proposed to be related to AD pathology although cholesterol stabilizes phospholipid bilayers against A $\beta$ .<sup>104</sup> Lipid ‘rafts’ or domains in the membrane enriched in cholesterol and sphingolipids could modulate A $\beta$  production, aggregation and toxicity.<sup>105</sup> Sanders and co-workers<sup>106</sup> showed that the C99 segment of APP bound to cholesterol and proposed that APP might act as a cholesterol sensor critical for the trafficking of APP to cholesterol-rich membrane domains. Cholesterol increases the thickness of phospholipid bilayers and may influence the proteolytic processing of APP and proportion of A $\beta$ 40 to A $\beta$ 42 produced. Lipid membranes are also susceptible to oxidative stress, as mentioned above as a mechanism for neurodegeneration in AD.<sup>98</sup>

## 2.6 A $\beta$ toxicity and Alzheimer’s disease

The physiological markers of AD are progressive cognitive decline, synaptic loss, presence of extracellular  $\beta$ -amyloid plaques and intracellular neurofibrillary tangles ultimately leading to neuronal cell death and a massive brain cell mass loss. To date, there is no drug that can prevent AD neurodegeneration probably because many pathways are activated during the uncontrolled production of A $\beta$  peptides, although several candidates are in ongoing clinical trials. Indeed, it has been demonstrated that A $\beta$  peptides accumulate at synapses, thereby disrupting the whole neuronal network.<sup>107</sup> More specifically, complex interactions between A $\beta$  peptides and both synaptic ion channels and mitochondria alter their physiological activities. A $\beta$  peptides and, more particularly, the oligomers of A $\beta$  have affinity for the glutamate<sup>108</sup> and acetylcholine<sup>109</sup> receptors, mediating the influx/efflux rate of critical mediators such as calcium ions. A $\beta$ -mediated deregulation of these receptors – particularly NMDAR and AMPAR – has been linked to the impairment of plasticity and degeneration of synapses during AD.<sup>110</sup>

The observation that A $\beta$  oligomers are able to co-localize within mitochondria has exposed another potential neurotoxic pathway.<sup>111</sup> A $\beta$  oligomers are able to alter the function of proteins involved in the mitochondrial fusion/fission process, which causes their fragmentation leading to the loss of neuron viability.<sup>112</sup> Moreover, accumulation of A $\beta$  peptides in synaptic mitochondria has been shown to decrease mitochondrial respiration and key respiratory enzyme activity, elevate oxidative stress, compromise calcium-handling capacity, and trigger apoptotic signals.<sup>113, 114</sup> Finally, intracellular accumulation of A $\beta$  peptides drastically reduces the lysosomal efficiency in removing damaged organelles and unfolded proteins, such as tau.<sup>115</sup> Better understanding of the cell biology of the downstream effects of A $\beta$  oligomers may uncover potential therapeutic targets for the prevention of AD.

## 2.7 Mitigation strategies and theranostics

With increased knowledge of the mechanism of fibril formation from the cleavage of APP to the kinetic modulation by extrinsic factors, several strategies to mitigate AD have emerged. Stabilizing the monomeric form of A $\beta$  peptides is a direct strategy to limit the formation of oligomeric species. Peptides that specifically interact with the pro-aggregating domains have been developed, as recently shown with a cyclopeptide, to inhibit A $\beta$  amyloidogenesis.<sup>116</sup> Antibody-based immunotherapy is another strategy to mitigate AD. For instance, a promising candidate, aducanumab, has shown high selectivity against aggregated A $\beta$ , induced significant reduction of insoluble and soluble A $\beta$  population and slowed clinical decline; although the outcome of ongoing Phase 3 clinical trials are needed to confirm these promising observations<sup>117</sup>. The affinity of A $\beta$  peptides for transition metals was seen as another area for potential development of AD therapeutics, but so far chelators, such as D-penicillamine, have not produced any clinical improvement.<sup>118</sup>

After drugs (e.g. bapineuzumab and solanezumab) which seek to lower existing A $\beta$  loads had failed, increasing attention was paid to BACE drugs that interfere with the process that creates A $\beta$ . However, Merck recently closed its trial for the BACE inhibitor, verubecestat, in mild-to-moderate AD after concluding that the drug had little chance of success.<sup>119</sup> A particular focus has been to decrease the production of apparently toxic A $\beta$  peptides by inhibiting BACE1 activity.<sup>120</sup> For instance, the cholesterol-rich endosomal environment, which promotes selective processing of APP by BACE1, has been pursued as a target using a membrane-anchored BACE1 transition-state inhibitor linked to a sterol moiety to generate highly effective BACE1 inhibitors.<sup>121</sup> Treatment with BACE inhibitor IV, which does not change the APP concentration level, was shown to prevent mitochondrial abnormalities caused by A $\beta$ .<sup>122</sup> Reducing the activation of caspases, such as caspase 3, can improve neuronal growth and decrease abnormal tau species, which may be an interesting therapeutic pathway for the treatment of AD.<sup>123</sup>

Since the approval of memantine in 2003, no new AD drug candidate has passed the FDA approval, with an alarming failure rate of 99.6%, the highest in all serious disease research programs.<sup>124</sup> A growing strategy in integrating therapeutics and personalized diagnostics has recently emerged as a promising route. Based on nanomedicine, small molecules – necessary to overcome prerequisite to cross the brain blood barrier – have been developed to label and simultaneously inhibit oligomerization of A $\beta$  peptides.<sup>125</sup> The term theranostic has thus

been coined to characterize these new inhibitor-biomarkers, many based on scaffolds of fluorescent probes such as ThT, to detect fibril formation *in vivo* and alter their accumulation.<sup>126</sup> These new strategies have been made possible by improved understanding of the assembly mechanism of A $\beta$  at the molecular level, which will continue to guide rational drug design against AD.

### 3. IAPP and type 2 diabetes

#### 3.1 Function of IAPP

Human islet amyloid polypeptide (IAPP, a.k.a amylin) is a 37-residue peptide hormone co-secreted with insulin from pancreatic  $\beta$ -cell islets. The IAPP physiology has been recently reviewed by Westermark et al.<sup>127</sup> Briefly, the peptide is synthesized from a 67-residue precursor peptide, proIAPP, by proteolysis and posttranslational modifications, such as the C-terminal amidation and a disulfide bond formation between residues 2 and 7 (Fig. 7a).<sup>128, 129</sup> Both IAPP and insulin are regulated by similar factors with a common regulatory promoter motif.<sup>130</sup> Before secreting to the circulation, IAPP is stored together with insulin inside the  $\beta$ -cell granules at high concentrations. IAPP functions as a synergistic partner of insulin to control the blood glucose level by slowing down gastric emptying, inhibiting digestive secretion, and promoting satiety.<sup>131, 132</sup> IAPP is also known to play a role in bone metabolism along with calcitonin and calcitonin gene-related peptides.<sup>133</sup>

A hallmark of type 2 diabetes (T2D) is the formation of IAPP-enriched amyloid plaques found in the pancreas of patients. Insulin resistance in T2D leads to increased production of insulin and also IAPP by  $\beta$ -cells because of their shared synthesis and secretion pathways. Since IAPP is one of the most amyloidogenic peptides known, over-production of IAPP in  $\beta$ -cells promotes the accumulation of toxic aggregates. Other studies also suggested that insufficient process of proIAPP and accumulation of intermediately processed peptides might promote the formation of amyloid fibrils, but the detailed molecular mechanisms remain unclear. The disease progression is marked by  $\beta$ -cell death and loss of  $\beta$ -cell functions, resulting in insulin deficiency and diabetic dependence on external insulin sources.

#### 3.2 Atomic structures of IAPP and IAPP amyloid fibrils

Structural characterization of IAPP monomers is extremely challenging due to the high aggregation propensity of the peptide. By reducing IAPP aggregation with detergent micelles, solution NMR studies have been used to study the structure of IAPP monomers.<sup>137–139</sup> It has been shown that SDS micelles stabilize IAPP in a highly helical form (Fig. 7b–d). At low pH, the peptide assumes an extended alpha-helix. At neutral pH, the peptide has been found to form a kinked helix around residue H18. Such structural difference is likely due to the electrostatic interaction of the protonated His18 at low pH with the anionic SDS. Combining low pH, low temperature, and low peptide concentrations to hinder IAPP aggregation in solution, an NMR study has recently revealed that the N-terminus of IAPP remains alpha-helical while the C-terminus is unstructured, which are consistent with molecular dynamics (MD) simulations of isolated IAPP monomers.<sup>140</sup>

The fibril aggregates of IAPPs share the same characteristic cross-beta structures of known fibrils.<sup>141</sup> Although the atomic structure of full-length IAPP amyloid fibrils is not available, several model structures have been proposed based on various experimental methods. Using constraints derived from solid-state NMR, Tycko et al. proposed a U-shaped fibrils model where residues 8–17 and 26–37 form two beta-sheets (Fig. 7e).<sup>134</sup> Based on X-ray microcrystallography structures of two short peptides, Eisenberg et al. reconstructed a similar fibril model with main differences in the side-chain packing (Fig. 7f).<sup>135</sup> Recently, EPR studies of disulfide-reduced IAPP led to a different fibril model (Fig. 7g), where the peptide still adopts a U-shape with two strands separated by a longer distance.<sup>136</sup> The two strands in a single peptide have to be staggered with respect to each other to have the appropriated inter  $\beta$ -sheet packing and distances.

### 3.3 Mesoscopic structure of IAPP amyloids

The morphology of IAPP amyloid fibril has been studied by both TEM and AFM.<sup>142, 143</sup> IAPP fibrils at the mesoscopic scale displayed significant structural polymorphism, including ribbon-like, sheet-like and helical fibril morphologies (Fig. 8). The ribbons and sheets were formed by lateral association of 5-nm wide protofibrils (Fig. 8a). Most of the fibrils were found in left-handed coil morphology with cross-over periodicities of either ~25 nm or ~50 nm (Fig. 8b). Based on these observations, Goldsbury et al. proposed that the building block of IAPP fibrils is the 5 nm protofibril which can either self-assemble laterally into ribbon-like or sheet-like arrays or coiled fibrils.<sup>143</sup> The atomic models of IAPP fibrils are consistent with these TEM and AFM observations.

### 3.4 IAPP toxicity and type 2 diabetes

Mounting studies suggest that IAPP aggregation and the related toxicity are associated with T2D. IAPP variants from diabetes-prone primates and cats form amyloid aggregates readily *in vitro*, while those from diabetes-free rodents and pigs feature significantly lower aggregation propensities.<sup>144</sup> A naturally-occurring polymorphic S20G mutation renders IAPP more aggregation prone,<sup>145</sup> and an Asian subpopulation carrying this mutation is subjected to early onset of T2D.<sup>146</sup> IAPP aggregated rapidly upon transplanting human islets into nude mice, and the aggregation process occurred before the recurrence of hyperglycemia and was correlated with  $\beta$ -cell death.<sup>147, 148</sup> Transgenic mice expressing human IAPP variant started to develop diabetes.<sup>149</sup> Moreover, as with other amyloid proteins,<sup>150, 151</sup> IAPP amyloid aggregates are toxic to pancreatic islet cells.<sup>152</sup> Therefore, amyloid aggregation of IAPP is related to  $\beta$ -cell death in T2D.<sup>153</sup>

**3.4.1 Oligomers vs amyloids**—Amyloid aggregation is a nucleation process, featuring a characteristic all-or-none sigmoidal kinetics. The final mature amyloid fibrils have been found relatively inert and have no significant cell toxicity. In contrast, freshly dissolved IAPP have been found to be highly toxic to islet cells and also cause membrane instability *in vitro*,<sup>154</sup> where the small and soluble aggregation intermediates of IAPP are expected to accumulate before the rapid fibril growth. IAPP oligomers have also been found to disrupt cell coupling, induce apoptosis, and impair insulin secretion in isolated human islets.<sup>155</sup> Additional evidence include transgenic mice studies,<sup>149, 156</sup> where amyloid deposits were not always observed under optical microscopy in animals starting to show diabetic

symptoms, and there was a lack of autocorrelation between beta cell loss and amyloid deposits in these models.<sup>157</sup> In addition, inhibition of the formation of insoluble IAPP aggregates but not oligomers by either small molecules<sup>158</sup> or proteins<sup>159</sup> did not reduce the cytotoxicity. Hence, these results among many others led to the toxic oligomer hypothesis in T2D.<sup>160, 161</sup>

As the aggregation intermediate species, IAPP oligomers are not well-defined and are extremely challenging to characterize due to their transient and heterogeneous nature. Many *in vitro* studies support the accumulation of helical intermediates populated along the aggregation pathway.<sup>162–164</sup> It has been suggested that the N-terminal helices of soluble IAPPs (Fig. 7d) are amphiphilic and hydrophobic interactions drive the helix association, which in turn increases the local concentration of the C-terminus containing the amyloidogenic sequence 20–29.<sup>165</sup> Both discrete molecular simulations (DMD) of IAPP dimers<sup>140</sup> and X-ray crystallography study of IAPP fused to a maltose-binding protein<sup>164</sup> supported this scenario. On the other hand, ion mobility mass spectroscopy (IM-MS) combined with MD simulations pointed to a different model of early intermediate states with beta-hairpin dimers.<sup>166</sup> The difference is possibly due to the enhanced sampling method - replica exchange<sup>167</sup> - used in the MD study, which reduced the free energy barrier of the helix unfolding in the N-terminus. Further experimental and computational studies are necessary to fully understand the structure and dynamics of IAPP oligomers in order to identify the toxic species and the molecular mechanism of IAPP toxicity.

**3.4.2 The endogenous inhibition of IAPP aggregation**—IAPP is highly aggregation prone and readily forms amyloid fibrils *in vitro* at  $\mu\text{M}$  concentrations within hours.<sup>168</sup> However, before its secretion to the bloodstream IAPP is stored inside  $\beta$ -cell granules at mM concentrations for hours without apparent formation of toxic aggregates in healthy individuals.<sup>169</sup> Therefore, the physiological environment inside  $\beta$ -cell granules natively inhibits the formation of toxic IAPP aggregates while disruption to the native inhibition environment may lead to amyloid aggregation of IAPP, causing  $\beta$ -cell death.

Islet  $\beta$ -cell granules have a distinct cellular environment.<sup>170</sup> First, the pH value inside the granules is 5.5, which is below the physiological pH of 7.4. Second,  $\beta$ -cell granules have one of the highest concentrations of  $\text{Zn}^{2+}$  ions in the entire human body. The high concentration of zinc in  $\beta$ -cell granules, maintained by a  $\beta$ -cell-specific zinc transporter — ZnT8,<sup>171</sup> is believed to be important for the efficient storage of insulin in  $\beta$ -cell granules: zinc coordinates the formation of insulin hexamers, which form insulin crystals as the dense core of  $\beta$ -cell granules.<sup>172</sup> Third, beside IAPP peptides  $\beta$ -cell granules also have other molecules in large quantities, including insulin and proinsulin C-peptide. Insulin is co-secreted with IAPP by  $\beta$ -cells at a ratio of  $\sim 100:1$  in healthy individuals, and such a high insulin-to-IAPP ratio is reduced to  $\sim 20:1$  in T2D patients.<sup>173</sup> The C-peptide is a part of the proinsulin sequence connecting A- and B-chains of insulin. Protease-processing of proinsulin results into mature insulin and C-peptide with an equal molar concentration inside  $\beta$ -cell granules.

**Low pH:** Inhibition of IAPP aggregation at low pH has been observed *in vitro*. At low pH, an increase in the lag time and a decrease in the growth rate of IAPP fibrillization was

observed.<sup>174, 175</sup> The electrostatic repulsion between IAPPs with protonated histidine18 (His18) is responsible for inhibiting the self-association of IAPP at low pH,<sup>176</sup> supported by DMD simulations of IAPP dimerization with and without protonation of His18.<sup>177</sup> However, since the pH value inside  $\beta$ -cell granules is close to the isoelectric point of His18<sup>174, 178</sup> and a significant portion of IAPP is still unprotonated, interactions of IAPP with other granule components are necessary for natively inhibiting the peptide amyloid aggregation at high concentrations.

**Insulin:** *In vitro* experiments have revealed that insulin is a potent IAPP aggregation inhibitor, which can significantly slow down aggregation at sub-stoichiometry concentrations.<sup>180</sup> Several studies, including peptide mapping,<sup>181</sup> IMS-MS combined with MD simulations,<sup>182</sup> and DMD studies<sup>140</sup> suggested that the B-chain of insulin can bind IAPP. Computational studies with atomistic DMD simulations showed that both insulin monomers and dimers (but not the zinc-bound hexamer as the IAPP-binding interface is buried) could bind IAPP monomer and inhibit IAPP self-association by competing with the amyloidogenic regions important for aggregation, subsequently preventing amyloid aggregation (Fig. 9a,b). The preferred binding of insulin with the amyloidogenic region in the beta-strand conformation (Fig. 9a) suggests that insulin can also cap the fibril growth, consistently with the observed sub-stoichiometric inhibition of IAPP aggregation by insulin. Comparing to high zinc concentrations where insulin is insoluble in the crystal form,<sup>183</sup> zinc-deficiency due to loss-of-function mutations of ZnT8 shifts the insulin oligomer/crystallization equilibrium toward soluble monomers and dimers, which can efficiently inhibit IAPP aggregation and reduce T2D risk in the subpopulation carrying these mutations.<sup>184</sup> However, since IAPP is found almost exclusively in the soluble halo fraction of  $\beta$ -cell granules while insulin is mostly insoluble in the core, the balance of other granule components such as  $\text{Zn}^{2+}$  and/or C-peptide co-localized with IAPP appears crucial for maintaining the native state of IAPP.

**Zinc:** In an early study by Steiner and co-workers where  $\text{ZnCl}_2$  was added to  $\sim 250 \mu\text{M}$  IAPP solution, aggregation promotion was observed.<sup>185</sup> This promotion effect leveled off till  $\sim 1 \text{ mM}$  zinc ion was added, but no data at higher salt concentrations was reported. In later experimental studies, IAPP aggregation inhibition was observed at low zinc concentrations ( $5$  and  $10 \mu\text{M}$ , but relatively high zinc/IAPP stoichiometry), followed by a partial recovery of aggregation at very high stoichiometry ( $\sim 50$ – $100$ ).<sup>186, 187</sup> A “two-site binding” model, where a high affinity binding with His18 stabilized non-aggregating oligomers but an unknown weaker secondary binding promoted amyloid fibril formation, was proposed.<sup>187</sup> However, this model cannot account for aggregation-promotion at low ion/protein stoichiometry<sup>185</sup> (e.g., in the case of  $10 \mu\text{M}$  of IAPP there was a single data point with increased aggregation at  $\sim 25 \mu\text{M}$  of zinc.<sup>186</sup>). Combining DMD simulations with experimental characterizations<sup>179</sup>, Govindan et al. developed an alternative model that was consistent with the experimentally-observed concentration-dependent effect of zinc on IAPP aggregation. At low zinc/IAPP stoichiometry, the IAPP oligomers cross-linked by zinc were aggregation-prone due to high local peptide concentrations (Fig. 9c). As ion/protein stoichiometry increased, each IAPP tended to bind only one zinc ion at His18. The electrostatic repulsion between the bound zinc ions ( $+2e$ ) inhibited IAPP aggregation,

similarly to the low pH condition where IAPP aggregation was inhibited by protonated His18 (+1e).<sup>176</sup> With zinc concentration kept increasing, the screening effect due to high salt concentrations reduced electrostatic repulsion, and allowed for the aggregation to recover (Fig. 9d).<sup>186, 187</sup>

**C-peptide:** Without zinc binding, C-peptide is disordered in water and weakly helical in trifluoroethanol (TFE) solution.<sup>188</sup> The peptide contains five acidic amino acids. Alanine scan coupled with MS experiments suggest that all these acidic amino acids bind zinc ions and the binding is 1:1 in stoichiometry.<sup>189</sup> It has been found that zinc-binding may induce structural changes.<sup>190</sup> It was hypothesized that multiple negatively charged acidic amino acids in C-peptide allow the binding with multiple IAPP peptides, locally increase IAPP concentration and subsequently promote IAPP aggregation. Upon binding zinc, C-peptide adopts specific secondary and tertiary structures with reduced net charges, which might bind and stabilize IAPP peptides in the aggregation incompetent state. In addition, other granule molecules including proIAPP<sup>191</sup> and proInsulin may also contribute to the native inhibition of IAPP aggregation and cytotoxicity in beta-cells and are subject to future investigations.

**3.4.3 IAPP-membrane interactions**—It has been proposed that IAPP exerts cytotoxicity by membrane disruption.<sup>154, 192, 193</sup> The positively charged IAPP can bind anionic cell membranes and lipid micelles, and the peptide conformational and aggregation propensity change upon binding also depending on the membrane curvature.<sup>192</sup> Binding of IAPP with small micelles was found to stabilize the peptide in helical conformation (Fig. 7), while absorption of IAPP on flat membrane accelerated the peptide aggregation.<sup>194</sup> Using a lipophilic Laurdan dye for examining MIN6 cell membranes upon exposure to freshly dissolved IAPP as well as mature amyloid fibrils, Pilkington et al. found that all species, especially fresh IAPP, enhanced membrane fluidity and caused losses in cell viability.<sup>195</sup> The cell generation of ROS, however, was the most pronounced with mature amyloid fibrils. This study suggested a correlation of cytotoxicity with changes in membrane fluidity rather than ROS production.

The exact mechanism by which IAPP oligomers disrupt the cell membrane is under active investigation. Pore formation by amyloid peptides has been suggested to be important for membrane disruption.<sup>196–198</sup> The amyloid pore model is strongly supported by single channel recordings of IAPP on planar membranes.<sup>196, 199, 200</sup> A detergent-like mechanism has also been advocated, where the mosaic-like opening and closing of transient defects within the membrane (also see Fig. 15d in section 4 for  $\alpha$ S) was supported by AFM studies showing large-scale defects in the lipid bilayer upon prolonged exposure to IAPP.<sup>201</sup> However, the strong correlation between fibril formation and membrane disruption by this mechanism<sup>202</sup> is inconsistent with the toxic oligomer hypothesis. Recently, biophysical measurements in conjunction with cytotoxicity studies showed that nonamyloidogenic rat IAPP is as effective as IAPP at disrupting standard anionic model membranes under conditions where rat IAPP did not induce cellular toxicity, suggesting that there is no direct relationship between disruption of model membranes and induction of cellular toxicity.<sup>203</sup> Therefore, the connection between IAPP cytotoxicity and membrane disruption remains inconclusive.

### 3.5 Mitigation strategies and theranostics

As with other amyloid diseases,<sup>204–206</sup> inhibition of IAPP aggregation is an attractive therapeutic strategy to prevent  $\beta$ -cell death<sup>207</sup> and halt the progression of diabetic conditions in T2D. Various approaches have been explored to reduce aggregation-induced IAPP cytotoxicity, through the use of peptides, peptide-mimetics,<sup>208–211</sup> small molecules<sup>212–223</sup>, and nanoparticles (NPs)<sup>224–226</sup>. Non-amyloidogenic sequence variants of IAPP including rat IAPP<sup>227</sup> have been found to inhibit the fibril formation of human IAPP,<sup>208, 209</sup> and the inhibition efficacies can be improved by synthesizing peptide mimetics with conformational restraints.<sup>210, 211</sup> Targeting the early helical intermediate states of IAPP aggregation<sup>162–164</sup>, small molecule peptidomimetics<sup>212, 213</sup> have been designed to mimic helices that complementarily bind to the N-terminal helix of IAPP. Another attractive set of amyloid aggregation inhibitors are small-molecule polyphenols<sup>221</sup> such as epigallocatechin gallate (EGCG),<sup>228</sup> curcumin,<sup>219, 220</sup> and resveratrol,<sup>229</sup> which inhibit aggregation and reduce the related cytotoxicity of IAPP<sup>230</sup> as well as other proteins and peptides such as A $\beta$ .<sup>231</sup> These polyphenols have the advantage of being naturally occurring, and are non-toxic at moderate concentrations. Despite well-known therapeutic benefits of small molecules,<sup>232</sup> however, pharmacological applications of these polyphenols are limited due to some common issues, such as their poor water solubility.<sup>233</sup>

Several studies have examined the anti-amyloid mechanisms of small molecules and NPs. For example, IMS-MS experiments showed that EGCG exerted an inhibitory effect on IAPP aggregation through direct binding of EGCG to the peptide<sup>215</sup> and alternating the aggregation pathways.<sup>228</sup> Using simulations of the amyloidogenic segment of IAPP, resveratrol was found to bind and prevent the lateral growth of the fibril-like  $\beta$ -sheets.<sup>235</sup> In another work, resveratrol was found to bind weakly to IAPP and reduce inter-peptide contacts.<sup>236</sup> A recent computational study showed that resveratrol altered the structure of an IAPP pentamer,<sup>237</sup> which was modelled by the amyloid fibril structure derived from solid-state NMR.<sup>134</sup> By modelling the effects of polyphenols like resveratrol and curcumin on the initial self-association and aggregation of IAPP in DMD simulation,<sup>234</sup> Nedumpully-Govindan et al. showed that these polyphenols inhibited IAPP aggregation by promoting “off-pathway” oligomers with the hydrophobic polyphenols forming the core (Fig. 10a). The peptides were stabilized in the aggregation-incompetent helix-rich state by burying their hydrophobic residues inside the core and exposing the hydrophilic residues. Graphene oxide nanosheets displayed strong inhibition effects on IAPP aggregation and associated cytotoxicity because strong binding affinity rendered the peptides to bind with the nanosheets rather than between themselves.<sup>225</sup> OH-terminated polyamidoamine (PAMAM-OH) dendrimers inhibited IAPP aggregation and cytotoxicity, where the polymeric NPs encapsulated and stabilized monomeric IAPP in their hydrophobic interior (Fig. 10b).<sup>224</sup> In general, these inhibitors all reduced the population of the oligomeric species, thereby reducing IAPP toxicity.



## 4. Alpha-synuclein and Parkinson's disease

### 4.1 Function of alpha-synuclein

Alpha synuclein ( $\alpha$ S) is a 140-residue small protein highly concentrated in presynaptic terminals,<sup>238</sup> making up as much as 1% of all proteins in the cytosol of brain cells. Small traces of  $\alpha$ S are also found in the heart, gut,<sup>239</sup> muscles and other tissues, reminiscent of the confounding bodily distributions of A $\beta$  and IAPP beyond their purported origins. In the intra-neuronal space,  $\alpha$ S assumes an equilibrium between an unfolded monomeric conformation and a membrane-bound state that is rich in alpha helices.<sup>240</sup> The precise physiological role of  $\alpha$ S is unclear, but is relevant to the modulation of neurotransmitter dopamine release, ER/Golgi trafficking, and synaptic vesicles.<sup>241</sup> The membrane-bound  $\alpha$ S influences lipid packing and induces vesicle clustering through physical and physicochemical interactions, while  $\alpha$ S in the multimeric form has been shown to promote SNARE complex assembly during synaptic exocytosis.<sup>240</sup>

Aggregated  $\alpha$ S mediates dopaminergic neurotoxicity *in vivo*.<sup>244</sup> However, the precise mechanisms by which  $\alpha$ S lends toxicity to host cells remain unclear. Pathologically,  $\alpha$ S is a major component of Lewy bodies and neurites, the intracellular protein aggregates first identified by Spillantini et al. in 1997 (Fig. 11)<sup>242</sup> and hallmarks of Parkinson's disease (PD), Parkinson's disease dementia (PDD) and dementia with Lewy bodies (DLB). Compared with the ambiguous pathology of  $\alpha$ S, the neuritic pathology of  $\beta$  and  $\gamma$  synuclein homologs does not appear widespread, and both neuroprotective and neurotoxic potentials of  $\beta$  synuclein have been reported.<sup>245</sup>

### 4.2 Atomic structures of alpha-synuclein and alpha-synuclein amyloid fibrils

The sequence of  $\alpha$ S is encoded by the *SNCA* gene and can be divided into three distinct domains: a) the amphipathic N-terminal domain (1–60), which contains consensus KTKEGV repeats and has alpha-helical propensity, b) the central domain (61–95) or the *non-amyloid-beta component* (NAC) that is highly hydrophobic and amyloidogenic, and c) the acidic C-terminal domain (96–140) which contains negatively charged and proline residues to afford protein flexibility but no apparent structural propensity.<sup>246</sup> High resolution ion-mobility mass spectroscopy has revealed that HPLC-purified  $\alpha$ S is autoproteolytic, giving rise to a number of small molecular weight fragments upon incubation. In particular, the fragment of residues 72–140 contains majority of the NAC region and aggregates faster than full-length  $\alpha$ S.<sup>247</sup> These autoproteolytic products may serve as intermediates or cofactors in the aggregation of  $\alpha$ S *in vivo*.

The atomic structures of fragmental and full-length  $\alpha$ S in the fibrillar form have been elucidated over the past decade (Fig. 12). Using quenched HD exchange Vilar et al. identified five  $\beta$ -strands within the fibril core comprising residues 35–96 and with solid-state NMR spectroscopy the presence of  $\beta$ -sheet secondary structure within the fibril core of residues 30–110.<sup>241</sup> This study has further detailed the mesoscopic features of  $\alpha$ S fibrils, as we will visit in the next sub-section.

Based on micro-electron diffraction Rodriguez et al. revealed small crystal structures of the toxic NAC core (68–78, or NACore) and the preNAC segment (47–56) of  $\alpha$ S, at spatial

resolution of 1.4 Å (Fig. 13a).<sup>248</sup> The NACore strands stacked in-register into  $\beta$ -sheets. The sheets were paired, forming steric-zipper protofilaments as observed for other types of amyloidogenic proteins. Notably, each pair of the sheets contained two water molecules, and each was associated with a threonine side chain within the interface. X-ray fiber diffraction patterns further revealed a similarity of the NACore to full-length  $\alpha$ S fibrils.<sup>248</sup>

In a more recent study, Tuttle et al. established the atomic structure of full-length  $\alpha$ S fibrils based on 68 spectra, using 2D and 3D ssNMR.<sup>249</sup> The fibrils were collected from cell culture and shown to adopt a  $\beta$ -serpentine arrangement (Fig. 13b–e). The fold exhibited hydrogen bonds in register along the fibril axis, orthogonal to the hydrogen bond geometry in a standard Greek-key motif unseen for other fibrils (Fig. 13d).<sup>249</sup> The innermost  $\beta$ -sheet contained amyloidogenic residues 71–82, while the sidechains in the core were tightly packed (Fig. 13e). Compact residues facilitated a close backbone-backbone interaction: A69–G93 bridged the distal loops of the Greek key, and G47–A78 rendered a stable intermolecular salt bridge between E46 and K80. Hydrophobic sidechain packing among I88, A91 and F94 established the innermost portion of the Greek key. Residues 55–62 were disordered, consistent with that reported by Comellas *et al.*<sup>250</sup> Collectively, the steric zippers, glutamine ladder and intermolecular salt bridge contributed to the structural complexity and stability of the fibril. However, it remains uncertain whether such atomic structure reflects that of  $\alpha$ S fibrils extracted directly from PD patients.

### 4.3 Mesoscopic structure of alpha-synuclein amyloids

The morphology of  $\alpha$ S fibrils has been examined with AFM<sup>251–253</sup> and cryoelectron microscopy.<sup>241</sup> A hierarchical assembly model (HAM) was proposed by Inonescu-Zanetti *et al.*<sup>254</sup> to describe the architecture of immunoglobulin light-chain protein SMA fibrils assembled from smaller subspecies and has shown general applicability to the nanoscale assemblies of A $\beta$ ,  $\alpha$ S and IAPP as well as SH3 domain, lysozyme, SMA,  $\beta_2$ -microglobulin and beta-lactoglobulin.<sup>142, 251, 252, 255–260</sup> Alternatively, a new packing model was proposed by Sweers *et al.*,<sup>261</sup> in attempt to reconcile the morphological and mechanical data observed for two distinct fibril species of E46K, a mutant of  $\alpha$ S. Nonetheless, according to the HAM, protofilaments are established by the nucleated polymerization kinetic model, in which the protofilaments elongate by the addition of monomeric, partially folded intermediates to their growing ends. The protofilaments then interact with each other to form protofibrils, each consisting of twisted 2–3 protofilaments, and two protofibrils entwine to form mature fibrils and, eventually, plaques. The driving force for such stepwise assembly is both electrostatic and hydrophobic.<sup>254</sup>

The HAM model predicts the occurrence of periodicity for protofilaments and fibrils, which assume twisted morphologies. Such periodicity is driven by a balance between mechanical forces dominated by the protofilament elasticity and electrostatic forces due to the distribution of hydrophobic regions and charge along the protofilament backbone,<sup>253</sup> as well as by the inherent chirality of constituting amino acids and  $\beta$ -sheets/helices of the fibrils. The average heights of  $\alpha$ S protofilaments and fibrils were 3.8 nm and 6.5 nm, respectively, while the periodicity of  $\alpha$ S fibrils ranged from 100–150 nm as determined by AFM (Fig. 14a).<sup>253</sup> These parameters are consistent with immunoelectron microscopy of filaments

extracted from the brains of patients with DLB and multiple system atrophy,<sup>262</sup> and agree with high-resolution cryoelectron microscopy where twisted protofilament of  $\sim 2 \times 3.5$  nm in boundaries and  $120 \pm 10$  nm in periodicity were observed leading to the proposal of a folded  $\alpha$ S fibril model (Fig. 14b).<sup>241</sup> The cross-section of individual  $\alpha$ S monomers in the fold was trapezoid instead of circular, resulting in a two-fold increase in moment of inertia (Sweers 2012).<sup>263</sup> Though not substantiated, such non-circular packing of monomers could also hold true for other  $\beta$ -sheet folded proteins.<sup>261, 263</sup> In addition, curly  $\alpha$ S fibrils prepared by filtration-like steps during aggregation possessed a persistence length of 170 nm, while straight  $\alpha$ S fibrils from unperturbed aggregation displayed persistence lengths of up to 140  $\mu$ m.<sup>264</sup>

#### 4.4 Alpha-synuclein toxicity and Parkinson's

**4.4.1 Oligomers vs amyloids**—Natively unfolded  $\alpha$ S undergoes a transition to partially folded intermediates prior to fibril formation.<sup>265</sup> Such partially folded conformations are favored by mutations<sup>266</sup> or changes in pH, ionic strength and temperature and are thought to be critical intermediates in the transition to amyloid fibrils.<sup>253</sup> Clearly, such dynamic transition has an important bearing on  $\alpha$ S toxicity, as evidenced by a body of literature focused on the complex roles of  $\alpha$ S oligomers and amyloids.

The aggregation of  $\alpha$ S follows a nucleation polymerization pathway involving prefibrillar species of remarkable conformational plasticity,<sup>267</sup> both transient and stable. Specifically, it is postulated that  $\alpha$ S aggregation takes place in the cytoplasm or in association with the cellular membrane. In the cytosol, soluble monomers interact to form unstable dimers, which develop into oligomers and, subsequently, fibrils.<sup>268</sup> The current understanding concerning  $\alpha$ S toxicity follows the narrative of the “toxic oligomer hypothesis”,<sup>251</sup> in that the oligomeric species are more toxic than the fibrillar form,<sup>251, 269–272</sup> as similarly proposed for  $A\beta$ <sup>273–279</sup> and IAPP.<sup>280</sup> However, due to the different structural characteristics and aggregation rates, different cellular environments, as well as prion-like cell to cell spreading and crosstalk of proteins of different origins and pathologies, this generalization remains putative.<sup>281, 282</sup>

In an early *in vitro* study, Conway et al. compared the rates of disappearance of monomeric  $\alpha$ S and appearance of fibrillar  $\alpha$ S for wild-type and two mutant proteins A53T and A30P.<sup>251</sup> The differences between the trends suggested the occurrence of nonfibrillar  $\alpha$ S oligomers. Using sedimentation and gel filtration chromatography, the researchers identified spheres (range of heights: 2–6 nm), chains of spheres (protofibrils), and rings/annulars (heights:  $\sim 4$  nm) from fibrils ( $\sim 8$  nm in diameter) by AFM. For a comprehensive account of  $\alpha$ S oligomers and their *in vitro* preparation protocols, readers may refer to a recent review by van Diggelen et al.<sup>283</sup>

Using attenuated total reflection-Fourier-transform infrared (ATR-FTIR) spectroscopy Celej et al. revealed that isolated  $\alpha$ S oligomers adopted an antiparallel  $\beta$ -sheet structure, whereas fibrils assumed a parallel arrangement.<sup>284</sup> Notably, antiparallel  $\beta$ -sheet structures have also been reported for the oligomeric structures of  $A\beta$ ,  $\beta_2$ -microglobulin and human prion peptide PrP82–146.<sup>284</sup> Such contrasting features in secondary structure between the oligomers and fibrils entail differences in conformational change, affinity and mode of

interaction when binding with the cell membrane, further compounded by the differences in aspect ratio and surface hydrophobicity between the two species. The toxicities of  $\alpha$ S oligomers and amyloid protein oligomers in general have been postulated as an inherent property.<sup>285</sup> Unlike amyloid fibrils, the oligomers share similar structural properties<sup>273, 286</sup> and possess higher portions of random coils and helical structures. Consequently, the exposed hydrophobic surfaces of the oligomers could mediate interactions with intracellular proteins to trigger aberrant cellular pathways.

Celej et al. found that purified  $\alpha$ S oligomers spheroidal and polydisperse (10–60 nm), while  $\alpha$ S fibrils were unbranched of 6–10 nm in diameter and micrometers long when examined under electron microscopy.<sup>287</sup> These isolated oligomers were on-pathway intermediates sharing the same structural motif with other prefibrillar oligomers and possessing no canonical cross- $\beta$  fibril structure.<sup>284</sup> Curiously, the  $\alpha$ S oligomers were recognized by A11 antibody, which also targeted the oligomeric but not monomeric or fibrillar forms of A $\beta$ , prions, and IAPP.<sup>273, 288</sup>

While it remains debatable whether  $\alpha$ S oligomers are intermediates in the process of amyloid formation, or precursors to fibrils, or byproducts of fibril elongation, or associated with a pathway of aggregation different from the standard amyloid fibrillization,<sup>269</sup> there is little ambiguity that  $\alpha$ S oligomers are toxic, as validated by *in vitro* and animal models.<sup>272, 273, 289, 290</sup>

**4.4.2 Alpha-synuclein-membrane interactions**—Towards understanding the origin of amyloid protein toxicity, much research over the past two decades has been focused on the interactions of the proteins as well as their aggregation products with cell membranes, model lipid vesicles, or lipid rafts. This focus is especially justified for  $\alpha$ S considering its strong functional association with synaptic vesicles and its cell-to-cell spreading.<sup>291</sup> From a biophysical standpoint such interactions may be understood as a manifestation of the structural attributes of  $\alpha$ S (sequence, charge and hydrophobicity), as well as the changing properties of  $\alpha$ S from soluble and disordered monomers to soluble and less random oligomers, and to waxy and highly ordered fibrils and plaques.

Research concerning protein-membrane interaction should take into consideration of two convoluting aspects: protein aggregation modulated by a model lipid bilayer or cell membrane, and membrane integrity perturbed by protein aggregation. Numerous studies have confirmed that lipid membranes can speed up the process of protein fibrillization due to the amphiphilicity of both interactants.<sup>292, 293</sup> Specifically, the N-terminal region of  $\alpha$ S, containing 7 amphiphilic imperfect repeats each of 11-residues, can initiate electrostatic interaction with anionic lipid head groups. The NAC region of the protein can establish hydrophobic interaction with lipid fatty acyl tails to promote membrane partitioning.<sup>294</sup> Upon membrane exposure, the protein concentration at the membrane surface is abruptly increased due to the 3D to 2D transition. Consequently, protein conformational entropy is reduced to favor aggregation.<sup>294, 295</sup> Specifically, the rate of  $\alpha$ S primary nucleation was enhanced by three orders of magnitude when exposed to small unilamellar vesicles (SUVs, 20–100 nm in diameter) of 1,2-dimyristoyl-*sn*-glycerol-3-phospho-L-serine (DMPS).<sup>296</sup>

Upon adsorption onto lipid membranes, monomeric amyloid proteins adopt an  $\alpha$  helical state, followed by a conversion to  $\beta$ -sheet rich oligomers and amyloid fibrils modulated by the curvature and charge of the membranes, presence of metal ions, peptide to lipid ratio, and ganglioside clusters, cholesterol and lipid rafts.<sup>299</sup>  $\alpha$ S assumes a fully extended  $\alpha$  helical state coming into contact with larger vesicles, likely representative of the protein conformation *in vivo*.<sup>300, 301</sup> In contrast, smaller vesicles with greater curvatures and smaller surface areas are associated with proteins in bent  $\alpha$  helices or antiparallel helix-turn-helix conformation to maximize protein-membrane binding.<sup>293</sup>

A high peptide/lipid ratio favors protein crowding on the membrane surface to induce nucleation.<sup>302</sup> Binding of  $\alpha$ S (isoelectric point of 4.74)<sup>303</sup> with membranes is elevated with increased acidic phospholipid content.<sup>304–306</sup>  $\alpha$ S oligomers also show propensity for the liquid disordered phase of anionic vesicles.<sup>307</sup> The exact mechanism of  $\alpha$ S association with lipid rafts is unclear, but is linked to the high lipid packing density of anionic head groups in the rafts. Such specific binding between  $\alpha$ S and lipid rafts may be essential to both the normal cellular function of  $\alpha$ S and its role in PD pathology.<sup>299</sup>

Elevated levels of metal ions have been found in the *substantia nigra* of PD patients.<sup>308</sup> Addition of metal cations of  $\text{Cu}^{2+}$ ,  $\text{Fe}^{3+}$  or  $\text{Co}^{3+}$  induced secondary structure in  $\alpha$ S and accelerated protein aggregation *in vitro*,<sup>265</sup> through metal ion-mediated amyloid protein-membrane interaction. Although  $\text{Ca}^{2+}$  (of  $\sim 300 \mu\text{M}$ ) in the ER serves to facilitate protein folding, addition of  $\text{Ca}^{2+}$  and other heavy metal ions to monomeric  $\alpha$ S rapidly produced annular oligomers,<sup>309</sup> while divalent metal ions also enabled the clustering of  $\alpha$ S on the surfaces of anionic 1-palmitoyl-2-oleoyl-*sn*-glycero-3-phospho(1'-*rac*-glycerol)/phosphatidylcholine bilayers.<sup>306</sup> It is possible that metal cations enabled the interaction of the likely charged C-terminus of  $\alpha$ S and membranes through charge neutralization. Such strong metal-hosting capacity of amyloid proteins has been utilized in entirely different contexts from amyloidogenesis, such as purification of wastewater and *in vitro* iron fortification using functional  $\beta$ -lactoglobulin amyloids.<sup>310–312</sup>

The adsorption of  $\alpha$ S has been shown to compromise membrane permeability.<sup>282</sup> One mechanism proposed for such perturbation is pore formation by the protein oligomers (Fig. 15a–c).<sup>271, 284, 293, 297</sup> In combination with biochemical and ultrastructural analysis, Tsigelny et al. revealed through MD simulations and docking that  $\alpha$ S monomers, upon adsorption onto lipid membranes through their N-termini, assembled into homodimers of both propagating (head to head) and non-propagating (head to tail) conformations. The propagating form docked on the membrane surface to recruit additional  $\alpha$ S molecules, rendering pentamers and hexamers to form ring-like structures partitioning in the membrane.<sup>313</sup> Consistently, addition of stable  $\alpha$ S oligomers has been shown to induce ion-channel activity (Fig. 15c),<sup>297</sup> while  $\text{Ca}^{2+}$  and dopamine exhibited much higher leakage rates than polymers of cytochrome *c* and fluorescein isothiocyanate-dextran from anionic vesicles in the presence of oligomeric A30P and A53T, two major  $\alpha$ S mutations.<sup>314</sup> Under conditions in which vesicular membranes were less stable due to the lack of counter-ion  $\text{Ca}^{2+}$ ,  $\alpha$ S permeation was less size selective and monomeric  $\alpha$ S permeated via a detergent-like mechanism.<sup>293</sup>

Another mechanism proposed for  $\alpha$ S-membrane interaction is illustrated in Fig. 15d.<sup>298</sup> Here the presence of a supported lipid bilayer facilitates the conversion of  $\alpha$ S from randomly structured monomers to alpha helices (top panel), which further aggregate into oligomers and fibrils while stripping lipids off the bilayer (middle and lower panels). Membrane thinning and depolarization, changing fluidity, lipid flip-flop, calcium leakage, and disruption of ionic homeostasis are plausible consequences of  $\alpha$ S membrane adsorption,  $\alpha$ S self-assembly, and  $\alpha$ S assembly with membrane lipids, through hydrophobic and electrostatic interactions as well as lipid micellar encasing of the protein species (i.e., the carpet model<sup>315</sup>). This mechanism is supported by experimental studies employing giant vesicles as well as reporters of ThT, calcein,  $\text{Ca}^{2+}$  and fluorescence recovery after photobleaching,<sup>316–319</sup> to name a few.

In close connection with  $\alpha$ S toxicity and  $\alpha$ S-membrane interaction, a body of literature has revealed links between  $\alpha$ S oligomers and mitochondrial dysfunction, cytoskeleton deformation, enhanced ROS production, neuroinflammation, ER stress, as well as impaired protein degradation systems.<sup>320–328</sup> An analysis of wide-type  $\alpha$ S and two mutational variants A30P and E46K interacting with synaptic-like SUVs suggested a mechanism by which a single  $\alpha$ S binds to two different synaptic vesicles via the NAC to promote their assembly and vesicle clustering.<sup>329</sup> In addition, promotion of SNARE-complex formation has been found to be associated with  $\alpha$ S assembly into high-order multimers upon their binding with plasma membranes, suggesting that  $\alpha$ S may act as a SNARE chaperone at the presynaptic terminal against neurodegeneration.<sup>240</sup>

#### 4.4.3 Parkinson's disease, mitigation strategies and theranostics

Synucleinopathies refer to a family of neurodegenerative diseases including PD, PDD and DLB, where inclusions of Lewy bodies and neurites are located within the neuronal cells (Fig. 11a). Multiple system atrophy (MSA) is a special type of synucleinopathy, since  $\alpha$ S-positive inclusions are found in oligodendroglia instead of in neurons. In these diseases,  $\alpha$ S pathology in the *substantia nigra* is closely correlated with motor symptoms and death of SN dopaminergic neurons stimulates the striatum.<sup>282</sup> The PD pathology involves progressive neuronal accumulation of aggregated  $\alpha$ S, and formation of Lewy bodies affects various functional structures throughout the human nervous system to compromise movement.<sup>330</sup>

Exogenous  $\alpha$ S fibrils seeded Lewy body- and Lewy neurite-like inclusions in cell culture models, and direct neuron to neuron  $\alpha$ S transmission throughout the brain propagated PD-like pathology.<sup>291, 331, 332</sup> Failure of the protein quality control systems, especially lysosomes, promoted accumulation of transmitted  $\alpha$ S and inclusion formation. Cells exposed to neuron-derived  $\alpha$ S displayed signs of apoptosis, such as nuclear fragmentation and caspase 3 activation, both *in vitro* and *in vivo*.<sup>291</sup> Inoculation of  $\alpha$ S fibrils into wide-type non-transgenic mice seeded aggregation of endogenous mouse  $\alpha$ S and reproduced key features of the neurodegenerative cascade.<sup>249</sup> A molecular level understanding of the pathological spreading of  $\alpha$ S in PD is lacking, but growing evidence suggests its origin lies in protein self-assembly through templated seeding, where the imported  $\alpha$ S aggregates catalyze the conversion of local soluble protein molecules into their aggregated forms. A recent study has revealed regulation of motor deficits and neuroinflammation by intestinal

microbiota in a PD model,<sup>239</sup> suggesting a role for microbial signals in PD.<sup>333</sup> Multiplication of the protein aggregates by recruiting additional  $\alpha$ S en route has been proposed as an additional mechanism to templated seeding, to ensure sustainable concentration of the aggregates spreading from cell to cell.<sup>332</sup> However, multiplication of  $\alpha$ S at neutral pH has not been observed, pointing to the involvement of other cellular processes in enabling the prion-like  $\alpha$ S spreading.

The ambiguities concerning the natural state, toxicity and aggregation pathway of  $\alpha$ S have hindered the development of mitigation and therapeutics against PD. The current approaches, still very much in the incubation stage, aim at exploiting the structural, functional and toxicological properties of  $\alpha$ S, or the self-assembly of the protein and its structural and pathological characteristics for therapeutic efficacy.<sup>268</sup>

Stabilization of the native  $\alpha$ S structure from misfolding is a logical strategy. This intervention may also help resolve the controversy concerning a tetrameric initial state of  $\alpha$ S.<sup>334</sup> One promising approach to slow down  $\alpha$ S synucleinopathies is to limit the role of extracellular  $\alpha$ S in disease progression, from interfering with  $\alpha$ S secretion to neuronal uptake. Removal of  $\alpha$ S from the extracellular space to minimize inflammations may be achieved with immunotherapy, as immunization with human  $\alpha$ S suppressed protein aggregation and decreased neurodegeneration in transgenic mice overexpressing the protein.<sup>335–337</sup> The use of small molecules and mutation is another feasible approach for stabilizing oligomeric species and ameliorating toxicity. The antioxidation and anti-inflammatory properties of the small molecules – often polyphenols or their structural derivatives with the capacity of interfering with protein aggregation through competing H-bonding, hydrophobic interaction and  $\pi$ -stacking with the protein – may counteract the toxicity elicited by the oligomeric species.<sup>338–340</sup> The presence of small molecules and other aggregation antagonists may also reduce accessibility to the oligomers by environmental chaperones, ligands and molecular organizations, thereby driving the aggregation off pathway to halt  $\alpha$ S pathology.

## 5. Prions and prion diseases

Transmissible spongiform encephalopathies (TSEs), also known as prion diseases, are a family of rare fatal neurodegenerative disorders associated with prion protein (PrP), and arise in several mammalian species by sporadic, inherited, or infectious means. Kuru, Creutzfeldt-Jakob disease (CJD), Gerstmann-Straussler-Scheinker (GSS), fatal familial insomnia (FFI) and fatal sporadic insomnia (FSI) are PrP-related human disorders,<sup>341</sup> whereas scrapie, bovine spongiform encephalopathy (BSE) and chronic wasting disease (CWD) are known sheep,<sup>342</sup> cattle<sup>343</sup> and cervids<sup>344</sup> prion diseases. The main characteristic symptoms of TSEs are brain vacuolation, astrogliosis and neuronal apoptosis,<sup>345, 346</sup> which are associated with accumulation of extracellular PrP amyloid deposits in the CNS.<sup>347–350</sup> Despite shared sequence between cellular non-pathological PrP (PrP<sup>C</sup>) and misfolded PrP (PrP<sup>Sc</sup>),<sup>351</sup> pathological PrP<sup>Sc</sup> aggregates are proteinase K resistant<sup>352</sup> and have a  $\beta$ -enriched secondary structure.<sup>353–355</sup>

The most distinct feature of TSEs, unique among diseases related to protein misfolding, is the infectivity of the pathogenic agent. Procedures that hydrolyze or modify proteins reduce scrapie infectivity, whereas procedures that alter nucleic acids have no effect.<sup>356–359</sup> The “protein-only hypothesis” has now been widely accepted,<sup>360–363</sup> contending that a protein structure can be replicated without the use of nucleic acids and the infectious pathogen is the misfolded PrP<sup>Sc</sup>.<sup>356, 357, 360–365</sup> In addition, prion diseases progress in host without any sign of immune responses to a “foreign infectious agent”.<sup>341</sup> When the protein requirement for infectivity was established, prions were defined as **proteinaceous infectious particles** that resisted inactivation by procedures that modified nucleic acids.<sup>341</sup>

Since prion pathology and infectivity<sup>366</sup> are closely related to a protein existing in two different conformations, much research in the last decade has been dedicated to understanding the structures of native PrP<sup>C</sup><sup>367</sup> and pathological PrP<sup>Sc</sup>.<sup>368</sup> PrP<sup>Sc</sup> is believed to act as a structural template, inducing conversion of other PrP<sup>C</sup> molecules into the pathological form.<sup>341</sup> Understanding PrP conformational structures is therefore essential for describing protein misfolding and the specific role of PrP in prion pathology.

### 5.1 Function of PrP

PrP is encoded by gene (*PRNP*) found in chromosome 20 (in human)<sup>369</sup> and expressed in many tissues, including the brain, circulating lymphocytes, heart, kidney, skin, digestive tract, endothelia, mammary gland and muscle. The physiological role of native PrP<sup>C</sup> remains unclear.<sup>370</sup> It has been shown that the protein is involved in several cellular processes including neuroprotection against excitotoxicity and serum starvation,<sup>371</sup> proliferation and cell-cell adhesion,<sup>370, 372</sup> formation of synapses<sup>373</sup> and ligand binding.<sup>374, 375</sup> PrP can protect cells against heavy metal overloading and subsequent oxidative stress by binding divalent ions of copper, zinc, manganese and nickel.<sup>375</sup> Due to the ability of PrP to modulate cell proliferation and apoptosis it is believed to play a role on cancer development.<sup>376</sup> Indeed, increased PrP<sup>C</sup> level has been found in gastric cancer,<sup>377</sup> colorectal cancer<sup>378</sup> and skin cancer.<sup>379</sup>

A common approach to study the function of PrP is using PrP knockout transgenic mice (Prnp<sup>-/-</sup>). The major finding in Prnp<sup>-/-</sup> mice was the lack of developmental differences and resistance to prion diseases.<sup>380</sup> However, Prnp<sup>-/-</sup> mice have shown cognitive abnormalities<sup>370</sup> such as depressive-like behavior, anxiety-related disorders and alterations in circadian activity.<sup>381</sup> In addition, decreased spatial learning of Prnp<sup>-/-</sup> mice has been noticed.<sup>382</sup> Using three Prnp knockout mice lines Firestein and colleagues found that PrP<sup>C</sup> was important in the normal processing of sensory information by the olfactory system.<sup>383</sup>

### 5.2 Atomic structures of prions and prion amyloids

The atomic structures of full-length and truncated PrP<sup>C</sup> were mostly solved by NMR.<sup>384–388</sup> Notably, X-ray crystallography studies were restricted to the C-terminal domain of PrP, suggesting an intrinsic tendency of the protein to avoid crystallization.<sup>389, 390</sup>

Proto-protein of human PrP (huPrP) is 253 residues long (Fig. 16a). After translation to mature form, the first 22 residues are removed and the last 23 residues are cleaved off prior



to the addition of a glycosyl phosphatidylinositol (GPI) anchor to Ser230. PrP is attached to the outer surface of the cellular membrane by a GPI anchor within the raft domains. The sequence of PrP is highly conserved amongst mammals:<sup>391, 392</sup> human PrP shares 99.2%, 94.9% and 92.8% of identical sequences with the proteins from chimpanzee, sheep and cow, respectively.

PrP<sup>C</sup> has two regions with distinct structural and dynamical properties.<sup>367</sup> In mammals, depending on the organism, the N-terminus contains a variable number of amino-terminal octapeptide repeats with sequence PHGGGWGQ. Each octapeptide is able to generate a divalent metals-binding domain via nitrogen atoms in the histidine imidazole side-chains.<sup>393</sup> The N-terminus is up to residue 120 and this region has been shown to constitute a pH-dependent folding: at pH 4.5 it is flexibly disordered,<sup>394</sup> however at pH 6.2 residues 61–84 of the octapeptides adopt a loop and a  $\beta$ -turn like conformation.<sup>386</sup> In contrast, the C-terminus of PrP<sup>C</sup> is structured, containing three  $\alpha$ -helices (H1, H2 and H3) and a short, two-stranded, antiparallel  $\beta$ -sheet (S1, S2)<sup>367</sup> (Fig. 16b). A disulphide bridge is between Cys179 and Cys214, which anchors H2 and H3 helices. This disulphide bridge is one of the major determinants of the tertiary structure of PrP. FTIR study of PrP secondary structure revealed 42% of  $\alpha$ -helices, 3% of  $\beta$ -sheets, 32% of turns and 23% of coils, respectively.<sup>395</sup>

The physicochemical properties of PrP<sup>Sc</sup> and PrP<sup>C</sup> greatly differ. Spectroscopic measurements indicated that PrP<sup>Sc</sup> contains about 34–43% of  $\beta$ -sheet structure,<sup>395, 396</sup> significantly higher than that of PrP<sup>C</sup>.<sup>395</sup> X-ray fiber diffraction of infectious prions revealed the presence of cross- $\beta$  diffraction patterns. Meridional diffraction at 4.8 Å specified the presence of  $\beta$ -strands, characteristic of a stacked-sheet amyloid structure. Thus,  $\beta$ -enriched structure of PrP<sup>Sc</sup> results from misfolding and self-assembly of protein PrP<sup>C</sup> into proteinase K-resistant amyloid-like aggregates. However, the high-resolution structures of infectious prions are not yet solved, as conventional structural methods have been hindered by the large and insoluble aggregates of PrP.

Several structural models of PrP<sup>Sc</sup> self-assembly have been proposed based on information derived from biophysical techniques. Parallel left-handed  $\beta$ -helical structure is the model proposed by Cohen and colleagues and based on electron microscopy analysis of 2D crystals<sup>368</sup> (Fig. 17a). The authors constructed a trimeric model of PrP 27–30 from a study of 119 all- $\beta$  folds globular proteins. PrP 27–30 is a protease-resistant 27–30 kDa core of PrP<sup>Sc</sup> (Fig. 16), and it retains prion infectivity.<sup>353, 397</sup> According to the  $\beta$ -helical model the N-terminal residues of PrP 27–30 form left-handed  $\beta$ -helices that are horizontally stacked, whereas the C-terminus maintains  $\alpha$ -helical secondary structure as in native PrP<sup>C</sup>. Larger aggregates are formed by vertically stacking of PrP trimers along the  $\beta$ -helical axis (Fig. 17a).

Based on MD simulations of PrP 27–30 conformational fluctuations under amyloidogenic conditions, DeMarco and Daggett proposed the  $\beta$ -spiral model<sup>398</sup> (Fig. 17b). Similarly to the  $\beta$ -helical model the C-terminal  $\alpha$ -helical characteristics of PrP<sup>C</sup> remain unchanged and natively unfolded N-terminus adopt a  $\beta$ -structure. The core structure is comprised of three short  $\beta$ -strands spanning 116–119, 129–132 and 160–164 residues.

Surewicz and colleagues proposed the in-register  $\beta$ -sheet model of PrP<sup>Sc</sup> using site-directed spin labelling and EPR spectroscopy<sup>399</sup> (Fig. 17c). In contrast to the other models, they observed that the refolding of PrP<sup>C</sup> involved major refolding of the C-terminal  $\alpha$ -helical region. According to this model PrP<sup>Sc</sup> structure possesses no  $\alpha$ -helices, consisting mainly of single molecules stacked on top of one another with parallel, in-register  $\beta$ -strands. Using MD simulations, Caughey and colleagues suggested that linear PrP<sup>Sc</sup> fibrils possessed a parallel in-register  $\beta$ -sheet structure<sup>400</sup> (Fig. 18e).

In addition, a number of structures have been proposed for mammalian<sup>401</sup> and fungal<sup>402</sup> prion protein segments. It is difficult to determine which of the proposed models is the closest to the PrP<sup>Sc</sup> structure, as they were established based on low-resolution experimental data. The diversity of the models could originate from the specimens used. For example, Wille and colleagues compared natural brain-delivered PrP<sup>Sc</sup> and synthetic bacteria-expressed recombinant PrP (with the same sequence) amyloid structure and found substantial differences in structure, heterogeneity and infectivity.<sup>403</sup> In addition, the existence of PrP tertiary structural diversity and prion strains have been experimentally proven,<sup>404–408</sup> including the formation of new strains during the passage of prions through animals with different PrP sequences.<sup>409, 410</sup> For instance, multiple scrapie prion strains were isolated with different incubation times and neuropathology.<sup>411</sup> However, these prion strains were encoded by the same PrP primary structure and were propagated in mice with the same PrP gene. Despite this, limited proteolysis generated different PrP<sup>Sc</sup> fragments, suggesting that these prion strains possessed different conformations.<sup>352</sup>

### 5.3 Mesoscopic structures of prions

The morphology of prions has been examined with TEM<sup>412–414</sup> and AFM.<sup>414</sup> Usually PrP<sup>Sc</sup> isolated from brain appears as large amorphous highly insoluble aggregates (Fig. 18a). Individual prion fibrils, termed prion rods (Fig. 18b), are not always visible probably because of heavy surface glycosylation<sup>415</sup> (Fig. 18c). Each PrP monomer has up to two large sugar moieties linked to the N-terminus to obscure the fibril core. Deficiencies in glucans and GPI anchorless PrP have been found suitable for analyzing the structural features of prion protofilaments (Fig. 18d), while neither glycosylation<sup>416, 417</sup> nor the GPI anchor<sup>348, 418</sup> is required for the infectivity of PrP<sup>Sc</sup>.

Majority of PrP fibrils, either wild-type, anchorless, or of different strains, possess a twisted morphology. Prion fibrils can be either left-handed or right-handed<sup>414</sup>, consisting of two or more protofilaments.<sup>412</sup> However, some fibrils also contain straight, parallel protofilaments.<sup>414</sup> In addition, fibrils occasionally resemble celery stalks or half-pipes<sup>414</sup> (Fig. 18c). In a recent study the gap previously thought to be the spacing between two protofilaments of celery stalk fibrils was assigned to represent the trough between the major hairpins. Accordingly, an in-register  $\beta$ -sheet PrP amyloid model was proposed.<sup>400</sup> The periodicity of PrP fibrils, on the other hand, ranged between 40 nm to 133 nm<sup>412, 414, 419</sup> while the width of each PrP protofilament varied from  $3.1 \pm 0.7$  nm<sup>414</sup> to 6.9 nm.<sup>368</sup>

## 5.4 Transmission of prions

Epidemiological transmission of PrP diseases is via the exposure of PrP<sup>C</sup> to PrP<sup>Sc</sup>. However, point mutations in the *PRNP* gene at K200E, D178N, L102P and V117A codons were observed in families initially diagnosed with vCJD and GSS.<sup>420–422</sup> Linear transmission in human has an early history in the fore people of Papua New Guinea who suffered from Kuru: a human variant of PrP disease with clinical symptoms of ataxia, shivering and death within year of manifestation. Although the endemic is ceased by terminating the ritual cannibalism in 1950s, Kuru is waning gradually due to long sub-clinical incubation period i.e. > 50 years.<sup>423</sup> In modern days, the inter-human transmission is via blood transfusions as person infected with vCJD carry PrP<sup>Sc</sup> load in all blood components with transmission efficiency of WBCs > platelets > RBCs > plasma and shed PrP<sup>Sc</sup> in saliva, urine and other bodily fluids.<sup>424, 425</sup> Less common ways of transmission in humans are surgical instruments and human derived growth hormones.<sup>426</sup>

The clinical symptoms of PrP diseases originate from pathological changes in CNS such as vacuolization, astrogilosis and neuronal apoptosis. However, once prion replication in CNS reaches its peak, the PrP<sup>Sc</sup> is disseminated centrifugally to the peripheral secretory organs and lymphoid tissues. PrP<sup>Sc</sup> excreted are detected in blood, urine, saliva, milk and bone-meat meal (MBM) of infected animal even at sub-clinical stage. The titre from urine and saliva of CWD infected cervid was able to reproduce infectivity in naïve cervid and transgenic mice models.<sup>427–429</sup> Salivary expression can contaminate drinking water and pose a risk of transmission to human and other animals.<sup>430</sup> Scrapie infected sheep shed PrP<sup>Sc</sup> in all components of colostrum and milk i.e. cells, cream and casein/whey proteins, which carried infectivity to lambs and dairy products.<sup>431, 432</sup> The titre of infectivity per mL of milk was equivalent to 6 µg of brain homogenate from terminally scrapie-infected sheep.<sup>433</sup> Bone and meat materials, either decaying in the soil or processed into MBM for cattle feeds, had PrP<sup>Sc</sup> attached to its particles. PrP<sup>Sc</sup> attached to MBM or soil particles had higher transmission efficiency.<sup>434</sup> Infectivity was retained and transmissible to animals even after processing of MBM for biodiesel productions.<sup>435</sup> Once attached to the soil particles, PrP<sup>Sc</sup> not detachable via surfactants and soil could retain infectivity up to 19 years.<sup>436–438</sup> However, hyperthermophilic bacteria were able to digest the PrP<sup>Sc</sup> particles from soil by secreting keratins and β-sheets proteases.<sup>439</sup>

Rasmussen et al. first showed that hamster PrP<sup>Sc</sup> were able to bind with wheat grass roots, from soil and brain homogenate, but neither absorbed in roots nor detected in areal parts of the plants.<sup>440</sup> Pritzkow et al. used protein misfolded cyclic amplification (PMCA) as a more sensitive detection method and transmitted hamster 263K PrP<sup>Sc</sup> to wheat grass roots via infected brain homogenate, excreta, contaminated soils and direct spray of PrP on areal parts.<sup>441</sup> The 263K PrP<sup>Sc</sup> were able to adsorb from the sources to the roots and travelled in the areal parts, which were further able to reproduce the infectivity in naïve hamster. Apart from the extraneous PrP<sup>Sc</sup> in plants, a protein named luminidependens from *Arabidopsis thaliana* was transformed and propagated like PrP when injected in yeast cells.<sup>442</sup>

## 5.5 Conversion and replication of prions

The molecular interaction between PrP<sup>Sc</sup> and PrP<sup>C</sup> is based on self-assembly driven by hydrogen bonding and  $\pi$ -stacking of the tyrosine residues. Two initial models described the mechanism of PrP replication.<sup>443</sup> The “template directed” model described PrP<sup>Sc</sup> as the more stable but thermodynamically inaccessible form of PrP<sup>C</sup>. In contrast, the “seeded nucleation” model described the contact of small oligomers of PrP<sup>Sc</sup> with PrP<sup>C</sup>: the seeds of PrP<sup>Sc</sup> recruit PrP<sup>C</sup> into conformationally changed form, and the growing fibril is broken down into various small seeds acting as nuclei for further recruitment. The PrP<sup>Sc</sup> monomers are less stable but become stabilized when joined in the seeded oligomer form.<sup>444, 445</sup> The seeded nucleation model was supported by later experiments where small amounts of preformed PrP<sup>Sc</sup> oligomers converted large quantities of PrP<sup>C</sup> as in PMCA, where seeds shredding was induced by sonication and the conversion process was amplified.<sup>446</sup> Makarava et al. refined the conversion phenomenon by studying the conformation switch (R and S) within single, mouse-hamster cross-seeded PrP amyloids and introduced the concepts of catalytic versus templated conversion and amyloid flexibility.<sup>447</sup> Hamster PrP (S conformation), when incubated with mouse PrP monomers, catalyzed the conversion by accelerating the fibrillation rate and shortening the lag phase, but the newly formed daughter fibrils retained R conformation only. In contrast, when hamster PrP seeds were introduced to hamster PrP monomers, it accelerated fibrillation and templated the same S conformation in daughter fibrils. Molecular events occurring in template-directed PrP conversion started from  $\pi$ - $\pi$  interaction of PrP<sup>C</sup> and PrP<sup>Sc</sup> in 6 different binding and conversion domains (BCD) of PrP. In the absence of PrP<sup>Sc</sup>, when human and hamster PrP<sup>C</sup> BCD were probed with monoclonal antibody (mAb), it resulted in structural denaturation of PrP<sup>C</sup>, regional loss of tertiary structure, dissociation of  $\beta$ -sheets, and exposure of bityrosine regions (YYR) at  $\alpha_1$  and  $\alpha_2$  helices. The exposure of YYR regions was confirmed with binding of anti-YYR mAb in these loose regions.<sup>448</sup> In contrast to mAb, PrP<sup>Sc</sup> binding induced melting and exposure of YYR regions from  $\beta_2$ - $\alpha_2$ ,  $\alpha_2$ - $\alpha_3$  and  $\alpha_1$  regions.<sup>448-450</sup> The exposed YYR could be the site of further PrP<sup>C</sup> attachment and connected the oligomer and monomer.<sup>450</sup> The loose structure induced by mAb was not able to acquire any conformation or secondary structure from mAb. However, when PrP<sup>Sc</sup> oligomers induced this structural loosening, it acquired  $\beta$ -sheets from oligomer's hydrogen bonded backbone and stabilized the whole fibril column.<sup>447</sup>

## 5.6 Co-factors in prion assembly

Co-factors, initially recognized as “Protein X” by Prusiner, stabilize the PrP<sup>C</sup>-PrP<sup>Sc</sup> assembly and may further facilitate the spontaneous conversion of PrP<sup>C</sup> into protease resistant form.<sup>451</sup> Biomacromolecules of polysaccharides, sphingolipids, phospholipids, cholesterol, detergents like SDS, lipopolysaccharides from bacterial membranes, and polyanions like RNA have been found to interact with PrP<sup>C</sup> and are co-localized with PrP<sup>Sc</sup> from infected animals.<sup>452-454</sup> The interaction with co-factors melted the secondary structure of PrP<sup>C</sup> and converted it into protease resistant but non-infectious  $\beta$ -sheet structure, differently from the  $\beta$ -sheets of PrP<sup>Sc</sup>, even though PrP<sup>Sc</sup> and co-factors exposed YYR from the same regions of PrP<sup>C</sup>.<sup>449, 450</sup>

## 5.7 Transmission barriers: sequence and conformation

A transmission barrier appears when there is no clinical neuropathology of spongiform encephalopathies upon inoculation of PrP<sup>Sc</sup> from infected species A into the naïve species B. The molecular etiology for the transmission barrier is attributed to i) difference in the sequences of host and donor PrP, ii) conformational misfit during assembly, and iii) post conversion maturation in host. The exact residual regions responsible for the transmission barrier are i) 165–175 ( $\beta_2$ - $\alpha_2$ ) with switches at 170 (S/N), 174 (N/T), 169 (Y/G), ii) 138–143 ( $\beta_1$ - $\alpha_1$ ) with switches at 139 (M/I) and iii) 129 ( $\beta_1$ ) for M/V switch (Fig. 19).<sup>455–458</sup> Sheep's scrapie and cattle's BSE are inter-transmissible with clinical symptoms as both are 170S homozygous. However, transmission between mice (170S) and hamster (170N) does not produce clinical disease.<sup>459, 460</sup> Sigurdson et al. demonstrated the 170 S/N and 174 N/T switches at the molecular level.<sup>458</sup> Inoculation of deer scrapie PrP<sup>Sc</sup> (170N, 174N) into wild type tg20 mice (170S, 174N) didn't express clinical symptoms at first passage but inoculation in rigid loop tg1020 mice (S170N, N174T) produced terminal symptoms in 74 days. Furthermore, hamster PrP<sup>Sc</sup> (170N, 174T) accelerated clinical disease in tg1020 mice (S170N, N174T) but not in tg20 mice (170S, 174N). In contrast, cattle and sheep PrP<sup>Sc</sup> (170S, 174N) produced disease in tg20 mice (170S, 174N) but not in tg1020 mice (S170N, N174T).<sup>458</sup> Similarly, 139I in humans and mice PrP<sup>Sc</sup> induced parallel  $\beta$ -sheet stacking and R conformation in fibril while 139M in hamster induced anti-parallel  $\beta$ -sheet stacking and S conformation.<sup>447, 456</sup> The region 138–143 has been demonstrated as a steric zipper in stabilizing PrP<sup>Sc</sup> fibril by hydrogen bonding between inter-monomeric  $\beta$ -sheets. Incompatibility at the steric zipper also erects a cross-species barrier.<sup>461</sup> The tyrosine residue at 169 is responsible for initial  $\pi$ - $\pi$  interaction between PrP<sup>Sc</sup> oligomers and host PrP<sup>C</sup> monomers and is conserved in all mammalian PrP. Eliminating tyrosine or replacing it with glycine completely blocked PrP<sup>Sc</sup> interaction with PrP<sup>C</sup> and halted the conversion.<sup>457</sup> Another molecular switch between human TSE and mad cow BSE is at 129 residue (M/V). vCJD infected human possessed 129M homologues with bovine 129M. However, 129V PrP peptide was still converted to the PrP<sup>Sc</sup> form *in-vitro*, but at a low efficiency. Hence the possibility of bovine 129M infection to 129V heterozygous human can not be excluded.<sup>455, 462</sup>

## 5.8 PrP evolution and conformational adaptation: sub-clinical stages

Cross-species transmission of PrP<sup>Sc</sup> infection produced no clinical symptoms in first passage due to dissimilar residual sequence and thus conformation as discussed above. However, the clinically silent phase led to the understanding of i) long sub-clinical stage, with no disease symptoms but undergoing PrP replication in brain, spleen and lymphoid tissues and ii) concepts of PrP<sup>Sc</sup> maturation, stability, selection and evolution.<sup>464, 465</sup> First passage of cattle BSE to human PrP<sup>Sc</sup> transgenic mice produced only a 0.6% attack rate after 739 days but a 75% attack rate after 639 days on second passage.<sup>466</sup> The decrease in incubation time and increase in attack rate were also observed by passaging the inoculum *in vitro* with PCMA rounds, which led to the emergence of mutated and phenotypically distinct PrP strains.<sup>467–469</sup> Kimberlin et al. inoculated 139A PrP<sup>Sc</sup> from mouse to hamster and then back to mouse resulting in 139H/M strain.<sup>470</sup> Colby et al. infected mice with rPrP of different conformational stability and resulted in phenotypically different strains with different physical morphologies, shorter incubation time, higher attack rate and varying clinical

pathologies.<sup>471</sup> It was hypothesized that the original inoculum consisted of different rPrP strains and upon infecting into the host, the strain having close conformational fit with host PrP replicated at a faster rate, induced the clinical disease and subsequently appeared in animal tissues.<sup>471</sup> Similarly, Bruce et al. raised 22C natural PRNP<sup>a</sup> strain in PRNP<sup>b</sup> mice and ended up with 22H strain. However, upon passaging the recombinant and pure 22C strain, only 22C was resulted in the host indicating the presence of both 22C and 22H in natural inoculum but 22H with shorted incubation time and close fit with host PrP was able to replicate at a faster rate.<sup>472</sup> Makarava et al. annealed hamster rPrP<sup>Sc</sup> with normal hamster brain homogenate and inoculated in naïve hamster. On first passage, 50% attack was observed but all hamster succumbed to disease on second passage and clinical symptoms were different from original rPrP<sup>Sc</sup> which was used to prepare the inoculum.<sup>464</sup> The explanation is that i) original inoculum lacked the GPI anchor and failed to penetrate the cell to initiate neurotoxicity, ii) conformational adaptation and stability were observed upon serial PCMA and iii) rPrP<sup>Sc</sup>-NBH failed to acquire co-factors, which it acquired on subsequent passages in the host.<sup>464</sup> Serial passages of donor PrP<sup>Sc</sup> with host PrP<sup>C</sup> by PCMA *in vivo* or *in vitro* also changed the biochemical parameters like electrophoretic mobility, protease digestion and degree of glycosylation.<sup>473</sup> The efficiency and properties of evolutionary adaptation was also found to be tissue dependant, i.e., occurring at a faster rate in spleen than brain and cell and brain adapting different strains.<sup>465, 474</sup>

### 5.9 Toxicity of prions and mitigation

Two and a half decades on, the mechanism of prion toxicity has been narrowed down to the distortion of neuronal cell membranes due to the assembly of PrP<sup>Sc</sup> oligomers with GPI anchored PrP<sup>C</sup>.<sup>475, 476</sup> Deletion of GPI anchored PrP<sup>C</sup> from the membrane or expression of anchorless PrP<sup>C</sup> in transgenic mice resulted a minimum infectivity or reversal of clinical symptoms in infected mice, which implicated anchored PrP<sup>C</sup> for neurotoxicity.<sup>348, 477</sup> However, the extracellular accumulation of PrP<sup>Sc</sup> continued as plaques as in terminally-ill wild-type mice.<sup>78, 79</sup> Apart from PrP<sup>Sc</sup>, when anchorless PrP<sup>C</sup> was exposed to lipid membrane or expressed in transgenic mice they adhered to the membranes, underwent conformational changes into the protease resistant form, oligomerized locally, and caused membrane disruption and ion channel formation.<sup>478–480</sup> Although PrP<sup>C</sup> has a neuroprotective role against cellular stress, it also intervenes toxic signals to neuronal cell and initiates an apoptotic cascade when probed by PrP<sup>Sc</sup>,  $\beta$ -sheet conformers, yeast prions, A $\beta$  or other amyloid oligomers and even anti-PrP<sup>C</sup> antibodies.<sup>481–483</sup> The mechanism is postulated as either through blocking the physiological binding domains of PrP<sup>C</sup> or disruption of neuronal membranes by PrP<sup>C</sup>-PrP<sup>Sc</sup> oligomer adducts.<sup>484, 485</sup> The adduct formed on the membrane can be internalized and disrupt endosomal trafficking or distort the local fluidity, structure and function of lipid bilayers like channel formation in GSS.<sup>476, 486</sup> In addition to adduct formation, PrP<sup>Sc</sup> oligomers can independently interact with membranes via their own GPI anchors, which they tend to develop during sequel passages.<sup>487</sup> The oligomer form of PrP<sup>Sc</sup> has been shown to be the toxic species, other than the monomers or amyloids.<sup>480</sup> PrP<sup>Sc</sup> oligomers possess the necessary hydrogen bonding backbone running up and own in the column to induce conformational change in PrP<sup>C</sup> and recruit the latter at the growing end.<sup>447</sup> PrP<sup>Sc</sup> oligomers corrupt PrP<sup>C</sup> function and deliver a neurotoxic signal.<sup>476</sup>

Initial therapeutic strategies considered silencing of the PrP<sup>C</sup> gene. Silencing was well tolerated in animals apart from minor disturbance in sleep cycle and electrophysiology of hippocampus.<sup>500</sup> However, as the PrP<sup>C</sup> is associated with neuroprotection excitotoxicity outcomes are being predicted for silencing PrP<sup>C</sup> in human.<sup>501</sup> RNA is physiologically found co-localized with PrP<sup>Sc</sup> which triggered research for RNA as an anti PrP drug.<sup>452</sup> RNA based aptamers can bind PrP<sup>C</sup> to prevent PrP<sup>Sc</sup>-induced conversion or with PrP<sup>Sc</sup> oligomers to block their activity.<sup>502</sup> The subsequent interaction of PrP<sup>C</sup> with the same aptamer increases the binding efficiency due to the adaptation flexibility of PrP<sup>C</sup>.<sup>503</sup> Different ways of delivering aptamer RNA across the blood brain barrier (BBB) include conjugation with transferrin, cell penetrating peptides, NPs, liposomes and dendrimer.<sup>503</sup> Polyethylene glycol-conjugated polycyanoacrylate NPs were able to penetrate the brain and spleen of scrapie infected animals, however their ability to delivery therapeutic cargo and mode of interaction with PrP<sup>Sc</sup> fibrils are questioned.<sup>504</sup> Branched polyamines degraded PrP<sup>Sc</sup> amyloids to undetectable levels and reversed PrP<sup>Sc</sup> toxicity in neuroblastoma cell culture (Fig. 20h).<sup>499</sup> Pre-treatment of PrP<sup>Sc</sup> amyloids with polyamines rendered them susceptible to proteolytic digestion. Tran et al. used polyallylamine (+) and polystyrenesulfonate (-) as two oppositely charged polyamines for layer-by-layer coating of gold NPs (AuNPs) (Fig. 20c). The AuNPs translocated across the BBB, disrupted the PrP<sup>Sc</sup> amyloids, and mitigated the toxicity in scrapie-infected cells. Nanomolar concentrations of AuNPs, with poly(allylamine) as the outermost layer, prolonged incubation time and delayed the disease onset in infected mice.<sup>497</sup> Polyamine-based dendrimers coated with maltose or maltotriose stimulated PrP fibrillization at lower concentrations by breaking long fibrils into small seeds, but at higher concentrations blocked the fibrillization by stabilizing individual seeds (Fig. 20h).<sup>491</sup>

NP-PrP interactions have been explored for diagnostic and sensing applications. Monothiolation of RNA aptamers makes them a good ligand to cap AuNPs or AgNPs. These NPs then specifically interact with PrP<sup>Sc</sup> and sequester the latter on their surfaces. The binding of PrP<sup>Sc</sup> or cell bound PrP<sup>C</sup> is sensed in a concentration dependant manner via changes in the surface plasmon resonance or Raman signals of the AuNPs/nanorods (NRs) and aptamer ligated AgNPs (Fig. 20j).<sup>489, 495</sup> PrP binding with aptamer-conjugated NPs induces controlled aggregation which can be sensed via resonance light scattering of metal NPs aggregation (Fig. 20b).<sup>488</sup> Henry et al. employed fluorescence turn-on and turn-off sensing for PrP detection.<sup>498</sup> The fluorescence of fluorescein-GABA-QYQRES-COOH peptide bound to antibody-conjugated AuNPs (turned-off) was turned-on by replacing the peptide with competitive binding of PrP<sup>Sc</sup> with the antibody (Fig. 20a). The fluorescence property of biotin-avidin or monoclonal antibody bound quantum dots (QDs) has also been explored for the detection of PrP *in vitro* and *in vivo* (Fig. 20g).<sup>490</sup> Xiao et al. used the dual-aptamer technique by ligating aptamer 1 on Fe magnetic NPs (MNPs) and aptamer 2 on QDs. MNPs and QDs sandwiched PrP<sup>Sc</sup> or PrP<sup>C</sup> in between and the technique was used to detect and isolate PrP by fluorescent QDs and magnetic NPs even from 0.1 % infected brain homogenate (Fig. 20f).<sup>496</sup> MNPs directly capped with aspartic acid or Au-mercaptopropionic acid were able to sequester PrP via carbodiimide coupling (Fig. 20d).<sup>505</sup> Miller et al. engaged the aptamer-ligated MNPs to capture and clear PrP<sup>Sc</sup> from solution. The sequestered PrP<sup>Sc</sup> on MNPs were able to act as seeds in PCMA and enabled the detection and amplification of small quantities of PrP<sup>Sc</sup> (Fig. 20e).<sup>506</sup>

On the medicinal chemistry front, amphotericin B,<sup>507, 508</sup> quinacrine, dimeric analogues of statins, pyrazolones and pyridyl hydrozones are available drugs for prolonging the lifespan of PrP infected animals.<sup>493, 509</sup> Tacrolimus and astemizole reduce the PrP expression on cell membranes and inhibit PrP<sup>Sc</sup> replication.<sup>510</sup> Drug discovery for small organic molecules led to 2-aminothiazoles which cap PrP<sup>Sc</sup> seeds and inhibit their replication activity.<sup>511</sup> Lipoic acid, an endogenous anti-oxidant compounds and when conjugated with acridine and quinolone, inhibited PrP<sup>Sc</sup> fibril formation.<sup>494</sup> A structure-activity relationship study of the pyrazole derivative of carbazole led to the understanding that a tricyclic aromatic ring with hydroxyl and amino groups inhibited PrP<sup>Sc</sup> fibrillization in PrP<sup>Sc</sup>-infected neuronal cells.<sup>492</sup>

### 5.10 Prions versus other neurodegenerative disorders

Cross-seeding and mutual stimulation of amyloid fibrils have revealed possible links between AD, PD and T2D.<sup>512, 513</sup> Mougenot et al. injected the PrP<sup>Sc</sup> from cattle BSE, human BSE and scrapie into mice over-expressing  $\alpha$ S. The incubation time was reduced significantly and mice died of cerebral spongiform pathologies of PrP<sup>Sc</sup> without accumulating insoluble fibrils of  $\alpha$ S.<sup>514</sup> AD and PD have different neuronal pathologies than PrP and their ability to transmit and infect like prions is inconclusive.<sup>515, 516</sup> More *in vitro* and *in vivo* cross seeding studies are necessary to elucidate the mechanisms and relationships between these diseases of different origins.

## 6. Summary

A survey of the literature has revealed striking similarities in the cross- $\beta$  motifs of amyloid fibrils held together by H-bonding, regardless of the sequence and origin of the proteins. However, a recent study reported a cross- $\alpha$  amyloid structure associated with PSM $\alpha$ 3, a 22-residue functional amyloid peptide secreted by *Staphylococcus aureus* for inflammatory response stimulation, human cell lysis and biofilm formation, representing a surprising departure from the common amyloid structure.<sup>517</sup> The suprastructure of amyloid fibrils – including that of all (S) A $\beta$ <sub>1-40</sub> and hen egg lysozyme – has been shown as predominantly left handed,<sup>518</sup> originated from the inherent left-handed chirality of the (S) amino acids. However, right-handed amyloids have been reported for truncated serum amyloid A (SAA) peptides (< 12 residues), resulting from the occurrence of  $\beta$  helices in SAA protofilaments prior to their assembly into fibrils.<sup>519</sup> A recent study on serum albumin amyloids, has revealed that handedness can be inverted from left to right handed, upon lateral addition of protofilaments of amyloid fibrils of a lower hierarchical level.<sup>520</sup>

There is compelling evidence that amyloid proteins can spread from cell to cell and cross talk *in vivo* to either speed up or slow down aggregation of the host protein.<sup>291, 519, 521-523</sup> Furthermore, aggregates of non-amyloidogenic proteins, such as bovine PI3-SH3 domain and *E. coli* HypF domain, can serve as seeds to promote cytotoxicity in brain cells. This phenomenon suggests a generic origin of protein misfolding diseases resulting from the emergence of trace amounts of aggregates, either introduced intracellularly through misfolding or mutations or externally through cross seeding.<sup>285</sup>

The development of neurodegenerative disorders appears to be correlated with aging, where misfolding of proteins down the free energy landscape towards the amyloid state is likely



prevented by metal ions (such as  $\text{Ca}^{2+}$  in the ER), molecular chaperones, ubiquitination enzymes and proteasomes, which kinetically trap the aggregating proteins off pathway.<sup>285, 524</sup> Compared with A $\beta$  or IAPP, the tremendous plasticity of  $\alpha\text{S}$  and PrP may originate from their much longer chain lengths and, therefore, greater populations of misfolded intermediates.

Although controversies remain, the observations that oligomers are more toxic than their fibrillar counterparts appear pervasive to amyloid proteins. In addition, oligomer-specific antibody developed for A $\beta$  also bound the oligomers of IAPP, lysozyme, prion<sup>106–126</sup>, human insulin, polyglutamine and  $\alpha\text{S}$ , suggesting a common tertiary structure<sup>273</sup> as well as a common mechanism of pathogenesis beyond the individuality of the proteins and compositions of their molecular chaperones and cellular environments. As amyloid proteins fibrillate along the kinetic pathway, both their solubility and reactivity appear to decline, consequently impacting protein self-assembly and their engagement with environmental ligands, proteins, cell membranes and organelles to elicit toxicity. While such conditions can be manipulated *in vitro*, such as through the regulation of temperature and pH or the introduction of metal ions, small molecules or engineered NPs, how to create *in vivo* conditions that prohibit trace amounts of aggregates from activating primary and/or secondary nucleation remains a tremendous challenge. Despite the complexity of protein structure, function and toxicity, as revealed by intensive research spanning the past two decades and highlighted in this review, protein aggregation through self-assembly and interaction with cellular environments constitutes hallmarks of neuronal and pancreatic  $\beta$ -cell degeneration. Consequently, understanding and exploiting molecular assembly under physiological conditions could make inroads on the development of therapeutics and diagnostics against amyloid diseases.

## Acknowledgments

The authors thank the support of ARC Project CE140100036 (Davis), DP160100959 (Separovic), NSF CAREER CBET-1553945 (Ding), NIH MIRA 1R35GM119691 (Ding) and Monash Institute of Pharmaceutical Sciences (Ke). Davis is thankful for an Australian Laureate Fellowship from the ARC. We apologize to those whose works are not cited in this review due to the tremendous amount of the relevant literature.

## List of abbreviations

<b>A<math>\beta</math></b>	amyloid-beta
<b>AD</b>	Alzheimer's disease
<b>AFM</b>	atomic force microscopy
<b>APP</b>	amyloid precursor protein
<b><math>\alpha\text{S}</math></b>	alpha-synuclein
<b>ATR-FTIR</b>	attenuated total reflection-Fourier-transform infrared
<b>BBB</b>	blood brain barrier
<b>BCD</b>	binding and conversion domains

<b>BSE</b>	bovine spongiform encephalopathy
<b>CD</b>	circular dichroism spectroscopy
<b>CJD</b>	Creutzfeldt-Jakob disease
<b>CNS</b>	central nervous system
<b>CWD</b>	chronic wasting disease
<b>DLB</b>	dementia with Lewy bodies
<b>DMD</b>	discrete molecular simulations
<b>EGCG</b>	epigallocatechin gallate
<b>EPR</b>	electron paramagnetic resonance
<b>ER</b>	endoplasmic reticulum
<b>FFI</b>	fatal familial insomnia
<b>FSI</b>	fatal sporadic insomnia
<b>FTIR</b>	Fourier transform infrared spectroscopy
<b>GPI anchor</b>	glycosyl phosphatidylinositol
<b>GSS</b>	Gerstmann-Straussler-Scheinker
<b>HAM</b>	hierarchical assembly model
<b>HD</b>	hydrogen-deuterium exchange
<b>huPrP</b>	human PrP
<b>IAPP</b>	islet amyloid polypeptide
<b>IDP</b>	intrinsically disorder protein
<b>IM-MS</b>	ion mobility mass spectroscopy
<b>mAb</b>	monoclonal antibody
<b>MBM</b>	bone-meat meal
<b>MD</b>	molecular dynamics
<b>MNPs</b>	Fe magnetic NPs
<b>NAC</b>	non-amyloid-beta component
<b>NFTs</b>	neurofibrillary tangles
<b>NMR</b>	nuclear magnetic resonance
<b>NSF</b>	N-ethylmaleimide-sensitive factor

<b>NPs</b>	nanoparticles
<b>PD</b>	Parkinson's disease
<b>PDD</b>	Parkinson's disease dementia
<b>PHFs</b>	paired helical filaments
<b>PMCA</b>	protein misfolded cyclic amplification
<b>PrP</b>	prion protein
<b>PrP<sup>C</sup></b>	non-pathological PrP
<b>PrP<sup>Sc</sup></b>	misfolded PrP
<b>ROS</b>	reactive oxygen species
<b>SAA</b>	serum amyloid A
<b>SDS</b>	sodium dodecyl sulfate
<b>SDSL</b>	site directed spin labelling
<b>SNARE</b>	soluble NSF attachment protein receptor
<b>ssNMR</b>	solid-state nuclear magnetic resonance
<b>SUVs</b>	small unilamellar vesicles
<b>T2D</b>	type 2 diabetes
<b>TEM</b>	transmission electron microscopy
<b>ThT</b>	thioflavin T assay
<b>TSEs</b>	transmissible spongiform encephalopathies
<b>UPS</b>	Ubiquitin proteasome system
<b>YYR</b>	bityrosine regions

## References

1. Knowles TPJ, Vendruscolo M, Dobson CM. *Nat Rev Mol Cell Biol.* 2014; 15:384–396. [PubMed: 24854788]
2. Cohen SIA, Linse S, Luheshi LM, Hellstrand E, White DA, Rajah L, Otzen DE, Vendruscolo M, Dobson CM, Knowles TPJ. *Proc Natl Acad Sci USA.* 2013; 110:9758–9763. [PubMed: 23703910]
3. Knowles TPJ, Waudby CA, Devlin GL, Cohen SIA, Aguzzi A, Vendruscolo M, Terentjev EM, Welland ME, Dobson CM. *Science.* 2009; 326:1533–1537. [PubMed: 20007899]
4. Guijarro JI, Sunde M, Jones JA, Campbell ID, Dobson CM. *Proc Natl Acad Sci USA.* 1998; 95:4224–4228. [PubMed: 9539718]
5. Chiti F, Webster P, Taddei N, Clark A, Stefani M, Ramponi G, Dobson CM. *Proc Natl Acad Sci USA.* 1999; 96:3590–3594. [PubMed: 10097081]
6. Urbanc B, Cruz L, Yun S, Buldyrev SV, Bitan G, Teplow DB, Stanley HE. *Proc Natl Acad Sci USA.* 2004; 101:17345–17350. [PubMed: 15583128]

7. Auer S, Meersman F, Dobson CM, Vendruscolo M. *PLoS Comp Biol.* 2008; 4:e1000222.
8. Ratha BN, Ghosh A, Brender JR, Gayen N, Ilyas H, Neeraja C, Das KP, Mandal AK, Bhunia A. *J Biol Chem.* 2016; 291:23545–23556. [PubMed: 27679488]
9. Hamley IW. *Angew Chem Int Ed.* 2007; 46:8128–8147.
10. Hamley IW. *Chem Rev.* 2012; 112:5147–5192. [PubMed: 22813427]
11. Alzheimer A, Stelzmann RA, Schnitzlein HN, Murtagh FR. *Clinical anatomy.* 1995; 8:429–431. [PubMed: 8713166]
12. Glenner GG, Wong CW. *Biochemical and biophysical research communications.* 1984; 120:885–890. [PubMed: 6375662]
13. Blessed G, Tomlinson BE, Roth M. *The British journal of psychiatry : the journal of mental science.* 1968; 114:797–811. [PubMed: 5662937]
14. Grundke-Iqbal I, Iqbal K, Tung YC, Quinlan M, Wisniewski HM, Binder LI. *Proc Natl Acad Sci USA.* 1986; 83:4913–4917. [PubMed: 3088567]
15. Skrabana R, Sevcik J, Novak M. *Cellular and molecular neurobiology.* 2006; 26:1085–1097. [PubMed: 16779670]
16. Avila J, Pallas N, Bolos M, Sayas CL, Hernandez F. *Expert opinion on therapeutic targets.* 2016; 20:653–661. [PubMed: 26652296]
17. Mukrasch MD, Bibow S, Korukottu J, Jeganathan S, Biernat J, Griesinger C, Mandelkow E, Zweckstetter M. *PLoS biology.* 2009; 7:e34. [PubMed: 19226187]
18. Ganguly P, Do TD, Larini L, LaPointe NE, Sercel AJ, Shade MF, Feinstein SC, Bowers MT, Shea JE. *The journal of physical chemistry B.* 2015; 119:4582–4593. [PubMed: 25775228]
19. Li W, Lee VM. *Biochemistry.* 2006; 45:15692–15701. [PubMed: 17176091]
20. Mandelkow E, von Bergen M, Biernat J, Mandelkow EM. *Brain pathology.* 2007; 17:83–90. [PubMed: 17493042]
21. von Bergen M, Friedhoff P, Biernat J, Heberle J, Mandelkow EM, Mandelkow E. *Proc Natl Acad Sci USA.* 2000; 97:5129–5134. [PubMed: 10805776]
22. Minoura K, Yao TM, Tomoo K, Sumida M, Sasaki M, Taniguchi T, Ishida T. *European journal of biochemistry.* 2004; 271:545–552. [PubMed: 14728681]
23. Adamcik J, Sanchez-Ferrer A, Ait-Bouziad N, Reynolds NP, Lashuel HA, Mezzenga R. *Angewandte Chemie.* 2016; 55:618–622. [PubMed: 26636567]
24. Sibille N, Huvent I, Fauquant C, Verdegem D, Amniai L, Leroy A, Wieruszkeski JM, Lippens G, Landrieu I. *Proteins.* 2012; 80:454–462. [PubMed: 22072628]
25. Sandbrink R, Masters CL, Beyreuther K. *Neurobiology of disease.* 1994; 1:13–24. [PubMed: 9216982]
26. Tanzi RE, McClatchey AI, Lamperti ED, Villa-Komaroff L, Gusella JF, Neve RL. *Nature.* 1988; 331:528–530. [PubMed: 2893290]
27. Burger PC, Vogel FS. *The American journal of pathology.* 1973; 73:457–476. [PubMed: 4271339]
28. Selkoe DJ. *Annual review of cell biology.* 1994; 10:373–403.
29. Zheng H, Jiang M, Trumbauer ME, Sirinathsinghji DJ, Hopkins R, Smith DW, Heavens RP, Dawson GR, Boyce S, Conner MW, Stevens KA, Slunt HH, Sisoda SS, Chen HY, Van der Ploeg LH. *Cell.* 1995; 81:525–531. [PubMed: 7758106]
30. White AR, Reyes R, Mercer JF, Camakaris J, Zheng H, Bush AI, Multhaup G, Beyreuther K, Masters CL, Cappai R. *Brain research.* 1999; 842:439–444. [PubMed: 10526140]
31. Grimm MO, Grimm HS, Patzold AJ, Zinser EG, Halonen R, Duering M, Tschape JA, De Strooper B, Muller U, Shen J, Hartmann T. *Nature cell biology.* 2005; 7:1118–1123. [PubMed: 16227967]
32. Meziane H, Dodart JC, Mathis C, Little S, Clemens J, Paul SM, Ungerer A. *Proc Natl Acad Sci USA.* 1998; 95:12683–12688. [PubMed: 9770546]
33. Roch JM, Masliah E, Roch-Levecq AC, Sundsmo MP, Otero DA, Veinbergs I, Saitoh T. *Proc Natl Acad Sci USA.* 1994; 91:7450–7454. [PubMed: 8052602]
34. Nikolaev A, McLaughlin T, O’Leary DD, Tessier-Lavigne M. *Nature.* 2009; 457:981–989. [PubMed: 19225519]

35. Ring S, Weyer SW, Kilian SB, Waldron E, Pietrzik CU, Filippov MA, Herms J, Buchholz C, Eckman CB, Korte M, Wolfer DP, Muller UC. *The Journal of neuroscience : the official journal of the Society for Neuroscience*. 2007; 27:7817–7826. [PubMed: 17634375]
36. Vassar R, Bennett BD, Babu-Khan S, Kahn S, Mendiaz EA, Denis P, Teplow DB, Ross S, Amarante P, Loeloff R, Luo Y, Fisher S, Fuller J, Edenson S, Lile J, Jarosinski MA, Biere AL, Curran E, Burgess T, Louis JC, Collins F, Treanor J, Rogers G, Citron M. *Science*. 1999; 286:735–741. [PubMed: 10531052]
37. Olubiyi OO, Strodel B. *J Phys Chem B*. 2012; 116:3280–3291. [PubMed: 22300010]
38. Caglayan S, Takagi-Niidome S, Liao F, Carlo AS, Schmidt V, Burgert T, Kitago Y, Fuchtbauer EM, Fuchtbauer A, Holtzman DM, Takagi J, Willnow TE. *Science translational medicine*. 2014; 6:223ra220.
39. Huse JT, Liu K, Pijak DS, Carlin D, Lee VM, Doms RW. *J Biol Chem*. 2002; 277:16278–16284. [PubMed: 11847218]
40. Liu K, Solano I, Mann D, Lemere C, Mercken M, Trojanowski JQ, Lee VM. *Acta neuropathologica*. 2006; 112:163–174. [PubMed: 16865398]
41. Hosoda R, Saido TC, Otvos L Jr, Arai T, Mann DM, Lee VM, Trojanowski JQ, Iwatsubo T. *Journal of neuropathology and experimental neurology*. 1998; 57:1089–1095. [PubMed: 9825946]
42. Gomez-Ramos P, Asuncion Moran M. *Journal of Alzheimer's disease : JAD*. 2007; 11:53–59. [PubMed: 17361035]
43. Wirths O, Multhaup G, Czech C, Blanchard V, Moussaoui S, Tremp G, Pradier L, Beyreuther K, Bayer TA. *Neuroscience letters*. 2001; 306:116–120. [PubMed: 11403971]
44. Cirrito JR, Yamada KA, Finn MB, Sloviter RS, Bales KR, May PC, Schoepp DD, Paul SM, Mennicker S, Holtzman DM. *Neuron*. 2005; 48:913–922. [PubMed: 16364896]
45. Kamenetz F, Tomita T, Hsieh H, Seabrook G, Borchelt D, Iwatsubo T, Sisodia S, Malinow R. *Neuron*. 2003; 37:925–937. [PubMed: 12670422]
46. Morley JE, Farr SA, Banks WA, Johnson SN, Yamada KA, Xu L. *Journal of Alzheimer's disease : JAD*. 2010; 19:441–449. [PubMed: 19749407]
47. Ghiso J, Frangione B. *Advanced drug delivery reviews*. 2002; 54:1539–1551. [PubMed: 12453671]
48. Strozzyk D, Blennow K, White LR, Launer LJ. *Neurology*. 2003; 60:652–656. [PubMed: 12601108]
49. Scheuner D, Eckman C, Jensen M, Song X, Citron M, Suzuki N, Bird TD, Hardy J, Hutton M, Kukull W, Larson E, Levy-Lahad E, Viitanen M, Peskind E, Poorkaj P, Schellenberg G, Tanzi R, Wasco W, Lannfelt L, Selkoe D, Younkin S. *Nature medicine*. 1996; 2:864–870.
50. Kurochkin IV, Goto S. *FEBS letters*. 1994; 345:33–37. [PubMed: 8194595]
51. Iwata N, Tsubuki S, Takaki Y, Watanabe K, Sekiguchi M, Hosoki E, Kawashima-Morishima M, Lee HJ, Hama E, Sekine-Aizawa Y, Saido TC. *Nature medicine*. 2000; 6:143–150.
52. Mueller-Steiner S, Zhou Y, Arai H, Roberson ED, Sun B, Chen J, Wang X, Yu G, Esposito L, Mucke L, Gan L. *Neuron*. 2006; 51:703–714. [PubMed: 16982417]
53. Tekirian TL, Saido TC, Markesbery WR, Russell MJ, Wekstein DR, Patel E, Geddes JW. *Journal of neuropathology and experimental neurology*. 1998; 57:76–94. [PubMed: 9600199]
54. Rezaei-Ghaleh N, Amininasab M, Kumar S, Walter J, Zweckstetter M. *Nature communications*. 2016; 7:11359.
55. Al-Hilaly YK, Williams TL, Stewart-Parker M, Ford L, Skaria E, Cole M, Bucher WG, Morris KL, Sada AA, Thorpe JR, Serpell LC. *Acta neuropathologica communications*. 2013; 1:83. [PubMed: 24351276]
56. Naslund J, Schierhorn A, Hellman U, Lannfelt L, Roses AD, Tjernberg LO, Silberring J, Gandy SE, Winblad B, Greengard P, et al. *Proc Natl Acad Sci USA*. 1994; 91:8378–8382. [PubMed: 8078890]
57. Ahmed M, Davis J, Aucoin D, Sato T, Ahuja S, Aimoto S, Elliott JI, Van Nostrand WE, Smith SO. *Nature structural & molecular biology*. 2010; 17:561–567.
58. Kirschner DA, Inouye H, Duffy LK, Sinclair A, Lind M, Selkoe DJ. *Proc Natl Acad Sci USA*. 1987; 84:6953–6957. [PubMed: 3477820]
59. Soto C, Branes MC, Alvarez J, Inestrosa NC. *Journal of neurochemistry*. 1994; 63:1191–1198. [PubMed: 7931272]

60. Sani MA, Gehman JD, Separovic F. *FEBS letters*. 2011; 585:749–754. [PubMed: 21320494]
61. Serpell LC. *Biochimica et biophysica acta*. 2000; 1502:16–30. [PubMed: 10899428]
62. Shirahama T, Cohen AS. *The Journal of cell biology*. 1967; 33:679–708. [PubMed: 6036530]
63. Tomaselli S, Esposito V, Vangone P, van Nuland NA, Bonvin AM, Guerrini R, Tancredi T, Temussi PA, Picone D. *Chembiochem : a European journal of chemical biology*. 2006; 7:257–267. [PubMed: 16444756]
64. Barrow CJ, Zagorski MG. *Science*. 1991; 253:179–182. [PubMed: 1853202]
65. Crescenzi O, Tomaselli S, Guerrini R, Salvadori S, D'Ursi AM, Temussi PA, Picone D. *Eur J Biochem*. 2002; 269:5642–5648. [PubMed: 12423364]
66. Vivekanandan S, Brender JR, Lee SY, Ramamoorthy A. *Biochemical and biophysical research communications*. 2011; 411:312–316. [PubMed: 21726530]
67. Coles M, Bicknell W, Watson AA, Fairlie DP, Craik DJ. *Biochemistry*. 1998; 37:11064–11077. [PubMed: 9693002]
68. Shao H, Jao S, Ma K, Zagorski MG. *Journal of molecular biology*. 1999; 285:755–773. [PubMed: 9878442]
69. Wood SJ, Maleeff B, Hart T, Wetzel R. *Journal of molecular biology*. 1996; 256:870–877. [PubMed: 8601838]
70. Narayanan S, Reif B. *Biochemistry*. 2005; 44:1444–1452. [PubMed: 15683229]
71. Danielsson J, Jarvet J, Damberg P, Graslund A. *The FEBS journal*. 2005; 272:3938–3949. [PubMed: 16045764]
72. Fezoui Y, Teplov DB. *J Biol Chem*. 2002; 277:36948–36954. [PubMed: 12149256]
73. Abedini A, Raleigh DP. *Physical biology*. 2009; 6:015005. [PubMed: 19208933]
74. Tycko R. *Quarterly reviews of biophysics*. 2006; 39:1–55. [PubMed: 16772049]
75. Kumar S, Rezaei-Ghaleh N, Terwel D, Thal DR, Richard M, Hoch M, Mc Donald JM, Wullner U, Glebov K, Heneka MT, Walsh DM, Zweckstetter M, Walter J. *The EMBO journal*. 2011; 30:2255–2265. [PubMed: 21527912]
76. He W, Barrow CJ. *Biochemistry*. 1999; 38:10871–10877. [PubMed: 10451383]
77. D'Arrigo C, Tabaton M, Perico A. *Biopolymers*. 2009; 91:861–873. [PubMed: 19562755]
78. Hortschansky P, Schroeckh V, Christopeit T, Zandomeneghi G, Fandrich M. *Protein science : a publication of the Protein Society*. 2005; 14:1753–1759. [PubMed: 15937275]
79. Meisl G, Yang X, Hellstrand E, Frohm B, Kirkegaard JB, Cohen SI, Dobson CM, Linse S, Knowles TP. *Proc Natl Acad Sci USA*. 2014; 111:9384–9389. [PubMed: 24938782]
80. Arosio P, Knowles TP, Linse S. *Physical chemistry chemical physics : PCCP*. 2015; 17:7606–7618. [PubMed: 25719972]
81. Meisl G, Yang X, Frohm B, Knowles TP, Linse S. *Scientific reports*. 2016; 6:18728. [PubMed: 26758487]
82. Adamcik J, Lara C, Usov I, Jeong JS, Ruggeri FS, Dietler G, Lashuel HA, Hamley IW, Mezzenga R. *Nanoscale*. 2012; 4:4426–4429. [PubMed: 22688679]
83. Petkova AT, Ishii Y, Balbach JJ, Antzutkin ON, Leapman RD, Delaglio F, Tycko R. *Proc Natl Acad Sci USA*. 2002; 99:16742–16747. [PubMed: 12481027]
84. Lu JX, Qiang W, Yau WM, Schwieters CD, Meredith SC, Tycko R. *Cell*. 2013; 154:1257–1268. [PubMed: 24034249]
85. Colvin MT, Silvers R, Ni QZ, Can TV, Sergeyev I, Rosay M, Donovan KJ, Michael B, Wall J, Linse S, Griffin RG. *Journal of the American Chemical Society*. 2016; 138:9663–9674. [PubMed: 27355699]
86. Xiao Y, Ma B, McElheny D, Parthasarathy S, Long F, Hoshi M, Nussinov R, Ishii Y. *Nature structural & molecular biology*. 2015; 22:499–505.
87. Walsh DM, Klyubin I, Fadeeva JV, Rowan MJ, Selkoe DJ. *Biochem Soc Trans*. 2002; 30:552–557. [PubMed: 12196135]
88. Schrag M, Mueller C, Oyoyo U, Smith MA, Kirsch WM. *Progress in neurobiology*. 2011; 94:296–306. [PubMed: 21600264]
89. Hallgren B, Sourander P. *Journal of neurochemistry*. 1960; 5:307–310. [PubMed: 14399117]

90. Schrag M, Dickson A, Jiffry A, Kirsch D, Vinters HV, Kirsch W. *Biometals : an international journal on the role of metal ions in biology, biochemistry, and medicine*. 2010; 23:1123–1127.
91. Bush AI, Pettingell WH, Multhaup G, Paradis Md, Vonsattel JP, Gusella JF, Beyreuther K, Masters CL, Tanzi RE. *Science*. 1994; 265:1464–1467. [PubMed: 8073293]
92. Markesbery WR. *Archives of neurology*. 1999; 56:1449–1452. [PubMed: 10593298]
93. Bush AI. *Current opinion in chemical biology*. 2000; 4:184–191. [PubMed: 10742195]
94. Butterfield DA, Sultana R. *Journal of amino acids*. 2011; 2011:198430. [PubMed: 22312456]
95. Cassagnes LE, Herve V, Nepveu F, Hureau C, Faller P, Collin F. *Angew Chem Int Ed*. 2013; 52:11110–11113.
96. Parthasarathy S, Yoo B, McElheny D, Tay W, Ishii Y. *J Biol Chem*. 2014; 289:9998–10010. [PubMed: 24523414]
97. Keskitalo S, Farkas M, Hanenberg M, Szodorai A, Kulic L, Semmler A, Weller M, Nitsch RM, Linnebank M. *Frontiers in aging neuroscience*. 2014; 6:237. [PubMed: 25249976]
98. Smith DG, Cappai R, Barnham KJ. *Biochimica et biophysica acta*. 2007; 1768:1976–1990. [PubMed: 17433250]
99. Eckert GP, Wood WG, Muller WE. *Current protein & peptide science*. 2010; 11:319–325. [PubMed: 20423299]
100. Aisenbrey C, Borowik T, Bystrom R, Bokvist M, Lindstrom F, Misiak H, Sani MA, Grobner G. *European biophysics journal : EBJ*. 2008; 37:247–255. [PubMed: 18030461]
101. Bystrom R, Aisenbrey C, Borowik T, Bokvist M, Lindstrom F, Sani MA, Olofsson A, Grobner G. *Cell biochemistry and biophysics*. 2008; 52:175–189. [PubMed: 18975139]
102. Weber DK, Gehman JD, Separovic F, Sani MA. *Aus J Chem*. 2012; 65:472–479.
103. Bhowmik D, Mote KR, MacLaughlin CM, Biswas N, Chandra B, Basu JK, Walker GC, Madhu PK, Maiti S. *ACS nano*. 2015; 9:9070–9077. [PubMed: 26391443]
104. Lau TL, Gehman JD, Wade JD, Masters CL, Barnham KJ, Separovic F. *Biochimica et biophysica acta*. 2007; 1768:3135–3144. [PubMed: 17920561]
105. Hicks DA, Nalivaeva NN, Turner AJ. *Frontiers in physiology*. 2012; 3:189. [PubMed: 22737128]
106. Beel AJ, Mobley CK, Kim HJ, Tian F, Hadziselimovic A, Jap B, Prestegard JH, Sanders CR. *Biochemistry*. 2008; 47:9428–9446. [PubMed: 18702528]
107. Lacor PN, Buniel MC, Chang L, Fernandez SJ, Gong Y, Viola KL, Lambert MP, Velasco PT, Bigio EH, Finch CE, Krafft GA, Klein WL. *The Journal of neuroscience : the official journal of the Society for Neuroscience*. 2004; 24:10191–10200. [PubMed: 15537891]
108. Garaschuk O, Schneggenburger R, Schirra C, Tempia F, Konnerth A. *The Journal of physiology*. 1996; 491(Pt 3):757–772. [PubMed: 8815209]
109. Wang HY, Lee DH, D'Andrea MR, Peterson PA, Shank RP, Reitz AB. *J Biol Chem*. 2000; 275:5626–5632. [PubMed: 10681545]
110. Snyder EM, Nong Y, Almeida CG, Paul S, Moran T, Choi EY, Nairn AC, Salter MW, Lombroso PJ, Gouras GK, Greengard P. *Nature neuroscience*. 2005; 8:1051–1058. [PubMed: 16025111]
111. Hansson Petersen CA, Alikhani N, Behbahani H, Wiehager B, Pavlov PF, Alafuzoff I, Leinonen V, Ito A, Winblad B, Glaser E, Ankarcrona M. *Proc Natl Acad Sci USA*. 2008; 105:13145–13150. [PubMed: 18757748]
112. Manczak M, Calkins MJ, Reddy PH. *Human molecular genetics*. 2011; 20:2495–2509. [PubMed: 21459773]
113. Du H, Guo L, Yan S, Sosunov AA, McKhann GM, Yan SS. *Proc Natl Acad Sci USA*. 2010; 107:18670–18675. [PubMed: 20937894]
114. D'Amelio M, Cavallucci V, Middei S, Marchetti C, Pacioni S, Ferri A, Diamantini A, De Zio D, Carrara P, Battistini L, Moreno S, Bacci A, Ammassari-Teule M, Marie H, Cecconi F. *Nature neuroscience*. 2011; 14:69–76. [PubMed: 21151119]
115. Berger Z, Ravikumar B, Menzies FM, Oroz LG, Underwood BR, Pangalos MN, Schmitt I, Wullner U, Evert BO, O'Kane CJ, Rubinsztein DC. *Human molecular genetics*. 2006; 15:433–442. [PubMed: 16368705]
116. Wen G, Qin W, Chen D, Wang Y, Yue X, Liu Z, Cao Y, Du J, Zhou B, Bu X. *Chemical communications*. 2017; 53:3886–3889. [PubMed: 28317984]

117. Sevigny J, Chiao P, Bussiere T, Weinreb PH, Williams L, Maier M, Dunstan R, Salloway S, Chen T, Ling Y, O'Gorman J, Qian F, Arastu M, Li M, Chollate S, Brennan MS, Quintero-Monzon O, Scannevin RH, Arnold HM, Engber T, Rhodes K, Ferrero J, Hang Y, Mikulskis A, Grimm J, Hock C, Nitsch RM, Sandrock A. *Nature*. 2016; 537:50–56. [PubMed: 27582220]
118. Squitti R, Lupoi D, Pasqualetti P, Dal Forno G, Vernieri F, Chioventa P, Rossi L, Cortesi M, Cassetta E, Rossini PM. *Neurology*. 2002; 59:1153–1161. [PubMed: 12391342]
119. Carroll J. *Science*. 2017; doi: 10.1126/science.aal0759
120. Vassar R, Kuhn PH, Haass C, Kennedy ME, Rajendran L, Wong PC, Lichtenthaler SF. *Journal of neurochemistry*. 2014; 130:4–28. [PubMed: 24646365]
121. Rajendran L, Schneider A, Schlechtingen G, Weidlich S, Ries J, Braxmeier T, Schulle P, Schulz JB, Schroeder C, Simons M, Jennings G, Knolker HJ, Simons K. *Science*. 2008; 320:520–523. [PubMed: 18436784]
122. Wang X, Su B, Siedlak SL, Moreira PI, Fujioka H, Wang Y, Casadesus G, Zhu X. *Proc Natl Acad Sci USA*. 2008; 105:19318–19323. [PubMed: 19050078]
123. Noble W, Garwood C, Stephenson J, Kinsey AM, Hanger DP, Anderton BH. *FASEB journal : official publication of the Federation of American Societies for Experimental Biology*. 2009; 23:739–750. [PubMed: 19001528]
124. Cummings JL, Morstorf T, Zhong K. *Alzheimer's research & therapy*. 2014; 6:37.
125. Fu H, Cui M, Zhao L, Tu P, Zhou K, Dai J, Liu B. *Journal of medicinal chemistry*. 2015; 58:6972–6983. [PubMed: 26262759]
126. Bolognesi ML, Gandini A, Prati F, Uliassi E. *J Med Chem*. 2016; 59:7759–7770. [PubMed: 27124551]
127. Westermark P, Andersson A, Westermark GT. *Physiol Rev*. 2011; 91:795–826. [PubMed: 21742788]
128. Marzban L, Trigo-Gonzalez G, Zhu X, Rhodes CJ, Halban PA, Steiner DF, Verchere CB. *Diabetes*. 2004; 53:141–148. [PubMed: 14693708]
129. Wang J, Xu J, Finnerty J, Furuta M, Steiner DF, Verchere CB. *Diabetes*. 2001; 50:534–539. [PubMed: 11246872]
130. German MS, Moss LG, Wang J, Rutter WJ. *Mol Cell Biol*. 1992; 12:1777–1788. [PubMed: 1549125]
131. Lutz TA. *Physiology & Behavior*. 2006; 89:465–471. [PubMed: 16697020]
132. Young A. *Adv Pharmacol*. 2005; 52:99–121. [PubMed: 16492543]
133. Naot D, Cornish J. *Bone*. 2008; 43:813–818. [PubMed: 18687416]
134. Luca S, Yau W-M, Leapman R, Tycko R. *Biochemistry*. 2007; 46:13505–13522. [PubMed: 17979302]
135. Wiltzius JJW, Sievers SA, Sawaya MR, Cascio D, Popov D, Riek C, Eisenberg D. *Protein science : a publication of the Protein Society*. 2008; 17:1467–1474. [PubMed: 18556473]
136. Bedrood S, Li Y, Isas JM, Hegde BG, Baxa U, Haworth IS, Langen R. *J Biol Chem*. 2012; 287:5235–5241. [PubMed: 22187437]
137. Patil SM, Xu S, Sheftic SR, Alexandrescu AT. *J Biol Chem*. 2009; 284:11982–11991. [PubMed: 19244249]
138. Nanga RPR, Brender JR, Vivekanandan S, Ramamoorthy A. *Biochimica et biophysica acta*. 2011; 1808:2337–2342. [PubMed: 21723249]
139. Camargo DCR, Tripsianes K, Buday K, Franko A, Göbl C, Hartlmüller C, Sarkar R, Aichler M, Mettenleiter G, Schulz M, Böddrich A, Erck C, Martens H, Walch AK, Madl T, Wanker EE, Conrad M, Angelis MHD, Reif B. *Scientific reports*. 2017; 7:44041. [PubMed: 28287098]
140. Nedumpully-Govindan P, Ding F. *Scientific reports*. 2015; 5:8240. [PubMed: 25649462]
141. Sumner Makin O, Serpell LC. *Journal of molecular biology*. 2004; 335:1279–1288. [PubMed: 14729343]
142. Goldsburly C, Kistler J, Aebi U, Arvinte T, Cooper GJS. *Journal of molecular biology*. 1999; 285:33–39. [PubMed: 9878384]
143. Goldsburly CS, Cooper GJS, Goldie KN, Müller SA, Saafi EL, Gruijters WTM, Misur MP, Engel A, Aebi U, Kistler J. *Journal of Structural Biology*. 1997; 119:17–27. [PubMed: 9216085]



144. Chakraborty S, Chatterjee B, Basu S. *Biophys Chem.* 2012; 168–169:1–9.
145. Sakagashira S, Hiddinga HJ, Tateishi K, Sanke T, Hanabusa T, Nanjo K, Eberhardt NL. *The American journal of pathology.* 2000; 157:2101–2109. [PubMed: 11106582]
146. Seino S. Study Group of Comprehensive Analysis of Genetic Factors in Diabetes M. *Diabetologia.* 2001; 44:906–909. [PubMed: 11508277]
147. Westermark P, Eizirik DL, Pipeleers DG, Hellerström C, Andersson A. *Diabetologia.* 1995; 38:543–549. [PubMed: 7489836]
148. Udayasankar J, Kodama K, Hull RL, Zraika S, Aston-Mourney K, Subramanian SL, Tong J, Faulenbach MV, Vidal J, Kahn SE. *Diabetologia.* 2009; 52:145–153. [PubMed: 19002432]
149. Janson J, Soeller WC, Roche PC, Nelson RT, Torchia AJ, Kreutter DK, Butler PC. *Proc Natl Acad Sci USA.* 1996; 93:7283–7288. [PubMed: 8692984]
150. Yankner BA, Dawes LR, Fisher S, Villa-Komaroff L, Oster-Granite ML, Neve RL. *Science.* 1989; 245:417–420. [PubMed: 2474201]
151. Yankner BA, Duffy LK, Kirschner DA. *Science.* 1990; 250:279–282. [PubMed: 2218531]
152. Lorenzo A, Razzaboni B, Weir GC, Yankner BA. *Nature.* 1994; 368:756–760. [PubMed: 8152488]
153. Lorenzo A, Yankner BA. *Ann N Y Acad Sci.* 1996; 777:89–95. [PubMed: 8624132]
154. Janson J, Ashley RH, Harrison D, McIntyre S, Butler PC. *Diabetes.* 1999; 48:491–498. [PubMed: 10078548]
155. Ritzel RA, Meier JJ, Lin C-Y, Veldhuis JD, Butler PC. *Diabetes.* 2007; 56:65–71. [PubMed: 17192466]
156. Wong WPS, Scott DW, Chuang C-L, Zhang S, Liu H, Ferreira A, Saafi EL, Choong YS, Cooper GJS. *Diabetes.* 2008; 57:2737–2744. [PubMed: 18633116]
157. Butler AE, Janson J, Soeller WC, Butler PC. *Diabetes.* 2003; 52:2304–2314. [PubMed: 12941770]
158. Meier JJ, Kaye R, Lin C-Y, Gurlo T, Haataja L, Jayasinghe S, Langen R, Glabe CG, Butler PC. *Am J Physiol Endocrinol Metab.* 2006; 291:E1317–1324. [PubMed: 16849627]
159. Pilkington EH, Xing Y, Wang B, Kakinen A, Wang M, Davis TD, Ding F, Ke PC. *Scientific reports.* 2017; doi: 10.1038/s41598-017-02597-0
160. Haataja L, Gurlo T, Huang CJ, Butler PC. *Endocrine Reviews.* 2008; 29:303–316. [PubMed: 18314421]
161. Zraika S, Hull RL, Verchere CB, Clark A, Potter KJ, Fraser PE, Raleigh DP, Kahn SE. *Diabetologia.* 2010; 53:1046–1056. [PubMed: 20182863]
162. Williamson JA, Miranker AD. *Protein science : a publication of the Protein Society.* 2007; 16:110–117. [PubMed: 17123962]
163. Williamson JA, Loria JP, Miranker AD. *Journal of molecular biology.* 2009; 393:383–396. [PubMed: 19647750]
164. Wiltzius JJW, Sievers SA, Sawaya MR, Eisenberg D. *Protein science : a publication of the Protein Society.* 2009; 18:1521–1530. [PubMed: 19475663]
165. Cao P, Abedini A, Raleigh DP. *Curr Opin Struct Biol.* 2013; 23:82–89. [PubMed: 23266002]
166. Dupuis NF, Wu C, Shea J-E, Bowers MT. *Journal of the American Chemical Society.* 2011; 133:7240–7243. [PubMed: 21517093]
167. Okamoto Y. *Journal of Molecular Graphics and Modelling.* 2004; 22:425–439. [PubMed: 15099838]
168. Padrick SB, Miranker AD. *Biochemistry.* 2002; 41:4694–4703. [PubMed: 11926832]
169. Hutton JC. *Diabetologia.* 32:271–281.
170. DeToma AS, Salamekh S, Ramamoorthy A, Lim MH. *Chem Soc Rev.* 2012; 41:608–621. [PubMed: 21818468]
171. Chimenti F, Favier A, Seve M. *Biometals : an international journal on the role of metal ions in biology, biochemistry, and medicine.* 2005; 18:313–317.

172. Lemaire K, Ravier MA, Schraenen A, Creemers JWM, Van de Plas R, Granvik M, Van Lommel L, Waelkens E, Chimienti F, Rutter GA, Gilon P, in't Veld PA, Schuit FC. *Proc Natl Acad Sci USA*. 2009; 106:14872–14877. [PubMed: 19706465]
173. Hull RL, Westermark GT, Westermark P, Kahn SE. *J Clin Endocrinol Metab*. 2004; 89:3629–3643. [PubMed: 15292279]
174. Jha S, Snell JM, Sheftic SR, Patil SM, Daniels SB, Kolling FW, Alexandrescu AT. *Biochemistry*. 2014; 53:300–310. [PubMed: 24377660]
175. Khemtémourian L, Doménech E, Doux JPF, Koorengevel MC, Killian JA. *Journal of the American Chemical Society*. 2011; 133:15598–15604. [PubMed: 21870807]
176. Abedini A, Raleigh DP. *Biochemistry*. 2005; 44:16284–16291. [PubMed: 16331989]
177. Nedumpully-Govindan P, Jemec DB, Ding F. *J Chem Inf Model*. 2015; doi: 10.1021/acs.jcim.5b00303
178. Hutton JC. *Biochem J*. 1982; 204:171–178. [PubMed: 6126183]
179. Nedumpully-Govindan P, Yang Y, Andorfer R, Cao W, Ding F. *Biochemistry*. 2015; 54:7335–7344. [PubMed: 26603575]
180. Larson JL, Miranker AD. *Journal of molecular biology*. 2004; 335:221–231. [PubMed: 14659752]
181. Gilead S, Wolfenson H, Gazit E. *Angew Chemie Int Ed*. 2006; 45:6476–6480.
182. Susa AC, Wu C, Bernstein SL, Dupuis NF, Wang H, Raleigh DP, Shea J-E, Bowers MT. *Journal of the American Chemical Society*. 2014; 136:12912–12919. [PubMed: 25144879]
183. Dodson G, Steiner D. *Curr Opin Struct Biol*. 1998; 8:189–194. [PubMed: 9631292]
184. Flannick J, Thorleifsson G, Beer NL, Jacobs SBR, Grarup N, Burtt NP, Mahajan A, Fuchsberger C, Atzmon G, Benediktsson R, Blangero J, Bowden DW, Brandslund I, Brosnan J, Burslem F, Chambers J, Cho YS, Christensen C, Douglas DA, Duggirala R, Dymek Z, Farjoun Y, Fennell T, Fontanillas P, Forsén T, Gabriel S, Glaser B, Gudbjartsson DF, Hanis C, Hansen T, Hreidarsson AB, Hveem K, Ingelsson E, Isomaa B, Johansson S, Jørgensen T, Jørgensen ME, Kathiresan S, Kong A, Kooner J, Kravic J, Laakso M, Lee J-Y, Lind L, Lindgren CM, Linneberg A, Masson G, Meitinger T, Mohlke KL, Molven A, Morris AP, Potluri S, Rauramaa R, Ribel-Madsen R, Richard A-M, Rolph T, Salomaa V, Segrè AV, Skärstrand H, Steinthorsdottir V, Stringham HM, Sulem P, Tai ES, Teo YY, Teslovich T, Thorsteinsdottir U, Trimmer JK, Tuomi T, Tuomilehto J, Vaziri-Sani F, Voight BF, Wilson JG, Boehnke M, McCarthy MI, Njølstad PR, Pedersen O, Go TDC, Groop L, Cox DR, Stefansson K, Altshuler D. *Nat Genet*. 2014; 46:357–363. [PubMed: 24584071]
185. Westermark P, Li Z-C, Westermark GT, Leckström A, Steiner DF. *FEBS letters*. 1996; 379:203–206. [PubMed: 8603689]
186. Brender JR, Hartman K, Nanga RPR, Popovych N, de la Salud Bea R, Vivekanandan S, Marsh ENG, Ramamoorthy A. *Journal of the American Chemical Society*. 2010; 132:8973–8983. [PubMed: 20536124]
187. Salamekh S, Brender JR, Hyung S-J, Nanga RPR, Vivekanandan S, Ruotolo BT, Ramamoorthy A. *Journal of molecular biology*. 2011; 410:294–306. [PubMed: 21616080]
188. Munte CE, Vilela L, Kalbitzer HR, Garratt RC. *The FEBS journal*. 2005; 272:4284–4293. [PubMed: 16098208]
189. Keltner Z, Meyer JA, Johnson EM, Palumbo AM, Spence DM, Reid GE. *Analyst*. 2010; 135:278–288. [PubMed: 20098759]
190. Giebink AW, Vogel PA, Medawala W, Spence DM. *Diabetes*. 2013; 29:44–52.
191. Meng F, Abedini A, Song B, Raleigh DP. *Biochemistry*. 2007; 46:12091–12099. [PubMed: 17924651]
192. Brender JR, Salamekh S, Ramamoorthy A. *Acc Chem Res*. 2012; 45:454–462. [PubMed: 21942864]
193. Khemtémourian L, Killian JA, Höppener JWM, Engel MFM. *Exp Diabetes Res*. 2008; 2008:421287. [PubMed: 18483616]
194. Hebda JA, Miranker AD. *Annu Rev Biophys*. 2009; 38:125–152. [PubMed: 19416063]

195. Pilkington EH, Gurzov EN, Kakinen A, Litwak SA, Stanley WJ, Davis TP, Ke PC. *Scientific reports*. 2016; 6:21274. [PubMed: 26880502]
196. Mirzabekov TA, Lin MC, Kagan BL. *J Biol Chem*. 1996; 271:1988–1992. [PubMed: 8567648]
197. Last NB, Rhoades E, Miranker AD. *Proc Natl Acad Sci USA*. 2011; 108:9460–9465. [PubMed: 21606325]
198. Anguiano M, Nowak RJ, Lansbury PT. *Biochemistry*. 2002; 41:11338–11343. [PubMed: 12234175]
199. Hirakura Y, Yiu WW, Yamamoto A, Kagan BL. *Amyloid*. 2000; 7:194–199. [PubMed: 11019860]
200. Quist A, Doudevski I, Lin H, Azimova R, Ng D, Frangione B, Kagan B, Ghiso J, Lal R. *Proc Natl Acad Sci USA*. 2005; 102:10427–10432. [PubMed: 16020533]
201. Green JD, Kreplak L, Goldsbury C, Li Blatter X, Stolz M, Cooper GS, Seelig A, Kistler J, Aepli U. *Journal of molecular biology*. 2004; 342:877–887. [PubMed: 15342243]
202. Engel MFM, Khemtémourian L, Kleijer CC, Meeldijk HJD, Jacobs J, Verkleij AJ, de Kruijff B, Killian JA, Höppener JWM. *Proc Natl Acad Sci USA*. 2008; 105:6033–6038. [PubMed: 18408164]
203. Cao P, Abedini A, Wang H, Tu L-H, Zhang X, Schmidt AM, Raleigh DP. *Proc Natl Acad Sci USA*. 2013; 110:19279–19284. [PubMed: 24218607]
204. Cohen FE, Kelly JW. *Nature*. 2003; 426:905–909. [PubMed: 14685252]
205. Klabunde T, Petrassi HM, Oza VB, Raman P, Kelly JW, Sacchettini JC. *Nat Struct Biol*. 2000; 7:312–321. [PubMed: 10742177]
206. Wang H, Duennwald ML, Roberts BE, Rozeboom LM, Zhang YL, Steele AD, Krishnan R, Su LJ, Griffin D, Mukhopadhyay S, Hennessy EJ, Weigele P, Blanchard BJ, King J, Deniz AA, Buchwald SL, Ingram VM, Lindquist S, Shorter J. *Proc Natl Acad Sci USA*. 2008; 105:7159–7164. [PubMed: 18480256]
207. Meng F, Abedini A, Plesner A, Middleton CT, Potter KJ, Zanni MT, Verchere CB, Raleigh DP. *Journal of molecular biology*. 2010; 400:555–566. [PubMed: 20452363]
208. Abedini A, Meng F, Raleigh DP. *Journal of the American Chemical Society*. 2007; 129:11300–11301. [PubMed: 17722920]
209. Sellin D, Yan L-M, Kapurniotu A, Winter R. *Biophys Chem*. 2010; 150:73–79. [PubMed: 20153100]
210. Yan L-M, Velkova A, Tatarek-Nossol M, Andreetto E, Kapurniotu A. *Angew Chemie Int Ed*. 2007; 46:1246–1252.
211. Yan L-M, Tatarek-Nossol M, Velkova A, Kazantzis A, Kapurniotu A. *Proc Natl Acad Sci USA*. 2006; 103:2046–2051. [PubMed: 16467158]
212. Saraogi I, Hebda JA, Becerril J, Estroff LA, Miranker AD, Hamilton AD. *Angew Chemie Int Ed*. 2010; 49:736–739.
213. Hebda JA, Saraogi I, Magzoub M, Hamilton AD, Miranker AD. *Chemistry & Biology*. 2009; 16:943–950. [PubMed: 19778722]
214. Meng F, Abedini A, Plesner A, Verchere CB, Raleigh DP. *Biochemistry*. 2010; 49:8127–8133. [PubMed: 20707388]
215. Young LM, Saunders JC, Mahood RA, Reville CH, Foster RJ, Tu LH, Raleigh DP, Radford SE, Ashcroft AE. *Nat Chem*. 2015; 7:73–81. [PubMed: 25515893]
216. Noor H, Cao P, Raleigh DP. *Protein science : a publication of the Protein Society*. 2012; 21:373–382. [PubMed: 22238175]
217. Zelus C, Fox A, Calciano A, Faridian BS, Nogaj LA, Moffet DA. *Open Biochem J*. 2012; 6:66–70. [PubMed: 22792130]
218. Tu L-H, Noor H, Cao P, Raleigh DP. *ACS Chem Biol*. 2014; 9:1632–1637. [PubMed: 24837419]
219. Daval M, Bedrood S, Gurlo T, Huang C-J, Costes S, Butler PC, Langen R. *Amyloid*. 2010; 17:118–128. [PubMed: 21067307]
220. Sparks S, Liu G, Robbins KJ, Lazo ND. *Biochemical and biophysical research communications*. 2012; 422:551–555. [PubMed: 22579683]
221. Cheng B, Gong H, Li X, Sun Y, Zhang X, Chen H, Liu X, Zheng L, Huang K. *Biochemical and biophysical research communications*. 2012; 419:495–499. [PubMed: 22366091]

222. Rigacci S, Guidotti V, Bucciattini M, Parri M, Nediani C, Cerbai E, Stefani M, Berti A. *The Journal of Nutritional Biochemistry*. 2010; 21:726–735. [PubMed: 19616928]
223. Mishra R, Sellin D, Radovan D, Gohlke A, Winter R. *ChemBioChem*. 2009; 10:445–449. [PubMed: 19165839]
224. Gurzov EN, Wang B, Pilkington EH, Chen P, Kakinen A, Stanley WJ, Litwak SA, Hanssen EG, Davis TP, Ding F, Ke PC. *Small*. 2016; 12:1615–1626. [PubMed: 26808649]
225. Nedumpully-Govindan P, Gurzov EN, Chen P, Pilkington EH, Stanley WJ, Litwak SA, Davis TP, Ke PC, Ding F. *Physical chemistry chemical physics : PCCP*. 2016; 18:94–100. [PubMed: 26625841]
226. Cabaleiro-Lago C, Quinlan-Pluck F, Lynch I, Dawson KA, Linse S. *ACS Chem Neurosci*. 2010; 1:279–287. [PubMed: 22778827]
227. Middleton CT, Marek P, Cao P, Chiu C-c, Singh S, Woys AM, de Pablo JJ, Raleigh DP, Zanni MT. *Nat Chem*. 2012; 4:355–360. [PubMed: 22522254]
228. Ehrhoefer DE, Bieschke J, Boeddrich A, Herbst M, Masino L, Lurz R, Engemann S, Pastore A, Wanker EE. *Nature structural & molecular biology*. 2008; 15:558–566.
229. Ladiwala ARA, Lin JC, Bale SS, Marcelino-Cruz AM, Bhattacharya M, Dordick JS, Tessier PM. *J Biol Chem*. 2010; 285:24228–24237. [PubMed: 20511235]
230. Mishra R, Bulic B, Sellin D, Jha S, Waldmann H, Winter R. *Angew Chemie Int Ed*. 2008; 47:4679–4682.
231. Yang F, Lim GP, Begum AN, Ubeda OJ, Simmons MR, Ambegaokar SS, Chen PP, Kaye R, Glabe CG, Frautschy SA, Cole GM. *J Biol Chem*. 2005; 280:5892–5901. [PubMed: 15590663]
232. Adessi C, Soto C. *Curr Med Chem*. 2002; 9:963–978. [PubMed: 11966456]
233. Santos AC, Veiga F, Ribeiro AJ. *Expert Opin Drug Deliv*. 2011; 8:973–990. [PubMed: 21668403]
234. Nedumpully-Govindan P, Kakinen A, Pilkington EH, Davis TP, Chun Ke P, Ding F. *Scientific reports*. 2016; 6:19463. [PubMed: 26763863]
235. Jiang P, Li W, Shea JE, Mu Y. *Biophys J*. 2011; 100:1550–1558. [PubMed: 21402038]
236. Lolicato F, Raudino A, Milardi D, La Rosa C. *Eur J Med Chem*. 2015; 92:876–881. [PubMed: 25638571]
237. Wang QQ, Ning LL, Niu YZ, Liu HX, Yao XJ. *J Phys Chem B*. 2015; 119:15–24. [PubMed: 25494644]
238. Maroteaux L, Campanelli J, Scheller R. *The Journal of neuroscience : the official journal of the Society for Neuroscience*. 1988; 8:2804–2815. [PubMed: 3411354]
239. Sampson TR, Debelius JW, Thron T, Janssen S, Shastri GG, Ilhan ZE, Challis C, Schretter CE, Rocha S, Gradinaru V, Chesselet M-F, Keshavarzian A, Shannon KM, Krajmalnik-Brown R, Wittung-Stafshede P, Knight R, Mazmanian SK. *Cell*. 2016; 167:1469–1480.e1412. [PubMed: 27912057]
240. Burré J, Sharma M, Südhof TC. *Proc Natl Acad Sci USA*. 2014; 111:E4274–E4283. [PubMed: 25246573]
241. Vilar M, Chou H-T, Lührs T, Maji SK, Riek-Loher D, Verel R, Manning G, Stahlberg H, Riek R. *Proc Natl Acad Sci USA*. 2008; 105:8637–8642. [PubMed: 18550842]
242. Spillantini MG, Schmidt ML, Lee VMY, Trojanowski JQ, Jakes R, Goedert M. *Nature*. 1997; 388:839–840. [PubMed: 9278044]
243. Irwin DJ, Lee VMY, Trojanowski JQ. *Nat Rev Neurosci*. 2013; 14:626–636. [PubMed: 23900411]
244. Periquet M, Fulga T, Myllykangas L, Schlossmacher MG, Feany MB. *The Journal of neuroscience : the official journal of the Society for Neuroscience*. 2007; 27:3338–3346. [PubMed: 17376994]
245. Stefanis L. *Cold Spring Harb Perspect Med*. 2012; 2:a009399. [PubMed: 22355802]
246. Villar-Piqué A, Lopes da Fonseca T, Outeiro TF. *Journal of neurochemistry*. 2016; 139:240–255. [PubMed: 26190401]
247. Vlad C, Lindner K, Karreman C, Schildknecht S, Leist M, Tomczyk N, Rontree J, Langridge J, Danzer K, Ciossek T, Petre A, Gross ML, Hengerer B, Przybylski M. *ChemBioChem*. 2011; 12:2740–2744. [PubMed: 22162214]

248. Rodriguez JA, Ivanova MI, Sawaya MR, Cascio D, Reyes FE, Shi D, Sangwan S, Guenther EL, Johnson LM, Zhang M, Jiang L, Arbing MA, Nannenga BL, Hattne J, Whitelegge J, Brewster AS, Messerschmidt M, Boutet S, Sauter NK, Gonen T, Eisenberg DS. *Nature*. 2015; 525:486–490. [PubMed: 26352473]
249. Tuttle MD, Comellas G, Nieuwkoop AJ, Covell DJ, Berthold DA, Kloepper KD, Courtney JM, Kim JK, Barclay AM, Kendall A, Wan W, Stubbs G, Schwieters CD, Lee VMY, George JM, Rienstra CM. *Nature structural & molecular biology*. 2016; 23:409–415.
250. Comellas G, Lemkau LR, Nieuwkoop AJ, Kloepper KD, Lador DT, Ebisu R, Woods WS, Lipton AS, George JM, Rienstra CM. *Journal of molecular biology*. 2011; 411:881–895. [PubMed: 21718702]
251. Conway KA, Lee S-J, Rochet J-C, Ding TT, Williamson RE, Lansbury PT. *Proc Natl Acad Sci USA*. 2000; 97:571–576. [PubMed: 10639120]
252. Rochet J-C, Conway KA, Lansbury PT. *Biochemistry*. 2000; 39:10619–10626. [PubMed: 10978144]
253. Khurana R, Ionescu-Zanetti C, Pope M, Li J, Nielson L, Ramírez-Alvarado M, Regan L, Fink AL, Carter SA. *Biophys J*. 2003; 85:1135–1144. [PubMed: 12885658]
254. Ionescu-Zanetti C, Khurana R, Gillespie JR, Petrick JS, Trabachino LC, Minert LJ, Carter SA, Fink AL. *Proc Natl Acad Sci USA*. 1999; 96:13175–13179. [PubMed: 10557293]
255. Harper JD, Lieber CM, Lansbury PT. *Chemistry & Biology*. 1997; 4:951–959. [PubMed: 9427660]
256. Stine WB, Snyder SW, Lador US, Wade WS, Miller MF, Perun TJ, Holzman TF, Krafft GA. *J Prot Chem*. 1996; 15:193–203.
257. Blackley HKL, Sanders GHW, Davies MC, Roberts CJ, Tendler SJB, Wilkinson MJ. *Journal of molecular biology*. 2000; 298:833–840. [PubMed: 10801352]
258. Chamberlain AK, MacPhee CE, Zurdo J, Morozova-Roche LA, Hill HA, Dobson CM, Davis JJ. *Biophys J*. 2000; 79:3282–3293. [PubMed: 11106631]
259. Kad NM, Thomson NH, Smith DP, Smith DA, Radford SE. *Journal of molecular biology*. 2001; 313:559–571. [PubMed: 11676539]
260. Adamcik J, Jung J-M, Flakowski J, De Los Rios P, Dietler G, Mezzenga R. *Nat Nanotech*. 2010; 5:423–428.
261. Sweers KKM, Segers-Nolten IMJ, Bennink ML, Subramaniam V. *Soft Matter*. 2012; 8:7215–7222.
262. Crowther RA, Daniel SE, Goedert M. *Neuroscience letters*. 2000; 292:128–130. [PubMed: 10998565]
263. Sweers KKM, Bennink ML, Subramaniam V. *J Phys Condens Matter*. 2012; 24:243101. [PubMed: 22585542]
264. Bhak G, Lee S, Park JW, Cho S, Paik SR. *Biomater*. 2010; 31:5986–5995.
265. Uversky VN, Li J, Fink AL. *J Biol Chem*. 2001; 276:10737–10744. [PubMed: 11152691]
266. Xu L, Ma B, Nussinov R, Thompson D. *ACS Chem Neurosci*. 2017; 8:837–849. [PubMed: 28075555]
267. Deleersnijder A, Gerard M, Debyser Z, Baekelandt V. *Trends Mol Med*. 2013; 19:368–377. [PubMed: 23648364]
268. Lashuel HA, Overk CR, Oueslati A, Masliah E. *Nat Rev Neurosci*. 2013; 14:38–48. [PubMed: 23254192]
269. Lorenzen N, Nielsen SB, Buell AK, Kaspersen JD, Arosio P, Vad BS, Paslawski W, Christiansen G, Valnickova-Hansen Z, Andreasen M, Enghild JJ, Pedersen JS, Dobson CM, Knowles TPJ, Otzen DE. *Journal of the American Chemical Society*. 2014; 136:3859–3868. [PubMed: 24527756]
270. Giehm L, Svergun DI, Otzen DE, Vestergaard B. *Proc Natl Acad Sci USA*. 2011; 108:3246–3251. [PubMed: 21300904]
271. Lashuel HA, Hartley D, Petre BM, Walz T, Lansbury PT. *Nature*. 2002; 418:291–291.

272. Winner B, Jappelli R, Maji SK, Desplats PA, Boyer L, Aigner S, Hetzer C, Loher T, Vilar M, Campioni S, Tzitzilonis C, Soragni A, Jessberger S, Mira H, Consiglio A, Pham E, Masliah E, Gage FH, Riek R. *Proc Natl Acad Sci USA*. 2011; 108:4194–4199. [PubMed: 21325059]
273. Kaye R, Head E, Thompson JL, McIntire TM, Milton SC, Cotman CW, Glabe CG. *Science*. 2003; 300:486–489. [PubMed: 12702875]
274. Walsh DM, Selkoe DJ. *Journal of neurochemistry*. 2007; 101:1172–1184. [PubMed: 17286590]
275. Luheshi LM, Tartaglia GG, Brorsson A-C, Pawar AP, Watson IE, Chiti F, Vendruscolo M, Lomas DA, Dobson CM, Crowther DC. *PLoS biology*. 2007; 5:e290. [PubMed: 17973577]
276. Dobson CM. *Nature*. 2003; 426:884–890. [PubMed: 14685248]
277. Lesné S, Koh MT, Kotilinek L, Kaye R, Glabe CG, Yang A, Gallagher M, Ashe KH. *Nature*. 2006; 440:352–357. [PubMed: 16541076]
278. Nilsberth C, Westlind-Danielsson A, Eckman CB, Condron MM, Axelman K, Forsell C, Sten C, Luthman J, Teplow DB, Younkin SG, Naslund J, Lannfelt L. *Nature neuroscience*. 2001; 4:887–893. [PubMed: 11528419]
279. Bernstein SL, Dupuis NF, Lazo ND, Wyttenbach T, Condron MM, Bitan G, Teplow DB, Shea J-E, Ruotolo BT, Robinson CV, Bowers MT. *Nat Chem*. 2009; 1:326–331. [PubMed: 20703363]
280. Haataja L, Gurlo T, Huang CJ, Butler PC. *Endocrine Rev*. 2008; 29:303–316. [PubMed: 18314421]
281. Krotee P, Rodriguez JA, Sawaya MR, Cascio D, Reyes FE, Shi D, Hattne J, Nannenga BL, Oskarsson ME, Philipp S, Griner S, Jiang L, Glabe CG, Westermark GT, Gonen T, Eisenberg DS. *eLife*. 2017; 6:e19273. [PubMed: 28045370]
282. Roberts H, Brown D. *Biomolecules*. 2015; 5:282–305. [PubMed: 25816357]
283. van Diggelen F, Tepper AWJW, Apetri MM, Otzen DE. *Isr J Chem*. 2017; doi: 10.1002/ijch.201600116
284. Celej, María S., Sarroukh, R., Goormaghtigh, E., Fidelio, Gerardo D., Ruysschaert, J-M., Raussens, V. *Biochem J*. 2012; 443:719–726. [PubMed: 22316405]
285. Bucciantini M, Giannoni E, Chiti F, Baroni F, Formigli L, Zurdo J, Taddei N, Ramponi G, Dobson CM, Stefani M. *Nature*. 2002; 416:507–511. [PubMed: 11932737]
286. Bolognesi B, Kumita JR, Barros TP, Esbjorner EK, Luheshi LM, Crowther DC, Wilson MR, Dobson CM, Favrin G, Yerbury JJ. *ACS Chem Biol*. 2010; 5:735–740. [PubMed: 20550130]
287. Serpell LC, Berriman J, Jakes R, Goedert M, Crowther RA. *Proc Natl Acad Sci USA*. 2000; 97:4897–4902. [PubMed: 10781096]
288. Glabe CG. *J Biol Chem*. 2008; 283:29639–29643. [PubMed: 18723507]
289. Danzer KM, Haasen D, Karow AR, Moussaud S, Habeck M, Giese A, Kretzschmar H, Hengerer B, Kostka M. *The Journal of neuroscience : the official journal of the Society for Neuroscience*. 2007; 27:9220–9232. [PubMed: 17715357]
290. Karpinar DP, Balija MBG, Kügler S, Opazo F, Rezaei-Ghaleh N, Wender N, Kim H-Y, Taschenberger G, Falkenburger BH, Heise H, Kumar A, Riedel D, Fichtner L, Voigt A, Braus GH, Giller K, Becker S, Herzig A, Baldus M, Jäckle H, Eimer S, Schulz JB, Griesinger C, Zweckstetter M. *The EMBO journal*. 2009; 28:3256–3268. [PubMed: 19745811]
291. Desplats P, Lee H-J, Bae E-J, Patrick C, Rockenstein E, Crews L, Spencer B, Masliah E, Lee S-J. *Proc Natl Acad Sci USA*. 2009; 106:13010–13015. [PubMed: 19651612]
292. Relini A, Cavalleri O, Rolandi R, Gliozzi A. *Chem Phys Lipids*. 2009; 158:1–9. [PubMed: 19056366]
293. Butterfield SM, Lashuel HA. *Angew Chem*. 2010; 49:5628–5654. [PubMed: 20623810]
294. Aisenbrey C, Borowik T, Byström R, Bokvist M, Lindström F, Misiak H, Sani M-A, Gröbner G. *European biophysics journal : EBJ*. 2008; 37:247–255. [PubMed: 18030461]
295. Hebda JA, Miranker AD. *Annu Rev Biophys*. 2009; 39:125–152.
296. Galvagnion C, Buell AK, Meisl G, Michaels TCT, Vendruscolo M, Knowles TPJ, Dobson CM. *Nat Chem Biol*. 2015; 11:229–234. [PubMed: 25643172]
297. Kim H-Y, Cho M-K, Kumar A, Maier E, Siebenhaar C, Becker S, Fernandez CO, Lashuel HA, Benz R, Lange A, Zweckstetter M. *Journal of the American Chemical Society*. 2009; 131:17482–17489. [PubMed: 19888725]

298. Reynolds NP, Soragni A, Rabe M, Verdes D, Liverani E, Handschin S, Riek R, Seeger S. *Journal of the American Chemical Society*. 2011; 133:19366–19375. [PubMed: 21978222]
299. Fortin DL, Troyer MD, Nakamura K, Kubo S-i, Anthony MD, Edwards RH. *The Journal of neuroscience : the official journal of the Society for Neuroscience*. 2004; 24:6715–6723. [PubMed: 15282274]
300. Georgieva ER, Ramlall TF, Borbat PP, Freed JH, Eliezer D. *Journal of the American Chemical Society*. 2008; 130:12856–12857. [PubMed: 18774805]
301. Trexler AJ, Rhoades E. *Biochemistry*. 2009; 48:2304–2306. [PubMed: 19220042]
302. Wong PT, Schauerte JA, Wisser KC, Ding H, Lee EL, Steel DG, Gafni A. *Journal of molecular biology*. 2009; 386:81–96. [PubMed: 19111557]
303. Morris AM, Finke RG. *Biophys Chem*. 2009; 140:9–15. [PubMed: 19101068]
304. Kjaer L, Giehm L, Heimburg T, Otzen D. *Biophys J*. 2009; 96:2857–2870. [PubMed: 19348768]
305. Smith DP, Tew DJ, Hill AF, Bottomley SP, Masters CL, Barnham KJ, Cappai R. *Biochemistry*. 2008; 47:1425–1434. [PubMed: 18179253]
306. Pandey AP, Haque F, Rochet J-C, Hovis JS. *Biophys J*. 2009; 96:540–551. [PubMed: 19167303]
307. van Rooijen BD, Claessens MMAE, Subramaniam V. *FEBS letters*. 2008; 582:3788–3792. [PubMed: 18930058]
308. Hirsch EC, Brandel JP, Galle P, Javoy-Agid F, Agid Y. *Journal of neurochemistry*. 1991; 56:446–451. [PubMed: 1988548]
309. Pountney DL, Voelcker NH, Gai WP. *Neurotox Res*. 2005; 7:59–67. [PubMed: 15639798]
310. Bolisetty S, Mezzenga R. *Nat Nanotech*. 2016; 11:365–371.
311. Shen Y, Posavec L, Bolisetty S, Hilty FM, Nyström G, Kohlbrecher J, Hilbe M, Rossi A, Baumgartner J, Zimmermann MB, Mezzenga R. *Nat Nanotech*. 2017 advance online publication.
312. Wei G, Su Z, Reynolds NP, Arosio P, Hamley IW, Gazit E, Mezzenga R. *Chem Soc Rev*. 2017; doi: 10.1039/C6CS00542J
313. Tsigelny IF, Bar-On P, Sharikov Y, Crews L, Hashimoto M, Miller MA, Keller SH, Platoshyn O, Yuan JXJ, Masliah E. *The FEBS journal*. 2007; 274:1862–1877. [PubMed: 17381514]
314. Volles MJ, Lansbury PT. *Biochemistry*. 2002; 41:4595–4602. [PubMed: 11926821]
315. Bechinger B, Lohner K. *Biochem Biophys Acta Biomembr*. 2006; 1758:1529–1539.
316. Kiskis J, Horvath I, Wittung-Stafshede P, Rocha S. *Quarterly Rev Biophys*. 2017:50.
317. Chaudhary H, Stefanovic AND, Subramaniam V, Claessens MMAE. *FEBS letters*. 2014; 588:4457–4463. [PubMed: 25448986]
318. Monsellier E, Bousset L, Melki R. *Scientific reports*. 2016; 6:19180. [PubMed: 26757959]
319. Iyer A, Schilderink N, Claessens MMAE, Subramaniam V. *Biophys J*. 2016; 111:2440–2449. [PubMed: 27926845]
320. Devi L, Raghavendran V, Prabhu BM, Avadhani NG, Anandatheerthavarada HK. *J Biol Chem*. 2008; 283:9089–9100. [PubMed: 18245082]
321. Luth ES, Stavrovskaya IG, Bartels T, Kristal BS, Selkoe DJ. *J Biol Chem*. 2014; 289:21490–21507. [PubMed: 24942732]
322. Chen L, Jin J, Davis J, Zhou Y, Wang Y, Liu J, Lockhart PJ, Zhang J. *Biochemical and biophysical research communications*. 2007; 356:548–553. [PubMed: 17374364]
323. Cremades N, Cohen Samuel I, Deas E, Abramov Andrey Y, Chen Allen Y, Orte A, Sandal M, Clarke Richard W, Dunne P, Aprile Francesco A, Bertocini Carlos W, Wood Nicholas W, Knowles Tuomas P, Dobson Christopher M, Klenerman D. *Cell*. 2012; 149:1048–1059. [PubMed: 22632969]
324. Junn E, Mouradian MM. *Neuroscience letters*. 2002; 320:146–150. [PubMed: 11852183]
325. Choi D-H, Cristóvão AC, Guhathakurta S, Lee J, Joh TH, Beal MF, Kim Y-S. *Antioxid Redox Signal*. 2012; 16:1033–1045. [PubMed: 22098189]
326. Lashuel HA, Petre BM, Wall J, Simon M, Nowak RJ, Walz T, Lansbury PT Jr. *Journal of molecular biology*. 2002; 322:1089–1102. [PubMed: 12367530]
327. Hoozemans JJM, van Haastert ES, Nijholt DAT, Rozemuller AJM, Scheper W. *Neurodegener Dis*. 2012; 10:212–215. [PubMed: 22302012]

328. Snyder H, Mensah K, Theisler C, Lee J, Matouschek A, Wolozin B. *J Biol Chem*. 2003; 278:11753–11759. [PubMed: 12551928]
329. Fusco G, Pape T, Stephens AD, Mahou P, Costa AR, Kaminski CF, Kaminski Schierle GS, Vendruscolo M, Veglia G, Dobson CM, De Simone A. *Nat Comm*. 2016; 7:12563.
330. Forno LS. *Journal of neuropathology and experimental neurology*. 1996; 55:259–272. [PubMed: 8786384]
331. Recasens A, Dehay B, Bové J, Carballo-Carbajal I, Dovero S, Pérez-Villalba A, Fernagut P-O, Blesa J, Parent A, Perier C, Fariñas I, Obeso JA, Bezard E, Vila M. *Ann Neurol*. 2014; 75:351–362. [PubMed: 24243558]
332. Iljina M, Garcia GA, Horrocks MH, Tosatto L, Choi ML, Ganzinger KA, Abramov AY, Gandhi S, Wood NW, Cremades N, Dobson CM, Knowles TPJ, Klenerman D. *Proc Natl Acad Sci USA*. 2016; 113:E1206–E1215. [PubMed: 26884195]
333. Malkki H. *Nat Rev Neurol*. 2017; 13:66–67.
334. Bartels T, Choi JG, Selkoe DJ. *Nature*. 2011; 477:107–110. [PubMed: 21841800]
335. Marques O, Outeiro TF. *Cell Death Dis*. 2012; 3:e350. [PubMed: 22825468]
336. Masliah E, Rockenstein E, Adame A, Alford M, Crews L, Hashimoto M, Seubert P, Lee M, Goldstein J, Chilcote T, Games D, Schenk D. *Neuron*. 46:857–868. [PubMed: 15953415]
337. Valera E, Masliah E. *Pharmacol Ther*. 2013; 138:311–322. [PubMed: 23384597]
338. Di Giovanni S, Eleuteri S, Paleologou KE, Yin G, Zweckstetter M, Carrupt P-A, Lashuel HA. *J Biol Chem*. 2010; 285:14941–14954. [PubMed: 20150427]
339. Masuda M, Suzuki N, Taniguchi S, Oikawa T, Nonaka T, Iwatsubo T, Hisanaga S-i, Goedert M, Hasegawa M. *Biochemistry*. 2006; 45:6085–6094. [PubMed: 16681381]
340. Porat Y, Abramowitz A, Gazit E. *Chem Biol Drug Des*. 2006; 67:27–37. [PubMed: 16492146]
341. Prusiner SB. *Proc Natl Acad Sci USA*. 1998; 95:13363–13383. [PubMed: 9811807]
342. Huang Z, Prusiner SB, Cohen FE. *Fold Des*. 1996; 1:13–19. [PubMed: 9079359]
343. Campbell PN. *IUBMB Life*. 2005; 57:273–276. [PubMed: 16036610]
344. Sigurdson CJ, Aguzzi A. *Biochimica et biophysica acta*. 2007; 1772:610–618. [PubMed: 17223321]
345. Westaway D, Cooper C, Turner S, Da Costa M, Carlson GA, Prusiner SB. *Proc Natl Acad Sci USA*. 1994; 91:6418–6422. [PubMed: 7912827]
346. Mastrianni J, Nixon F, Layzer R, DeArmond SJ, Prusiner SB. *Neurology*. 1997; 48:A296.
347. Westermarck P, Benson MD, Buxbaum JN, Cohen AS, Frangione B, Ikeda S-I, Masters CL, Merlini G, Saraiva MJ, Sipe JD. *Amyloid*. 2005; 12:1–4. [PubMed: 16076605]
348. Chesebro B, Trifilo M, Race R, Meade-White K, Teng C, LaCasse R, Raymond L, Favara C, Baron G, Priola S, Caughey B, Masliah E, Oldstone M. *Science*. 2005; 308:1435. [PubMed: 15933194]
349. Aguzzi A. *Science*. 2005; 308:1420. [PubMed: 15933188]
350. Aguzzi A, Heikenwalder M. *Nat Rev Microbiol*. 2006; 4:765–775. [PubMed: 16980938]
351. Baskakov IV, Legname G, Baldwin MA, Prusiner SB, Cohen FE. *J Biol Chem*. 2002; 277:21140–21148. [PubMed: 11912192]
352. Bessen RA, Marsh RF. *J Virol*. 1994; 68:7859–7868. [PubMed: 7966576]
353. McKinley MP, Meyer RK, Kenaga L, Rahbar F, Cotter R, Serban A, Prusiner SB. *J Virol*. 1991; 65:1340–1351. [PubMed: 1704926]
354. Sunde M, Blake CC. *Quarterly reviews of biophysics*. 1998; 31:1–39. [PubMed: 9717197]
355. Leffers K-W, Wille H, Stöhr J, Junger E, Prusiner Stanley B, Riesner D. *Biol Chem*. 2005; 386:569. [PubMed: 16006244]
356. Safar JG, Kellings K, Serban A, Groth D, Cleaver JE, Prusiner SB, Riesner D. *J Virol*. 2005; 79:10796–10806. [PubMed: 16051871]
357. Caughey B, Baron GS. *Nature*. 2006; 443:803–810. [PubMed: 17051207]
358. Manuelidis L. *Virulence*. 2013; 4:373–383. [PubMed: 23633671]
359. Bastian FO. *Arch Pathol Lab Med*. 1979; 103:665–669. [PubMed: 389196]
360. Griffith JS. *Nature*. 1967; 215:1043–1044. [PubMed: 4964084]



361. Prusiner SB. *Annu Rev Microbiol.* 1989; 43:345–374. [PubMed: 2572197]
362. Soto C, Castilla J. *Nature medicine.* 2004; 10:63–67.
363. Abid K, Soto C. *Cell Mol Life Sci.* 2006; 63:2342–2351. [PubMed: 16927029]
364. Stefani M, Dobson CM. *J Mol Med.* 2003; 81:678–699. [PubMed: 12942175]
365. Novitskaya V, Bocharova OV, Bronstein I, Baskakov IV. *J Biol Chem.* 2006; 281:13828–13836. [PubMed: 16554307]
366. Chiesa R, Piccardo P, Quaglio E, Drisaldi B, Si-Hoe SL, Takao M, Ghetti B, Harris DA. *J Virol.* 2003; 77:7611–7622. [PubMed: 12805461]
367. Wüthrich K, Riek R. *Adv Protein Chem.* 2001; 57:55–82. [PubMed: 11447697]
368. Govaerts C, Wille H, Prusiner SB, Cohen FE. *Proc Natl Acad Sci USA.* 2004; 101:8342–8347. [PubMed: 15155909]
369. Sparkes RS, Simon M, Cohn VH, Fournier RE, Lem J, Klisak I, Heinzmann C, Blatt C, Lucero M, Mohandas T. *Proc Natl Acad Sci USA.* 1986; 83:7358–7362. [PubMed: 3094007]
370. Linden R, Martins VR, Prado MAM, Cammarota M, Izquierdo I, Brentani RR. *Physiol Rev.* 2008; 88:673–728. [PubMed: 18391177]
371. Llorens F, del Río JA. *Prion.* 2012; 6:245–251. [PubMed: 22437735]
372. Aguzzi A, Heikenwalder M, Polymenidou M. *Nat Rev Mol Cell Biol.* 2007;8.
373. Kanaani J, Prusiner SB, Diacovo J, Baekkeskov S, Legname G. *Journal of neurochemistry.* 2005; 95:1373–1386. [PubMed: 16313516]
374. Brown DR, Qin K, Herms JW, Madlung A, Manson J, Strome R, Fraser PE, Kruck T, von Bohlen A, Schulz-Schaeffer W, Giese A, Westaway D, Kretzschmar H. *Nature.* 1997; 390:684–687. [PubMed: 9414160]
375. Prina M, Kontseková E, Novák M. *Acta Virol.* 2015; 59:179–184. [PubMed: 26104335]
376. Mehrpour M, Codogno P. *Cancer Letters.* 2010; 290:1–23. [PubMed: 19674833]
377. Du J, Pan Y, Shi Y, Guo C, Jin X, Sun L, Liu N, Qiao T, Fan D. *Int J Cancer.* 2005; 113:213–220. [PubMed: 15386405]
378. Li Q-Q, Sun Y-P, Ruan C-P, Xu X-Y, Ge J-H, He J, Xu Z-D, Wang Q, Gao W-C. *Cancer Sci.* 2011; 102:400–406. [PubMed: 21265952]
379. de Wit M, Jimenez CR, Carvalho B, Belien JAM, Delis-van Diemen PM, Mongera S, Piersma SR, Vikas M, Navani S, Pontén F, Meijer GA, Fijneman RJA. *Gut.* 2012; 61:855–864. [PubMed: 21890811]
380. Büeler H, Aguzzi A, Sailer A, Greiner RA, Autenried P, Aguet M, Weissmann C. *Cell.* 1993; 73:1339–1347. [PubMed: 8100741]
381. Steele AD, Lindquist S, Aguzzi A. *Prion.* 2007; 1:83–93. [PubMed: 19164918]
382. Criado JR, Sánchez-Alavez M, Conti B, Giacchino JL, Wills DN, Henriksen SJ, Race R, Manson JC, Chesebro B, Oldstone MBA. *Neurobiology of disease.* 2005; 19:255–265. [PubMed: 15837581]
383. Le Pichon CE, Valley MT, Polymenidou M, Chesler AT, Sagdullaev BT, Aguzzi A, Firestein S. *Nature neuroscience.* 2009; 12:60–69. [PubMed: 19098904]
384. Riek R, Hornemann S, Wider G, Billeter M, Glockshuber R, Wüthrich K. *Nature.* 1996; 382:180–182. [PubMed: 8700211]
385. Zahn R, Liu A, Lührs T, Riek R, von Schroetter C, López García F, Billeter M, Calzolari L, Wider G, Wüthrich K. *Proc Natl Acad Sci USA.* 2000; 97:145–150. [PubMed: 10618385]
386. Zahn R, Güntert P, von Schroetter C, Wüthrich K. *Journal of molecular biology.* 2003; 326:225–234. [PubMed: 12547204]
387. Calzolari L, Zahn R. *J Biol Chem.* 2003; 278:35592–35596. [PubMed: 12826672]
388. Calzolari L, Lysek DA, Güntert P, von Schroetter C, Riek R, Zahn R, Wüthrich K. *Proc Natl Acad Sci USA.* 2000; 97:8340–8345. [PubMed: 10900000]
389. Pastore A, Zagari A. *Prion.* 2007; 1:185–197. [PubMed: 19164911]
390. Knaus KJ, Morillas M, Swietnicki W, Malone M, Surewicz WK, Yee VC. *Nature structural & molecular biology.* 2001; 8:770–774.

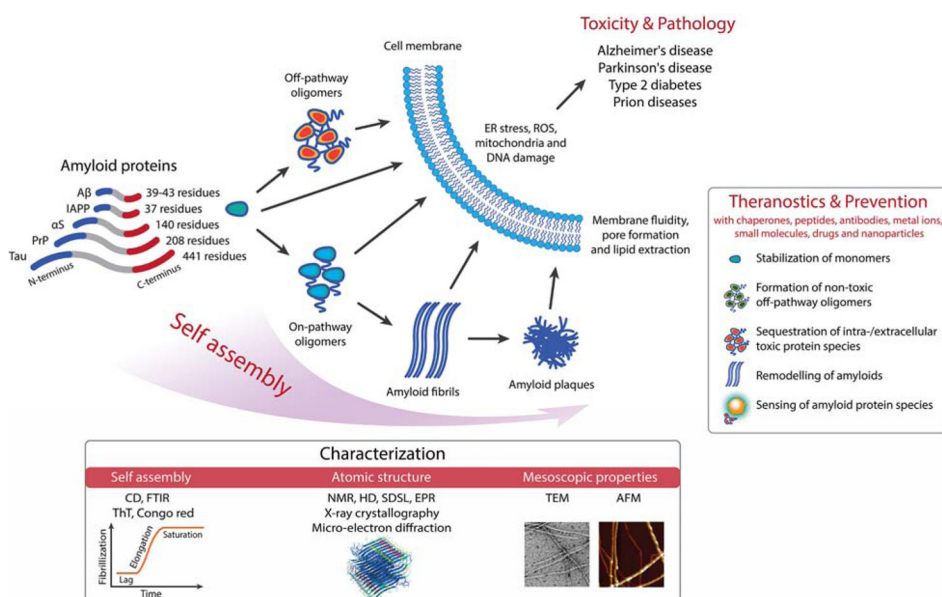
391. Wopfner F, Weidenhöfer G, Schneider R, von Brunn A, Gilch S, Schwarz TF, Werner T, Schätzl HM. *Journal of molecular biology*. 1999; 289:1163–1178. [PubMed: 10373359]
392. Rivera-Milla E, Oidtmann B, Panagiotidis CH, Baier M, Sklaviadis T, Hoffmann R, Zhou Y, Solis GP, Stuermer CAO, Málaga-Trillo E. *FASEB journal : official publication of the Federation of American Societies for Experimental Biology*. 2005; doi: 10.1096/fj.05-4279fje
393. Millhauser GL. *Annu Rev Phys Chem*. 2007; 58:299–320. [PubMed: 17076634]
394. Donne DG, Viles JH, Groth D, Mehlhorn I, James TL, Cohen FE, Prusiner SB, Wright PE, Dyson HJ. *Proc Natl Acad Sci USA*. 1997; 94:13452–13457. [PubMed: 9391046]
395. Pan KM, Baldwin M, Nguyen J, Gasset M, Serban A, Groth D, Mehlhorn I, Huang Z, Fletterick RJ, Cohen FE. *Proc Natl Acad Sci USA*. 1993; 90:10962–10966. [PubMed: 7902575]
396. Safar J, Roller PP, Gajdusek DC, Gibbs CJ. *J Biol Chem*. 1993; 268:20276–20284. [PubMed: 8104185]
397. McKinley MP, Prusiner SB. *Int Rev Neurobiol*. 1986; 28:1–57. [PubMed: 3100471]
398. DeMarco ML, Daggett V. *Proc Natl Acad Sci USA*. 2004; 101:2293–2298. [PubMed: 14983003]
399. Cobb NJ, Sönnichsen FD, McHaourab H, Surewicz WK. *Proc Natl Acad Sci USA*. 2007; 104:18946–18951. [PubMed: 18025469]
400. Groveman BR, Dolan MA, Taubner LM, Kraus A, Wickner RB, Caughey B. *J Biol Chem*. 2014; 289:24129–24142. [PubMed: 25028516]
401. Sawaya MR, Sambashivan S, Nelson R, Ivanova MI, Sievers SA, Apostol MI, Thompson MJ, Balbirnie M, Wiltzius JJW, McFarlane HT, Madsen AO, Riek C, Eisenberg D. *Nature*. 2007; 447:453–457. [PubMed: 17468747]
402. Wasmer C, Lange A, Van Melckebeke H, Siemer AB, Riek R, Meier BH. *Science*. 2008; 319:1523–1526. [PubMed: 18339938]
403. Wille H, Bian W, McDonald M, Kendall A, Colby DW, Bloch L, Ollesch J, Borovinskiy AL, Cohen FE, Prusiner SB, Stubbs G. *Proc Natl Acad Sci USA*. 2009; 106:16990–16995. [PubMed: 19805070]
404. Dickinson AG, Meikle VMH, Fraser H. *J Comp Pathol*. 1968; 78:293–299. [PubMed: 4970191]
405. Bruce ME, Dickinson AG. *J Gen Virol*. 1987; 68:79–89. [PubMed: 3100717]
406. Bessen RA, Marsh RF. *J Gen Virol*. 1992; 73:329–334. [PubMed: 1531675]
407. Monari L, Chen SG, Brown P, Parchi P, Petersen RB, Mikol J, Gray F, Cortelli P, Montagna P, Ghetti B. *Proc Natl Acad Sci USA*. 1994; 91:2839–2842. [PubMed: 7908444]
408. Collinge J, Clarke AR. *Science*. 2007; 318:930–936. [PubMed: 17991853]
409. Scott MR, Groth D, Tatzelt J, Torchia M, Tremblay P, DeArmond SJ, Prusiner SB. *J Virol*. 1997; 71:9032–9044. [PubMed: 9371560]
410. Kimberlin RH, Walker CA, Fraser H. *J Gen Virol*. 1989; 70:2017–2025. [PubMed: 2504883]
411. Fraser H, Dickinson AG. *J Comp Pathol*. 1973; 83:29–40. [PubMed: 4199908]
412. Merz PA, Somerville RA, Wisniewski HM, Iqbal K. *Acta neuropathologica*. 1981; 54:63–74. [PubMed: 7195134]
413. Prusiner SB, McKinley MP, Bowman KA, Bolton DC, Bendheim PE, Groth DF, Glenner GG. *Cell*. 1983; 35:349–358. [PubMed: 6418385]
414. Sim VL, Caughey B. *Neurobiol Aging*. 2009; 30:2031–2042. [PubMed: 18394757]
415. Kascsak RJ, Rubenstein R, Merz PA, Carp RI, Robakis NK, Wisniewski HM, Diring H. *J Virol*. 1986; 59:676–683. [PubMed: 2426470]
416. Neuendorf E, Weber A, Saalmueller A, Schatzl H, Reifenberg K, Pfaff E, Groschup MH. *J Biol Chem*. 2004; 279:53306–53316. [PubMed: 15448157]
417. Zanusso G, Polo A, Farinazzo A, et al. Consortium Td-G. *Archives of neurology*. 2007; 64:595–599. [PubMed: 17420324]
418. Lewis, Patrick A., Properzi, F., Prodromidou, K., Clarke, Anthony R., Collinge, J., Jackson, Graham S. *Biochem J*. 2006; 395:443–448. [PubMed: 16441239]
419. Stack MJ, Aldrich AM, Kitching AD, Scott AC. *Res Vet Sci*. 1995; 59:247–254. [PubMed: 8588101]
420. Hsiao K, Prusiner SB. *Neurology*. 1990; 40:1820–1820. [PubMed: 2247227]

421. Prusiner SB. *Archives of neurology*. 1993; 50:1129–1153. [PubMed: 8105771]
422. Gajdusek D. *Eur J Epidemiol*. 1991; 7:567–577. [PubMed: 1684758]
423. Collinge J, Whitfield J, McKintosh E, Beck J, Mead S, Thomas DJ, Alpers MP. *The Lancet*. 2006; 367:2068–2074.
424. McCutcheon S, Blanco ARA, Houston EF, de Wolf C, Tan BC, Smith A, Groschup MH, Hunter N, Hornsey VS, MacGregor IR. *PloS One*. 2011; 6:e23169. [PubMed: 21858015]
425. Andréoletti O, Litaïe C, Simmons H, Corbière F, Lugan S, Costes P, Schelcher F, Vilette D, Grassi J, Lacroux C. *PLoS Pathog*. 2012; 8:e1002782. [PubMed: 22737075]
426. Bonda DJ, Manjila S, Mehndiratta P, Khan F, Miller BR, Onwuzulike K, Puoti G, Cohen ML, Schonberger LB, Cali I. *Neurosurg Focus*. 2016; 41:E10.
427. Mathiason CK, Powers JG, Dahmes SJ, Osborn DA, Miller KV, Warren RJ, Mason GL, Hays SA, Hayes-Klug J, Seelig DM. *Science*. 2006; 314:133–136. [PubMed: 17023660]
428. Mathiason CK, Hays SA, Powers J, Hayes-Klug J, Langenberg J, Dahmes SJ, Osborn DA, Miller KV, Warren RJ, Mason GL. *PLoS One*. 2009; 4:e5916. [PubMed: 19529769]
429. Haley NJ, Seelig DM, Zabel MD, Telling GC, Hoover EA. *PLoS One*. 2009; 4:e4848. [PubMed: 19293928]
430. DeJoia C, Moreaux B, O’Connell K, Bessen RA. *J Virol*. 2006; 80:4546–4556. [PubMed: 16611915]
431. Konold T, Moore SJ, Bellworthy SJ, Simmons HA. *BMC Vet Res*. 2008; 4:14. [PubMed: 18397513]
432. Ligios C, Sigurdson CJ, Santucci C, Carcassola G, Manco G, Basagni M, Maestrale C, Cancedda MG, Madau L, Aguzzi A. *Nature medicine*. 2005; 11:1137–1139.
433. Lacroux C, Simon S, Benestad SL, Maïllet S, Mathey J, Lugan S, Corbière F, Cassard H, Costes P, Bergonier D. *PLoS Pathog*. 2008; 4:e1000238. [PubMed: 19079578]
434. Johnson CJ, McKenzie D, Pedersen JA, Aiken JM. *J Toxicol Environ Health Part A*. 2011; 74:161–166. [PubMed: 21218345]
435. Bruederle CE, Hnasko RM, Kraemer T, Garcia RA, Haas MJ, Marmer WN, Carter JM. *PloS One*. 2008; 3:e2969. [PubMed: 18698417]
436. Miller MW. *Emerg Infect Diseases*. 2004; 10:1003–1006. [PubMed: 15207049]
437. Georgsson G, Sigurdarson S, Brown P. *J Gen Virol*. 2006; 87:3737–3740. [PubMed: 17098992]
438. Saunders SE, Bartz JC, Bartelt-Hunt SL. *Environ Sci Technol*. 2009; 43:5242. [PubMed: 19708348]
439. Tsirolnikov K, Rezai H, Bonch-Osmolovskaya E, Nedkov P, Gousterova A, Cuff V, Godfroy A, Barbier G, Métro F, Chobert J-M. *J Agric Food Chem*. 2004; 52:6353–6360. [PubMed: 15453713]
440. Rasmussen J, Gilroyed BH, Reuter T, Dudas S, Neumann NF, Balachandran A, Kav NN, Graham C, Czub S, McAllister TA. *Prion*. 2014; 8:136–142. [PubMed: 24509640]
441. Pritzkow S, Morales R, Moda F, Khan U, Telling GC, Hoover E, Soto C. *Cell Rep*. 2015; 11:1168–1175. [PubMed: 25981035]
442. Chernoff YO. *Proc Natl Acad Sci USA*. 2016; 113:6097–6099. [PubMed: 27217577]
443. Brandner S, Klein MA, Frigg R, Pekarik V, Parizek P, Raeber A, Glatzel M, Schwarz P, Rüllicke T, Weissmann C. *Exp Physiol*. 2000; 85:705–712. [PubMed: 11187965]
444. Aguzzi A, Polymenidou M. *Cell*. 2004; 116:313–327. [PubMed: 14744440]
445. Aguzzi A, Calella AM. *Physiol Rev*. 2009; 89:1105–1152. [PubMed: 19789378]
446. Soto C, Estrada L, Castilla J. *Trends Biochem Sci*. 2006; 31:150–155. [PubMed: 16473510]
447. Makarava N, Ostapchenko VG, Savtchenko R, Baskakov IV. *J Biol Chem*. 2009; 284:14386–14395. [PubMed: 19329794]
448. Li L, Guest W, Huang A, Plotkin SS, Cashman NR. *Protein Eng Des Sel*. 2009; 22:523–529. [PubMed: 19602568]
449. Legname G. *Prion*. 2012; 6:37–39. [PubMed: 22453176]
450. Paramithiotis E, Pinard M, Lawton T, LaBoissiere S, Leathers VL, Zou W-Q, Estey LA, Lamontagne J, Lehto MT, Kondejewski LH. *Nature medicine*. 2003; 9:893–899.

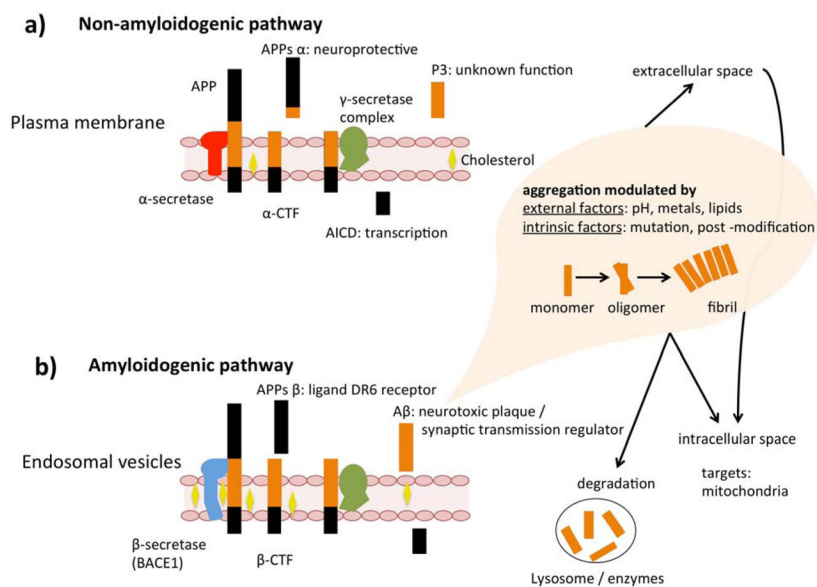
451. Kaneko K, Zulianello L, Scott M, Cooper CM, Wallace AC, James TL, Cohen FE, Prusiner SB. *Proc Natl Acad Sci USA*. 1997; 94:10069–10074. [PubMed: 9294164]
452. Geoghegan JC, Valdes PA, Orem NR, Deleault NR, Williamson RA, Harris BT, Supattapone S. *J Biol Chem*. 2007; 282:36341–36353. [PubMed: 17940287]
453. Baskakov IV, Breydo L. *BBA Mol Basis Dis*. 2007; 1772:692–703.
454. Caughey B. *Br Med Bull*. 2003; 66:109–120. [PubMed: 14522853]
455. Bishop M, Hart P, Aitchison L, Baybutt H, Plinston C, Thomson V, Tuzi N, Head M, Ironside J, Will R. *Lancet Neurol*. 2006; 5:393–398. [PubMed: 16632309]
456. Apostol MI, Wiltzius JJ, Sawaya MR, Cascio D, Eisenberg D. *Biochemistry*. 2011; 50:2456. [PubMed: 21323366]
457. Kurt TD, Bett C, Fernández-Borges N, Joshi-Barr S, Hornemann S, Rüllicke T, Castilla J, Wüthrich K, Aguzzi A, Sigurdson CJ. *The Journal of neuroscience : the official journal of the Society for Neuroscience*. 2014; 34:1022–1027. [PubMed: 24431459]
458. Sigurdson CJ, Nilsson KPR, Hornemann S, Manco G, Fernández-Borges N, Schwarz P, Castilla J, Wüthrich K, Aguzzi A. *J Clin Invest*. 2010; 120:2590–2599. [PubMed: 20551516]
459. Hill AF, Collinge J. *Trends Microbiol*. 2003; 11:578–584. [PubMed: 14659690]
460. Thuring C, Erkens J, Jacobs J, Bossers A, Van Keulen L, Garssen G, Van Zijderveld F, Ryder S, Groschup M, Sweeney T. *J Clin Microbiol*. 2004; 42:972–980. [PubMed: 15004040]
461. Jones EM, Surewicz WK. *Cell*. 2005; 121:63–72. [PubMed: 15820679]
462. Jones M. *Emerg Infect Diseases*. 2009
463. Liu H, Farr-Jones S, Ulyanov NB, Llinas M, Marqusee S, Groth D, Cohen FE, Prusiner SB, James TL. *Biochemistry*. 1999; 38:5362–5377. [PubMed: 10220323]
464. Makarava N, Kovacs GG, Bocharova O, Savtchenko R, Alexeeva I, Budka H, Rohwer RG, Baskakov IV. *Acta Neurol*. 2010; 119:177–187.
465. Béringue V, Herzog L, Jaumain E, Reine F, Sibille P, Le Dur A, Vilotte J-L, Laude H. *Science*. 2012; 335:472–475. [PubMed: 22282814]
466. Padilla D, Béringue V, Espinosa JC, Andreoletti O, Jaumain E, Reine F, Herzog L, Gutierrez-Adan A, Pintado B, Laude H. *PLoS Pathog*. 2011; 7:e1001319. [PubMed: 21445238]
467. Castilla J, Gonzalez-Romero D, Saá P, Morales R, De Castro J, Soto C. *Cell*. 2008; 134:757–768. [PubMed: 18775309]
468. Asante EA, Linehan JM, Desbruslais M, Joiner S, Gowland I, Wood AL, Welch J, Hill AF, Lloyd SE, Wadsworth JD. *The EMBO journal*. 2002; 21:6358–6366. [PubMed: 12456643]
469. Wadsworth JD, Asante EA, Desbruslais M, Linehan JM, Joiner S, Gowland I, Welch J, Stone L, Lloyd SE, Hill AF. *Science*. 2004; 306:1793–1796. [PubMed: 15539564]
470. Kimberlin RH, Cole S, Walker CA. *J Gen Virol*. 1987; 68:1875–1881. [PubMed: 3110370]
471. Colby DW, Giles K, Legname G, Wille H, Baskakov IV, DeArmond SJ, Prusiner SB. *Proc Natl Acad Sci USA*. 2009; 106:20417–20422. [PubMed: 19915150]
472. Bruce ME. *Br Med Bull*. 2003; 66:99–108. [PubMed: 14522852]
473. Barria MA, Telling GC, Gambetti P, Mastrianni JA, Soto C. *J Biol Chem*. 2011; 286:7490–7495. [PubMed: 21209079]
474. Li J, Browning S, Mahal SP, Oelschlegel AM, Weissmann C. *Science*. 2010; 327:869–872. [PubMed: 20044542]
475. Caughey B, Baron GS, Chesebro B, Jeffrey M. *Annu Rev Biochem*. 2009; 78:177–204. [PubMed: 19231987]
476. Aguzzi A, Falsig J. *Nature neuroscience*. 2012; 15:936–939. [PubMed: 22735515]
477. Mallucci G, Dickinson A, Linehan J, Klöhn P-C, Brandner S, Collinge J. *Science*. 2003; 302:871–874. [PubMed: 14593181]
478. Bahadi R, Farrelly PV, Kenna BL, Kourie JI, Tagliavini F, Forloni G, Salmona M. *Am J Physiol-Cell Ph*. 2003; 285:C862–C872.
479. Sanghera N, Pinheiro TJ. *Journal of molecular biology*. 2002; 315:1241–1256. [PubMed: 11827491]

480. Simoneau S, Rezaei H, Salès N, Kaiser-Schulz G, Lefebvre-Roque M, Vidal C, Fournier J-G, Comte J, Wopfner F, Grosclaude J. *PLoS Pathog.* 2007; 3:e125. [PubMed: 17784787]
481. Resenberger UK, Harmeier A, Woerner AC, Goodman JL, Müller V, Krishnan R, Vabulas RM, Kretzschmar HA, Lindquist S, Hartl FU. *The EMBO journal.* 2011; 30:2057–2070. [PubMed: 21441896]
482. Um JW, Nygaard HB, Heiss JK, Kostylev MA, Stagi M, Vortmeyer A, Wisniewski T, Gunther EC, Strittmatter SM. *Nature neuroscience.* 2012; 15:1227–1235. [PubMed: 22820466]
483. Linden R, Martins VR, Prado MA, Cammarota M, Izquierdo I, Brentani RR. *Physiol Rev.* 2008; 88:673–728. [PubMed: 18391177]
484. Kristiansen M, Deriziotis P, Dimcheff DE, Jackson GS, Ovaa H, Naumann H, Clarke AR, van Leeuwen FW, Menéndez-Benito V, Dantuma NP. *Mol Cell.* 2007; 26:175–188. [PubMed: 17466621]
485. Westergaard L, Christensen HM, Harris DA. *BBA Mol Basis Dis.* 2007; 1772:629–644.
486. Jeffrey M, McGovern G, Goodsir CM, González L. *Brain Pathol.* 2009; 19:1–11. [PubMed: 18400047]
487. Caughey B. *Trends Biochem Sci.* 2001; 26:235–242. [PubMed: 11295556]
488. Zhang H-J, Lu Y-H, Long Y-J, Wang Q-L, Huang X-X, Zhu R, Wang X-L, Liang L-P, Teng P, Zheng H-Z. *Anal Method.* 2014; 6:2982–2987.
489. Zhan L, Peng L, Huang C-Z. *Chin Sci Bull.* 2014; 59:964–970.
490. Sobrova P, Blazkova I, Chomoucka J, Drbohlovova J, Vaculovicova M, Kopel P, Hubalek J, Kizek R, Adam V. *Prion.* 2013; 7:349–358. [PubMed: 24055838]
491. Ottaviani MF, Cangiotti M, Fiorani L, Fattori A, Wasiak T, Appelhans D, Klajnert B. *Curr Med Chem.* 2012; 19:5907–5921. [PubMed: 22834819]
492. Kimura T, Hosokawa-Muto J, Asami K, Murai T, Kuwata K. *Eur J Med Chem.* 2011; 46:5675–5679. [PubMed: 21906853]
493. Gallardo-Godoy A, Gever J, Fife KL, Silber BM, Prusiner SB, Renslo AR. *J Med Chem.* 2011; 54:1010. [PubMed: 21247166]
494. Bongarzone S, Tran HNA, Cavalli A, Roberti M, Rosini M, Carloni P, Legname G, Bolognesi ML. *ChemMedChem.* 2011; 6:601–605. [PubMed: 21412985]
495. Alvarez-Puebla RA, Agarwal A, Manna P, Khanal BP, Aldeanueva-Potel P, Carbó-Argibay E, Pazos-Pérez N, Vigderman L, Zubarev ER, Kotov NA. *Proc Natl Acad Sci USA.* 2011; 108:8157–8161. [PubMed: 21536908]
496. Xiao SJ, Hu PP, Wu XD, Zou YL, Chen LQ, Peng L, Ling J, Zhen SJ, Zhan L, Li YF. *Anal Chem.* 2010; 82:9736–9742. [PubMed: 21038863]
497. Tran HNA, Sousa F, Moda F, Mandal S, Chanana M, Vimercati C, Morbin M, Krol S, Tagliavini F, Legname G. *Nanoscale.* 2010; 2:2724–2732. [PubMed: 20944860]
498. Henry J, Anand A, Chowdhury M, Coté G, Moreira R, Good T. *Anal Biochem.* 2004; 334:1–8. [PubMed: 15464948]
499. Supattapone S, Wille H, Uyechi L, Safar J, Tremblay P, Szoka FC, Cohen FE, Prusiner SB, Scott MR. *J Virol.* 2001; 75:3453–3461. [PubMed: 11238871]
500. Rangel A, Madroñal N, Gavín R, Llorens F, Sumoy L, Torres JM, Delgado-García JM, Del Río JA. *PloS One.* 2009; 4:e7592. [PubMed: 19855845]
501. Khosravani H, Zhang Y, Tsutsui S, Hameed S, Altier C, Hamid J, Chen L, Villemaire M, Ali Z, Jirik FR. *The Journal of cell biology.* 2008; 181:551–565. [PubMed: 18443219]
502. Weiss S, Proske D, Neumann M, Groschup MH, Kretzschmar HA, Famulok M, Winnacker E-L. *J Virol.* 1997; 71:8790–8797. [PubMed: 9343239]
503. Boese AS, Majer A, Saba R, Booth SA. *Exp Op Drug Disc.* 2013; 8:1265–1284.
504. Calvo P, Gouritin B, Brigger I, Lasmezas C, Deslys J-P, Williams A, Andreux JP, Dormont D, Couvreur P. *J Neurosc Method.* 2001; 111:151–155.
505. Kouassi GK, Wang P, Sreevatan S, Irudayaraj J. *Biotechnol Progr.* 2007; 23:1239–1244.
506. Miller MB, Supattapone S. *J Virol.* 2011; 85:2813–2817. [PubMed: 21228242]

507. Mangé A, Milhavel O, McMahon HEM, Casanova D, Lehmann S. *Journal of neurochemistry*. 2000; 74:754–762. [PubMed: 10646527]
508. Mangé A, Nishida N, Milhavel O, McMahon HEM, Casanova D, Lehmann S. *J Virol*. 2000; 74:3135–3140. [PubMed: 10708429]
509. Mangé A, Nishida N, Milhavel O, McMahon HE, Casanova D, Lehmann S. *J Virol*. 2000; 74:3135–3140. [PubMed: 10708429]
510. Karapetyan YE, Sferrazza GF, Zhou M, Ottenberg G, Spicer T, Chase P, Fallahi M, Hodder P, Weissmann C, Lasmézas CI. *Proc Natl Acad Sci USA*. 2013; 110:7044–7049. [PubMed: 23576755]
511. Ghaemmaghami S, May BC, Renslo AR, Prusiner SB. *J Virol*. 2010; 84:3408–3412. [PubMed: 20032192]
512. Oskarsson ME, Paulsson JF, Schultz SW, Ingelsson M, Westermark P, Westermark GT. *The American journal of pathology*. 2015; 185:834–846. [PubMed: 25700985]
513. Ono K, Takahashi R, Ikeda T, Yamada M. *Journal of neurochemistry*. 2012; 122:883–890. [PubMed: 22734715]
514. Mougénot A-LJ, Bencsik A, Nicot S, Vulin J, Morignat E, Verchère J, Bétemps D, Lakhdar L, Legastelois S, Baron TG. *J Neuropath Exp Neur*. 2011; 70:377–385. [PubMed: 21487306]
515. Olanow CW, Prusiner SB. *Proc Natl Acad Sci USA*. 2009; 106:12571–12572. [PubMed: 19666621]
516. Beekes M, Thomzig A, Schulz-Schaeffer WJ, Burger R. *Acta Neurol*. 2014; 128:463–476.
517. Tayeb-Fligelman E, Tabachnikov O, Moshe A, Goldshmidt-Tran O, Sawaya MR, Coquelle N, Colletier J-P, Landau M. *Science*. 2017; 355:831–833. [PubMed: 28232575]
518. Rubin N, Perugia E, Goldschmidt M, Fridkin M, Addadi L. *Journal of the American Chemical Society*. 2008; 130:4602–4603. [PubMed: 18338897]
519. Rubin N, Perugia E, Wolf SG, Klein E, Fridkin M, Addadi L. *Journal of the American Chemical Society*. 2010; 132:4242–4248. [PubMed: 20218685]
520. Usov I, Adamcik J, Mezzenga R. *ACS nano*. 2013; 7:10465–10474. [PubMed: 24171389]
521. Lee S-J, Desplats P, Sigurdson C, Tsigelny I, Masliah E. *Nat Rev Neurol*. 2010; 6:702–706. [PubMed: 21045796]
522. Jackson K, Barisone GA, Diaz E, Jin L-w, DeCarli C, Despa F. *Ann Neurol*. 2013; 74:517–526. [PubMed: 23794448]
523. Horvath I, Wittung-Stafshede P. *Proc Natl Acad Sci USA*. 2016; 113:12473–12477. [PubMed: 27791129]
524. Horwich A. *J Clin Invest*. 2002; 110:1221–1232. [PubMed: 12417558]

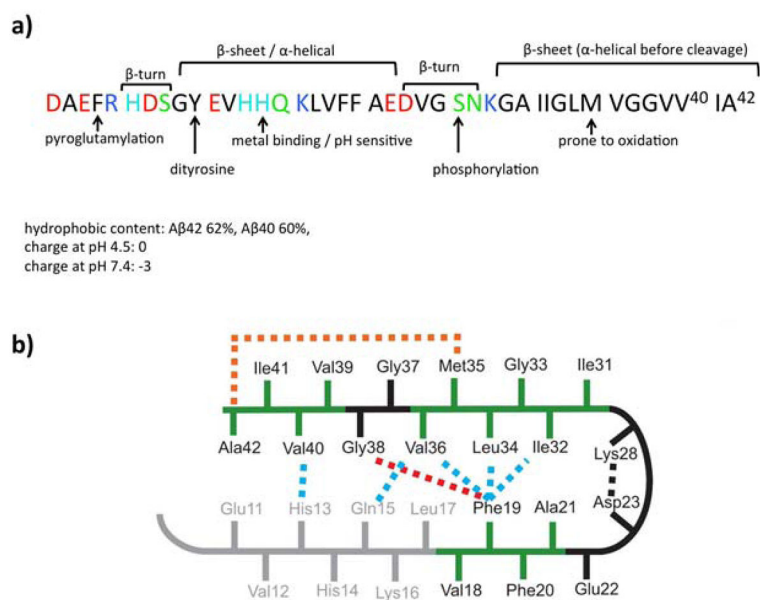


**Figure 1.** Scope of the present review, highlighting protein self-assembly, its biological and pathological implications, therapeutics and prevention. Aβ: amyloid-beta; IAPP: islet amyloid polypeptide; αS: alpha-synuclein; PrP: prion protein; CD: circular dichroism spectroscopy; FTIR: Fourier transform infrared spectroscopy; ThT: thioflavin T assay; NMR: nuclear magnetic resonance; HD: hydrogen-deuterium exchange; SDSL: site directed spin labelling; EPR: electron paramagnetic resonance; TEM: transmission electron microscopy; AFM: atomic force microscopy. ER: endoplasmic reticulum; ROS: reactive oxygen species.

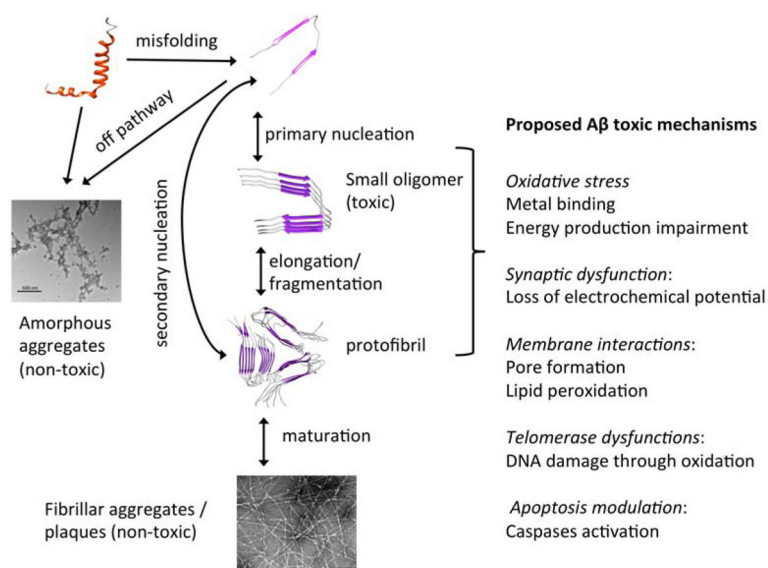


**Figure 2.** (a) Non-amyloidogenic pathway triggered by the location of APP at the plasma membrane interface; and (b) Amyloidogenic pathway induced through APP endocytosis into endosomal vesicles containing the protease BACE1. A $\beta$  peptides are then prone to aggregation and can be either secreted extracellularly or remain in the intracellular space to target other organelles, such as mitochondria, or be degraded by proteases such as cathepsin B.



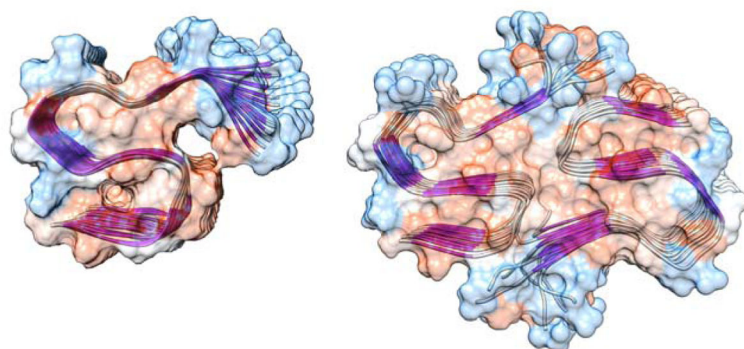


**Figure 3.** (a) A $\beta$  peptide sequence (CINEMA color code), potential post-modification sites and physicochemical properties; and (b) Intramolecular interactions stabilizing the typical hairpin  $\beta$ -sheet structure. Red and orange dashes: molecular contacts. Blue dashes: side-chain packing. Green: hydrophobic residues. Black: salt bridge. Adapted from reference 57. Copyright Nature Publishing Group.

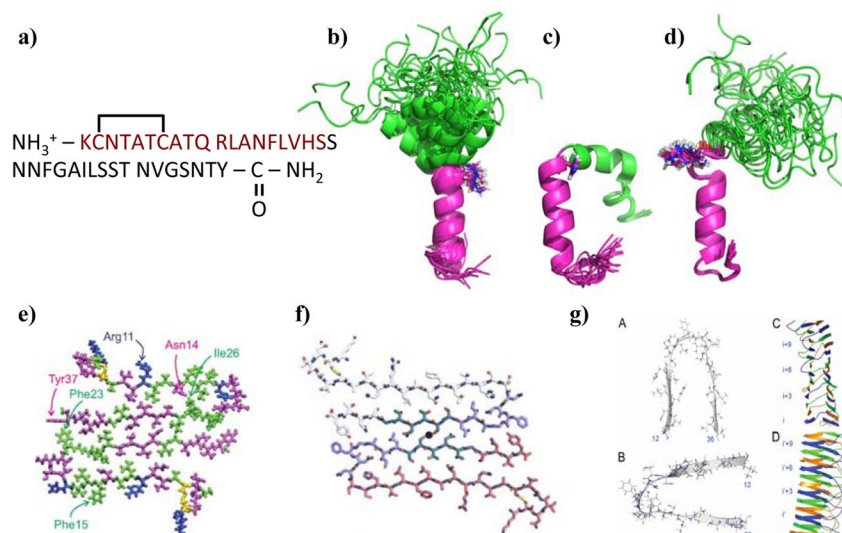


**Figure 4.**  
Aβ aggregation pathways from monomer to fibril formation and toxic outcomes.

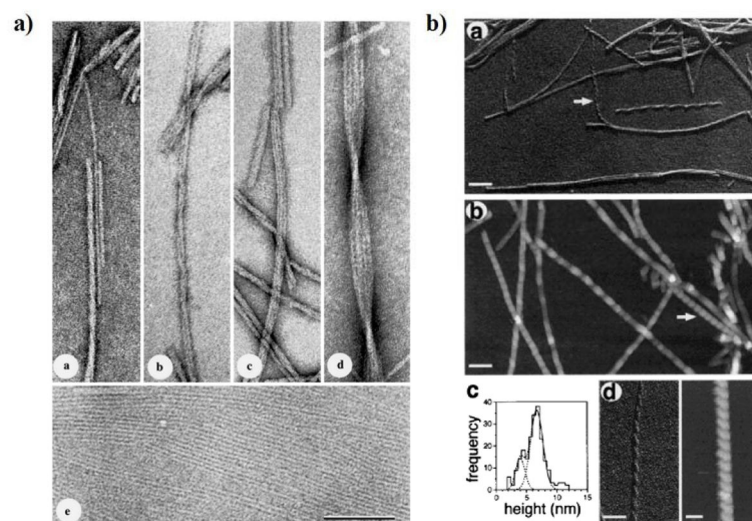




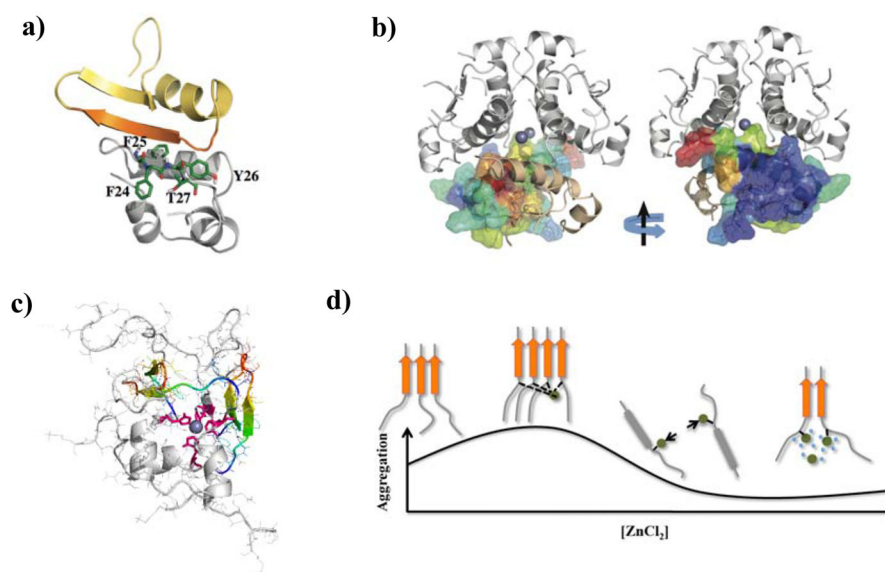
**Figure 6.** Two recent solid-state NMR A $\beta$ 42 fibril structures identifying different assemblies by (left) Griffin and co-workers (PDB: 5kk3)<sup>85</sup> and (right) Ishii and co-workers (2MXU).<sup>86</sup> High similarity is apparent with the  $\beta$ -sheet domain (purple ribbons) and the unstructured strand (gray ribbons) forming an S-shape. The hydrophobic surfaces are based on Kyte-Doolittle scale (red: hydrophobic, white: neutral, blue: hydrophilic).



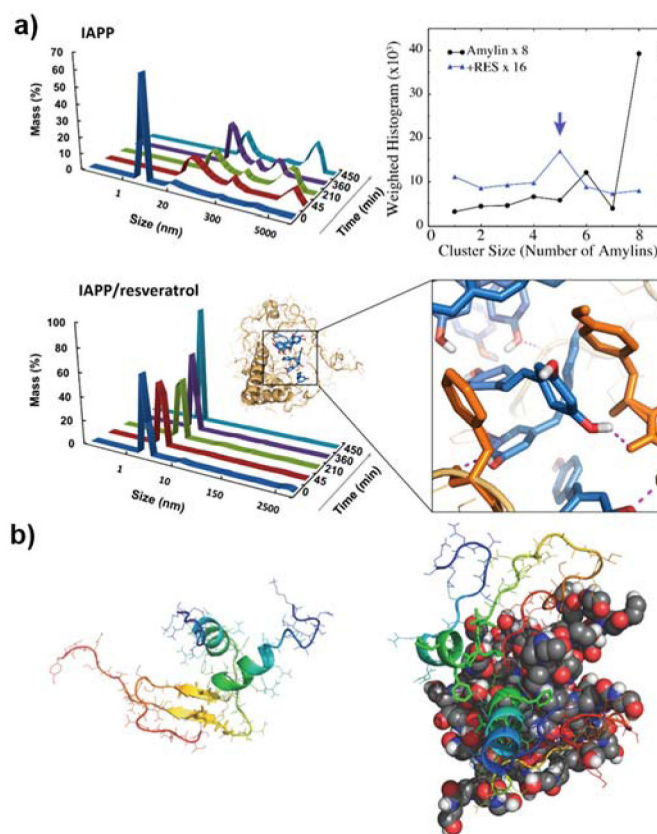
**Figure 7.** Structural studies of IAPP. (a) The primary structure of IAPP peptide. Solution NMR structures of IAPP monomers stabilized by SDS micelle at (b) pH 4.2 (PDB: 2KB8) and (c) pH 7.3 (PDB: 2L86). (d) Solution NMR structure of IAPP whose aggregation is reduced at pH 5.3, 4 °C, and 100 μM in concentration (PDB: 5MGQ). Residues 1–19 are colored purple and His18 is in sticks. The overall U-shaped IAPP fibril models are derived from experimental constraints by (e) solid-state NMR<sup>134</sup> and (f) X-ray crystallography of short peptides.<sup>135</sup> In panels (e) and (f), two peptides in the fibril cross-section are shown in sticks viewed along the fibril axis. (g) EPR constraints were applied to reconstruct the fibril model of disulfide reduced IAPP. The sub-panels A and B correspond to views along and perpendicular to the fibril axis, and sub-panels C and D are the accordingly reconstructed fibril models with two different views perpendicular to the fibril axis.<sup>136</sup> Copyright The American Chemical Society, John Wiley & Sons, and The American Society for Biochemistry and Molecular Biology.



**Figure 8.** Morphology of IAPP amyloid fibrils. (a) Lateral association of ribbon-like IAPP protofibrils revealed by TEM of freeze-dried tungsten-shadowed samples. Subpanels *a–d* depict ribbons assembled by lateral association of 1 to 4 protofibrils. Ribbons with multiple protofibrils often crossed over in a left-handed sense at moderately regular intervals. Subpanel *e* corresponds to lateral assembly of protofibrils into single-layered, sheet-like arrays. Scale bar: 100 nm. (b) IAPP fibrils with coiled morphologies.<sup>142, 143</sup> Subpanels *a* and *b* denote coiled fibrils visualized by TEM and AFM, respectively. Arrows point to a left-handed fibril with a 25 nm cross-over periodicity. Longer periodicities of approximately 50 nm can also be seen in both subpanels. Subpanel *c* shows the AFM height distribution, and *d* compares the 25 nm periodicity fibril in TEM and AFM. Scale bars: 100 nm in subpanels *a, b*; and 50 nm in *d*. Copyright Elsevier.

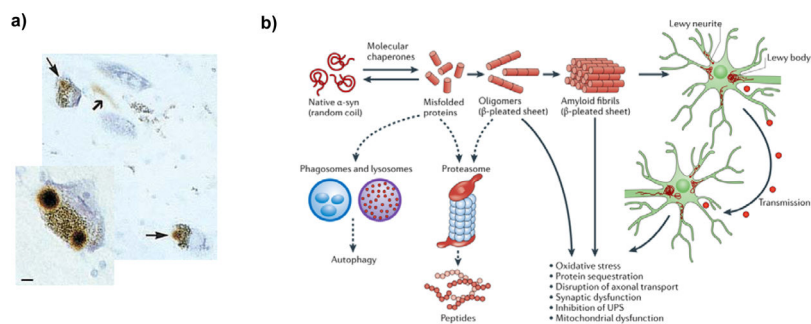


**Figure 9.** Effects of  $\beta$ -cell granule components on IAPP aggregation. (a) A representative IAPP-insulin complex from DMD simulations,<sup>140</sup> where the amyloidogenic residues of IAPP (residues 22–29) are shown in orange. The residues in the B-chain of insulin important for binding IAPP are highlighted in stick representation. (b) The residues of an insulin monomer are colored according to IAPP binding frequencies in the structure of an insulin hexamer. The view with an 180° rotation is also presented. The residues with strong IAPP-binding are located at the insulin monomer–monomer interface. (c) A representative IAPP tetramer with His18 (highlighted as sticks in pink) coordinated by a Zn<sup>2+</sup> (blue sphere) from DMD simulations.<sup>179</sup> The amyloidogenic sequences from each IAPP monomer are highlighted in rainbow colors. (d) A mechanistic scheme demonstrating the dependence of IAPP aggregation on relative zinc concentration. Copyright The American Chemical Society and Elsevier.



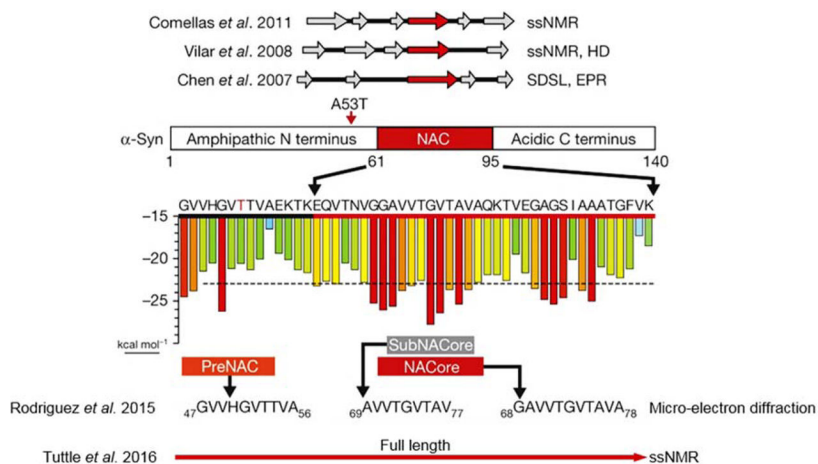
**Figure 10.** Inhibition of IAPP aggregation. (a) Left: High-throughput dynamic light scattering measurement of IAPP size distributions with and without resveratrol (2:1 ligand/IAPP ratio). Right: Distribution of IAPP aggregates of different molecular weights with and without resveratrol *in silico*. Stable IAPP/resveratrol oligomer has the resveratrol molecules forming a nano-sized core and IAPP peptides a corona, which prevents aggregation.<sup>234</sup> (b) Left: a typical IAPP dimer in DMD simulations. Right: Binding to a PAMAM-OH dendrimer (spheres) inhibits self-association of the amyloidogenic sequences (yellow region) between two IAPP peptides.<sup>224</sup> The peptides are shown in cartoon representation with rainbow color from blue (N-terminus) to red (C-terminus). Copyright Nature Publishing Group and John Wiley & Sons.





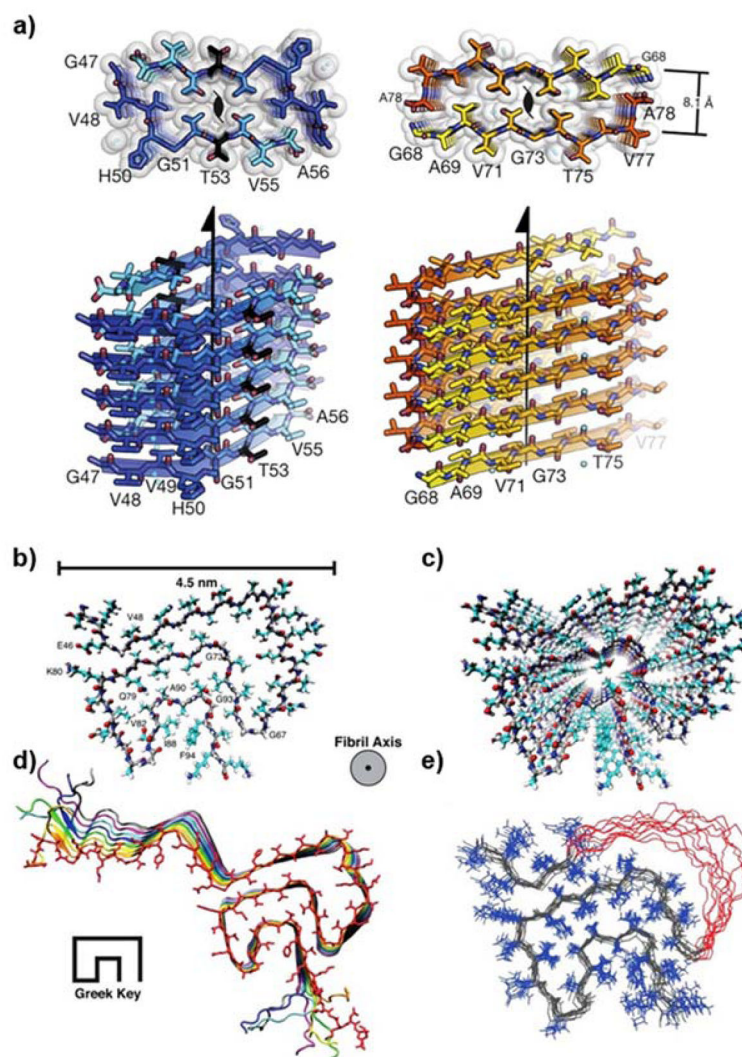
**Figure 11.**

(a) (Large image) Pigmented nerve cells containing  $\alpha$ S-positive Lewy body (thin arrows) and Lewy neurites (thick arrow).<sup>242</sup> Small image: a pigmented nerve cell with two  $\alpha$ S-positive Lewy bodies. Scale bar: 8  $\mu$ m. (b) Hypothesized  $\alpha$ S toxicity and spread of pathology in Parkinson's disease (PD) and Parkinson's disease dementia (PDD). UPS: Ubiquitin proteasome system.<sup>243</sup> Copyright Nature Publishing Group.



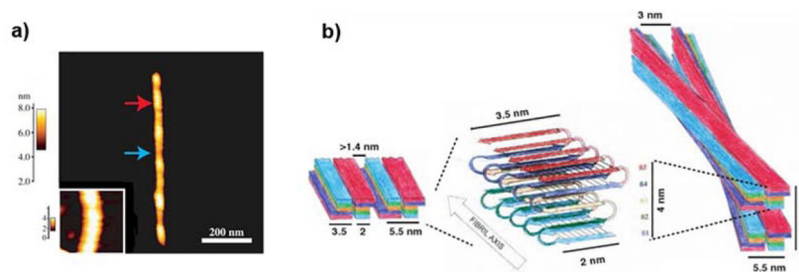
**Figure 12.**

Landmark studies concerning the structures of  $\alpha$ S fragments with respect to its full 140 residues consisting of N terminus, NAC and C terminus.<sup>248</sup> The researcher teams are chronicled on the left while the employed techniques are abbreviated on the right. EPR: electron paramagnetic resonance; ssNMR: solid-state nuclear magnetic resonance; HD: hydrogen-deuterium exchange; SDSL: site directed spin labelling. Copyright Nature Publishing Group.



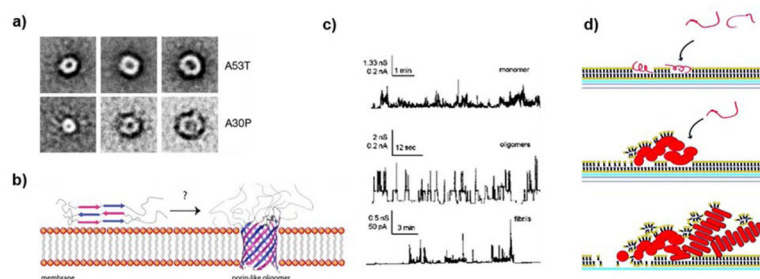
**Figure 13.**

(a) Top and side views of the structures of NACore (orange; residues 68–78, sequence also see Fig. 12) and PreNAC segments (blue; residues 47–56, sequence also see Fig. 12). The A53T mutation in PreNAC is shown in black.<sup>248</sup> (b–e) Three-dimensional structure of a full  $\alpha$ S fibril. (b) A central monomer from residues 44 to 96 looking down the fibril axis showing the Greek-key motif of the fibril core. (c) Stacked monomers showing the sidechain alignment between each monomer down the fibril axis. (d) Residues 25 to 105 of 8 monomers displaying the  $\beta$ -sheet alignment of each monomer in the fibril and the Greek-key topology of the core. (e) Overlaid ten lowest energy structures, showing sidechain positions within the core. Residues 51–57 are indicated in red with side chains removed.<sup>249</sup> Copyright Nature Publishing Group.



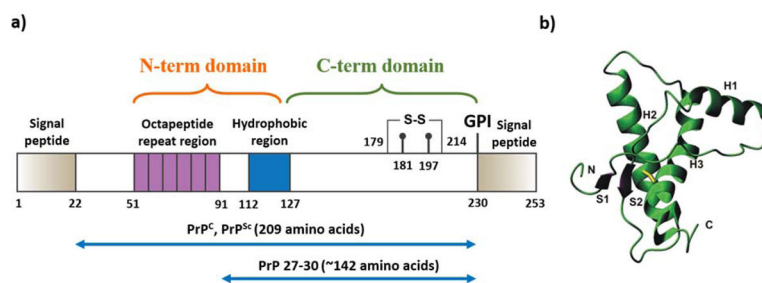
**Figure 14.**

(A) AFM image showing a periodicity of 100–150 nm along an  $\alpha$ S protofibril. The peak (red arrow) to trough (blue arrow) differs by  $\sim 1$  nm in height. (Inset) A section of a protofilament with an average height of 3.8 nm.<sup>253</sup> (B) Proposed fold of an  $\alpha$ S fibril. A monomeric  $\alpha$ S within a protofilament (center). Incorporation of protofilaments into a straight or twisted fibril is illustrated in the left and right panel, respectively.<sup>241</sup> Copyright Cell Press and National Academy of Sciences.



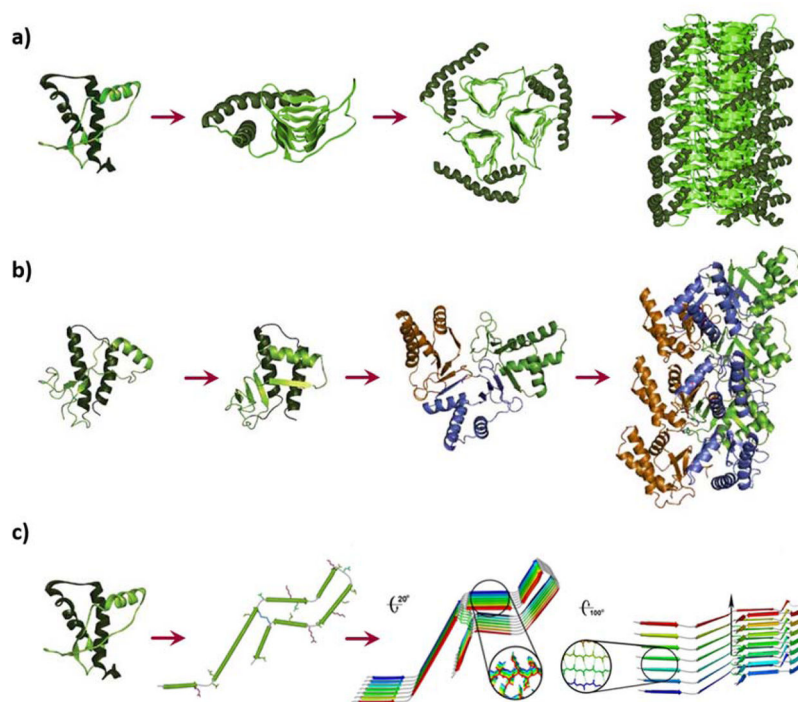
**Figure 15.**

Proposed mechanisms of membrane damage induced by  $\alpha$ S aggregation. (a) Projection averages of annular oligomers formed by  $\alpha$ S mutants A53T and A30P.<sup>271</sup> (b)  $\alpha$ S oligomer spans the membrane in a porin-like fashion to induce toxicity.<sup>284</sup> (c) Oligomers but not monomers or fibrils induced frequent channel formation in planar lipid bilayers formed from diphytanoylphosphatidylcholine dissolved in *n*-decane in 1 M KCl, at a bias of +100 mV.<sup>297</sup> (d) (Top panel) Monomeric  $\alpha$ S adsorbed to a lipid bilayer. (Middle panel) Aggregation of  $\alpha$ S monomers causes membrane thinning and lipid extraction. (Lower panel) Further incubation results in assembly of mature  $\alpha$ S fibrils and disassembly of the lipid membrane.<sup>298</sup> Copyright Nature Publishing Group, Portland Press and The American Chemical Society.

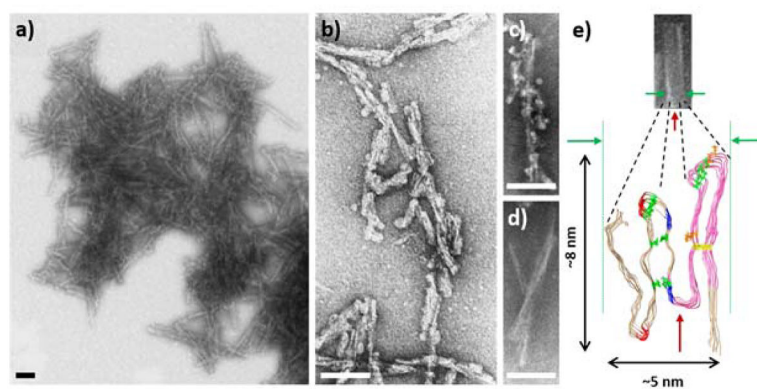


**Figure 16.**

(a) Overview of the PrP sequence and architecture.<sup>341, 389</sup> The residue numbering refers to human PrP. (b) 3D representation of the secondary structure of mouse PrP<sup>C</sup>.<sup>384</sup> The unordered N-terminus is omitted and the sulphur bridge between Cys179 and Cys214 is indicated in yellow. Copyright Nature Publishing Group.



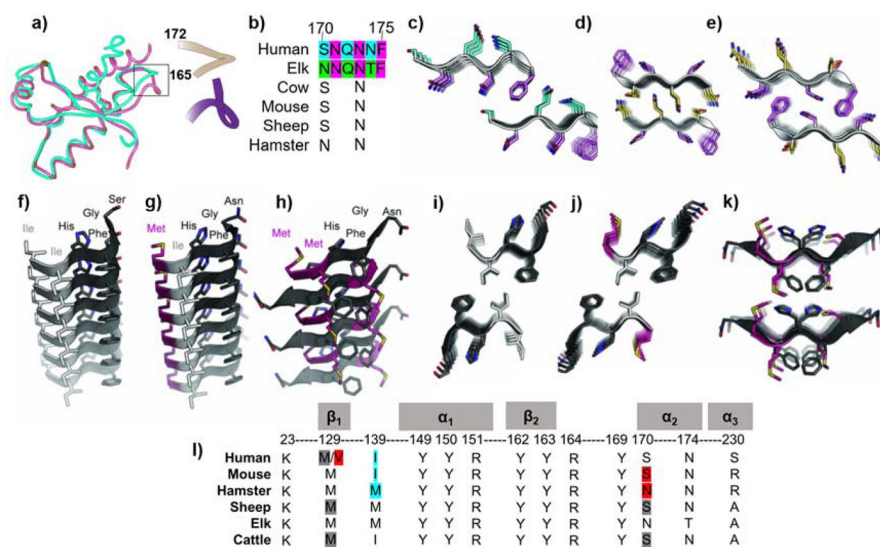
**Figure 17.** Structural models for the PrP<sup>Sc</sup> aggregates: (a) In the  $\beta$ -helical model the N-terminal region (90–177 residues, light green) of PrP 27–30 refolds into a  $\beta$ -helix motif and the C-terminal region (residues 178–230, dark green) maintains  $\alpha$ -helical secondary structure as in native PrP<sup>C</sup>.<sup>368</sup> (b) The  $\beta$ -spiral model consists of a spiralling core of extended sheets consisting of short  $\beta$ -strands, comprising residues 116–119, 129–132 and 160–164. The three  $\alpha$ -helices in C-terminus maintain this conformational motif.<sup>398</sup> (c) The parallel in-register extended  $\beta$ -sheet model of PrP<sup>Sc</sup>, where PrP<sup>C</sup> refolds into a structure consisting mainly of  $\beta$ -sheets.<sup>399</sup> Copyright National Academy of Sciences.



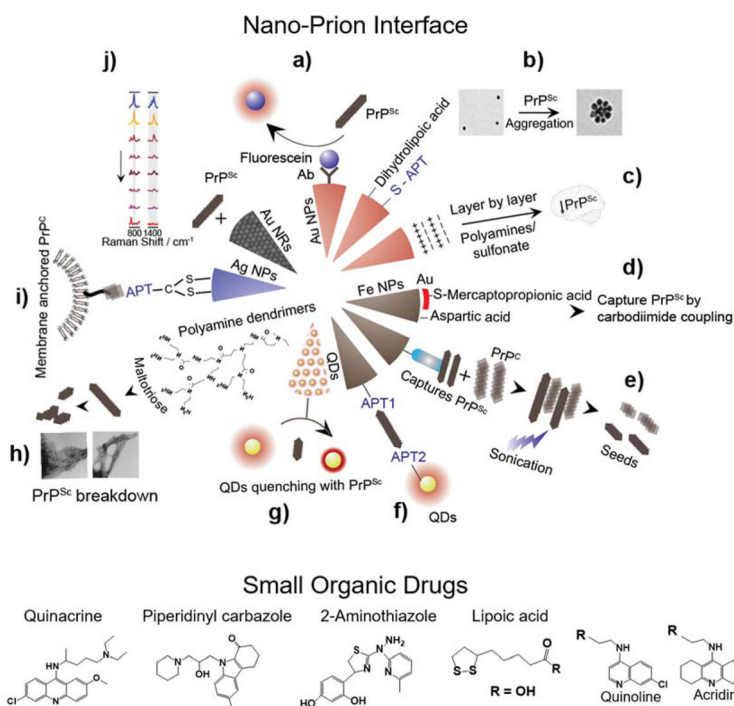
**Figure 18.**

Electron microscopy of prion fibrils. (a) Aggregates of wild-type 22L scrapie prion aggregates.<sup>414</sup> (b) Prion rods of PrP 27–30.<sup>341</sup> (c) Wild type RML scrapie prion structure obscured by non-fibrillar material, while (d) anchorless RML fibril morphology was much cleaner.<sup>414</sup> (e) Celery stalk-like brain-derived GPI-anchorless 22L fibril<sup>414</sup> and proposed parallel in-register  $\beta$ -sheet model of PrP (90–231) octameric segment.<sup>400</sup> Scale bars: 100 nm. Copyright Elsevier, National Academy of Sciences and American Society for Biochemistry and Molecular Biology.



**Figure 19.**

Amino acid sequence and 3D structural comparison of  $\beta$ -sheet stacking from steric zones of PrP<sup>Sc</sup> in different mammalian species. Superimposition of mouse (grey) and hamster (blue) PrP<sup>Sc</sup> with 165–172 backbone fold (a). Amino acid sequence from 170–175 backbone region (b).<sup>463</sup> Cyan highlights human while orange highlights elk specific residues. Stick representation of steric zipper interfacing  $\beta$ -sheet back bone region for human (c) and both alignments of elk (d, e). X-ray crystallographic atomic structures from barrier determining steric zippers from human, mouse and hamster, side view for single  $\beta$ -sheet stacking (f, g, h) and top view of steric zipper (i, j, k).<sup>456</sup> Sequence differences at molecular switches, defining the conformational and transmission barrier between different species (l).<sup>456, 463</sup> Grey and red indicate transmission and barrier while cyan at 139 presents molecular switch for parallel or anti-parallel sheet stacking in human, mouse and hamster. Copyright The American Chemical Society.

**Figure 20.**

Prion diagnostics and therapeutics at the nano and medicinal chemistry fronts.<sup>488–499</sup>

Compiled from references 488–499. PrP<sup>Sc</sup> can be sensed by turning on/off the fluorescence of fluorescein-AuNPs (a), free QDs (g) or QD-FeNP sandwiches (f), or by resonance light scattering (RLS) of lipoic acid-AuNP aggregates (b). Quantitative sensing can be performed by Raman spectroscopy of Au nanorods (j). PrP<sup>Sc</sup> can be captured by AuNPs with polyamines and sulphonates surface layers of (c) or by FeNPs with mercaptopropionic acid, aspartic acid (d) or RNA aptamer surface layers (e). Cell bound PrP<sup>Sc</sup> can be captured by aptamer-AgNP conjugates (i) while complete denaturation of PrP<sup>Sc</sup> can be observed with 5G polyamine dendrimers (h). The TEM images in h are reproduced from ref. 488 with permission from the Royal Society of Chemistry. The TEM images in b and Raman spectra in j are copyrights of The American Society of Chemistry and National Academy of Science.